MICROBIAL REGULATION OF SOIL GREENHOUSE GAS EMISSIONS IN A NON-BLOAT LEGUME GRAZING SYSTEM

A Thesis Submitted to the College of
Graduate and Postdoctoral Studies
in Partial Fulfillment of the Requirements
for the Degree of Master of Science
in the Department of Soil Science
University of Saskatchewan
Saskatoon
By
Jesse Christopher Reimer

PERMISSION TO USE

In presenting this thesis in partial fulfillment of the requirements for a Postgraduate degree from the University of Saskatchewan, I agree that the Libraries of this University may make it freely available for inspection. I further agree that permission for copying of this thesis in any manner, in whole or in part, for scholarly purposes may be granted by the professor or professors who supervised my thesis work or, in their absence, by the Head of the Department or the Dean of the College in which my thesis work was done. It is understood that any copying or publication or use of this thesis or parts thereof for financial gain shall not be allowed without my written permission. It is also understood that due recognition shall be given to me and to the University of Saskatchewan in any scholarly use which may be made of any material in my thesis.

Requests for permission to copy or to make other uses of materials in this thesis in whole or part should be addressed to:

Head of the Department of Soil Science
Agriculture Building
University of Saskatchewan
51 Campus Drive
Saskatoon, Saskatchewan S7N 5A8
Canada

OR

Dean
College of Graduate and Postdoctoral Studies
University of Saskatchewan
107 Administration Place
Saskatoon, Saskatchewan S7N 5A2
Canada

DISCLAIMER

Reference in this thesis to any specific commercial products, process, or service by trade name, trademark, manufacturer, or otherwise, does not constitute or imply its endorsement, recommendation, or favouring by the University of Saskatchewan. The views and opinions of the author expressed herein do not state or reflect those of the University of Saskatchewan and shall not be used for advertising or product endorsement purposes.

ABSTRACT

Cattle pastures are a source of greenhouse gas (GHG) emissions, including enteric methane from ruminating cattle, carbon dioxide (CO_2), and nitrous oxide (N_2O) from microbial respiration of soil carbon (C) and nitrogen (N). Producers may introduce non-bloat legumes to cattle pastures to improve soil N content, increase cattle protein uptake, and decrease enteric methane emissions. However, such land management changes can alter soil microbial communities, potentially increasing net system GHGs. The research goal was to determine whether non-bloat legumes alter soil microbial community structure, activity, and N_2O emissions. Grazed pastures with introduced Veldt cicer milkvetch and common sainfoin were surveyed for differences in GHGs, microbial community structure, and extracellular enzyme activity for two growing seasons. Seasonal shifts explained most microbial community changes; however, communities structured according to legume treatment and legume microbial community structure correlated with increasing soil nitrate (NO_3^-) content, particularly in cicer milkvetch plots. Soil N_2O fluxes did not differ on sampling dates, however cicer milkvetch tended towards larger N_2O emissions. Pasture soil microbial community changes did not translate to increased N_2O emissions on sampling dates. Additional protein found in non-bloat legumes may increase urine urea-N content in cattle affecting soil processes. Urine containing low or high concentrations of ^{15}N and ^{13}C labeled urea was added to soil microcosms under controlled conditions to better understand the impact of urine on soil N_2O emissions, microbial N cycling communities, and N_2O sources. Ammonia oxidizing bacteria (AOB) were the most active nitrifiers following urine addition. Denitrifiers contributed the most N_2O in urine amended soils and their dynamics varied. After urine deposition, *nirS* gene abundance and transcript increases were greater and more sustained than *nirK*, while *nirK* increased activity more rapidly but did not increase gene abundance. Urine toxicity and increased clade II *nosZ* transcription likely reduced initial N_2O emissions at high urea concentrations, resulting in no difference between cumulative soil N_2O fluxes between urea rates and a lower urine-N emission factor for high urea soils. These findings support the use of non-bloat legumes in pastures, particularly when considering the potential reduction in enteric methane emissions, reducing net pasture system GHG emissions.

ACKNOWLEDGEMENTS

First, I would like to thank the Department of Soil Science faculty and staff, past and present. The open, friendly nature of the department makes it a very welcoming place to study. The faculty's passion in teaching their discipline is what drew me to the department as an undergraduate. The undergraduate and graduate students, technicians, research associates, and faculty that have helped me along the way are too numerous to mention individually, but know that you are appreciated and each one of you is what makes the department a great place to work.

Thank you to my committee members Dr. J. Diane Knight and chair Dr. Jeff Schoenau for providing me with your expertise, guidance, and advice. To my co-supervisors, Dr. Bobbi Helgason and Dr. Melissa Arcand, thank you for your invaluable inspiration, encouragement, and insight.

Thank you to my parents, Elvin and Nancy Reimer, for fostering my interest in the natural world from an early age. My father could not witness my journey through university, but I know both he and my mother would be equally as proud.

Lastly, to Micah, for encouraging me to reach out and follow this path and motivating me once I was on it – thank you. Your support and inspiration have kept me motivated and grounded through the many successes and challenges that come with pursuing a thesis.

TABLE OF CONTENTS

LIST OF TABLES

LIST OF FIGURES

LIST OF ABBREVIATIONS

AGGP	Agricultural greenhouse gases program
AOA	Ammonia-oxidizing archaea
AOB	Ammonia-oxidizing bacteria
amoA	Gene encoding the ammonia monooxygenase α subunit
AMF	Arbuscular mycorrhizal fungi
ANOSIM	Analysis of similarity
AP	Acid phosphatase, which cleaves organically bound monophosphates
βG	β-glucosidase enzyme, which degrades cellulose
cDNA	Complimentary deoxyribonucleic acid
CRDS	Cavity ring down spectrometer
dbRDA	Distance-based redundancy analysis
DNA	Deoxyribonucleic acid
DOC	Dissolved organic carbon
ECD	Electron capture detector
EMM	Estimated marginal means
FAME	Fatty acid methyl ester
FID	Flame ionization detector
GC	Gas chromatograph
gDNA	Genomic deoxyribonucleic acid
GHG	Greenhouse gas
GLM	General linear model
GLME	General linear mixed effects model
G-	Gram-negative bacteria
G+	Gram-positive bacteria
hao	Gene encoding the enzyme hydroxylamine oxidoreductase
HU	High urea urine treatment
ln	Natural-base logarithm
log	Base-10 logarithm
LU	Low urea urine treatment

mRNA	Messenger ribonucleic acid
NAG	N-acetyl-β-D-glucosaminidase enzyme, which degrades chitin
NIR	Nitrite reductase
nirK	Gene encoding the copper-containing *c*-type cytochrome subunit of nitrite reductase
nirS	Gene encoding the cd_1-type cytochrome subunit of nitrite reductase
NMDS	Non-metric multidimensional scaling
NOR	Nitric oxide reductase
NOS	Nitrous oxide reductase
nosZ-I	Gene encoding a structural subunit of clade I nitrous oxide reductase
nosZ-II	Gene encoding a structural subunit of clade II nitrous oxide reductase
P450nor	Gene encoding the fungal cytochrome nitric oxide reductase
PerMANOVA	Permutational multivariate analysis of variance
PLFA	Phospholipid fatty acid
PEARL	Prairie Environmental Agriculture Research Laboratory
qPCR	Quantitative polymerase chain reaction
RNA	Ribonucleic acid
RT-qPCR	Reverse transcription quantitative polymerase chain reaction
SE	Standard error of the mean
SEM	Structural equation model
SIP	Stable isotope probing
SP	Site preference
TCD	Thermal conductivity detector
TDN	Total dissolved nitrogen
WFPS	Water-filled pore space

1. General Introduction

1.1 Introduction

Microbial life has long had a global impact on atmospheric composition. One such example is photosynthetic cyanobacteria oxygenating the atmosphere 2.45 billion years ago (Schirrmeister, de Vos, Antonelli, & Bagheri, 2013). Presently, microorganisms impact global climate by producing and consuming greenhouse gases (GHGs) through metabolic and nutrient cycling activities. Microbes are ubiquitous across all terrestrial ecosystems, with billions of microbial cells occupying a single gram of soil. They provide essential ecosystem services and curate the biogeochemical cycles which produce GHGs. Carbon dioxide (CO_2) is produced by microbes degrading organic materials, while nitrous oxide (N_2O) is derived from microbial nitrification and denitrification processes. Methane (CH_4) is both produced and consumed by methanogenic and methanotrophic microbes, respectively. Net GHG emissions from terrestrial agroecosystems, such as pasturelands where cattle are grazed, can be mitigated through land management practices that alter soil microbiome structure and activity. As such, pasture management practices can mitigate the effects of cattle production on global climate through field-scale manipulation of the soil microbiome.

In 2015, animal agriculture contributed 57% of Canada's total agricultural GHG emissions, with beef production comprising 40% of this total (Environment and Climate Change Canada, 2017, p. 164). There is much potential to mitigate these GHG emissions within pasture systems. Alemu et al. (2017) highlight the potential for GHG mitigation in beef grazing systems through manipulating diet quality and grazing management practices. For example, increased carbon (C) sequestration in pasture soils can be achieved by managing plant cover and grazing intensity, thereby decreasing net CO_2 emissions and net system effects on global climate. Climate change is increasing the variability of precipitation, which is predicted to compromise pasture plant productivity and beef production in regions reliant upon forage grazing (Sloat et al., 2018). Additionally, consumer interest in sustainably produced beef is continually increasing. Beef

production systems that decrease net GHG emissions could have a competitive market advantage. Reduced pasture plant production, market demands for sustainable products, and the implementation of carbon taxation mean that western Canadian beef producers have both an environmental and economic interest in reducing the impacts of their grazing systems on the global climate.

One management strategy that can alter net GHG emissions is to seed non-bloat forage legumes into grass pastures. Cattle producers grow non-bloat forage legumes to reduce pasture bloat, increase cattle protein uptake, and improve pasture soil quality. The reduction of pasture bloat has an added benefit of concurrently reducing enteric methane emissions, which is one of the largest sources of GHG emissions in beef production systems (Alemu et al., 2017). The higher protein content of forage legumes also provides additional protein to grazing cattle. The improved digestibility of non-bloat legumes increases protein uptake, increasing animal growth and value. Finally, forage legumes improve soil quality by increasing soil nitrogen (N) inputs. Legume N-fixation by *Rhizobia* increases soil N content through root exudates and plant litter inputs, thereby lowering C:N ratios and increasing soil productivity. In addition to local pasture benefits, non-bloat legumes can also mitigate the contributions of beef grazing systems to climate change.

However, the use of non-bloat legumes may also increase N_2O emissions through multiple routes. The presence of legumes in a pasture increases soil N, which also increases rates of N_2O emissions by providing additional N substrates. Increasing dietary protein in pasture-fed cattle also increases the urea-N content of urine excreted onto the soil (Garg et al., 2013). Excretion of N-rich urine provides readily-available N substrates to soil microorganisms and increases the potential for soil N_2O emissions from nitrifiers and denitrifiers. Increased soil N, osmotic stress, and shifts in soil pH caused by urine deposition can all cause shifts in soil microbiome composition and activity. As such, understanding the cumulative impacts of non-bloat legumes on N_2O-producing communities is essential for mitigating the contribution of soil GHG emissions to net grazing system emissions.

Understanding the responses of microorganisms to human activities with regards to GHG production and consumption is essential for achieving an environmentally sustainable future. Agricultural land use influences microbial community composition, thereby altering natural cycles

of C and N transformations in the soil and altering rates of GHG production and consumption. Microorganisms can contribute immensely to the effective mitigation of climate change through improved agricultural management practices, or to its exacerbation if the effects of human activities on microbial GHG production are left unstudied (Cavicchioli et al., 2019). A better understanding of how non-bloat legume introduction alters soil microbial GHG emissions in pastures will help improve agricultural outcomes, mitigating the impacts of cattle grazing on global climate.

The overall goal of this project was to determine how the introduction of non-bloat legumes to a grass pasture grazing system would influence the soil microbes responsible for GHG emissions. As the microbial component of the larger Agricultural Greenhouse Gases Program (AGGP) "Strategies for improving nutritional value of grazed forages: impact on greenhouse gas emissions and carbon sequestration", this project sought to answer how non-bloat legumes affect soil microbial community structure, enzyme activity, and how these factors relate to soil GHG fluxes. In addition, this project sought to answer how varying urine urea-N content affects key N-cycling gene and gene transcript abundances, and how these relate to N_2O emissions. These goals were achieved through a two-year microbial survey of pastures containing novel non-bloat legume forage blends and a laboratory study of pasture soils spiked with ^{13}C and ^{15}N labeled urea.

1.2 Organization of the Thesis

This thesis is presented in manuscript format. Following this introduction and the literature review in Chapter 2, two studies are presented in Chapters 3 and 4. These research chapters begin with a broad, microbial survey of pasture soils analyzing microbial community structure and nutrient cycling activity in relation to GHG emissions in Chapter 3. Chapter 4 specifically examines the effect of varying urine urea-N content on the abundance and expression of N-cycling genes linked to N_2O production, as well as the relative contributions of soil and urea C and N to observed CO_2 and N_2O fluxes.

The goal of Chapter 3 was to determine whether the introduction of non-bloat legumes to a grass pasture influences the structure and activity of the soil microbiome, and whether any observed changes might influence soil GHG fluxes. A pasture with replicated paddocks containing

non-bloat legume and grass mixtures was surveyed throughout the 2017 and 2018 grazing seasons and viable microbial biomass, enzyme activities, and GHG fluxes quantified. In Chapter 4, the effects of varying urine urea N content on N_2O-producing soil microbes is investigated. Soil microcosms were spiked with cattle urine containing dual isotope labeled ($^{15}N^{13}C$) urea and the resulting N_2O and CO_2 fluxes measured for isotope abundance and total flux. Nucleic acids were then extracted, followed by the quantification of archaeal and bacterial N-cycling gene and gene transcript abundances. Gene targets were selected for their known contributions to N_2O emissions. At the end of this thesis, Chapter 5 synthesizes the major findings of the studies and suggests future research directions.

2. LITERATURE REVIEW

2.1 The Nitrogen Cycle

The nitrogen (N) cycle is a large, complex biogeochemical cycle ubiquitous in many diverse environments. N is required for the synthesis of all amino and nucleic acids, meaning that life cannot exist without bioavailable forms. While the atmosphere is 78% nitrogen gas (N_2), this gaseous form is unavailable to most lifeforms. N-fixing bacteria in mutualistic relationships with plants mediate the primary entry point of N into the soil N cycle. From here, N undergoes a complex series of transformations through its range of -3 to +5 oxidative states. While heavily interconnected, these transformations are known collectively as the N cycle. The N cycle is highly diverse and mediated by all three domains of life throughout. The most prominent N-transformations in soils, besides N-fixation and mineralization, are nitrification and denitrification. These processes produce nitrous oxide (N_2O) in soils.

Nitrification (Fig. 2.1) begins with the oxidation of ammonium (NH_4^+) to hydroxylamine by ammonia monooxygenase (*amoA*) enzymes, which is then oxidized to nitrite (NO_2^-) and nitrate (NO_3^-). Incomplete oxidation can occur during nitrification, producing N_2O as a metabolic by-product (Gregorich, Janzen, Helgason, & Ellert, 2015). Denitrification contributes to losses of N through stepwise reductions of NO_3^- to N_2 gas, primarily through facultative anaerobic heterotrophs under suboxic conditions (Gregorich et al., 2015). However, not all N is fully reduced to N_2. The gaseous intermediates nitric oxide (NO) and N_2O are produced throughout the process and may be released to the soil and subsequently, the atmosphere. Denitrification begins with the reduction of NO_3^- to NO_2^-. Next, the enzyme nitrite reductase (*nirK* or *nirS*) produces NO from NO_2^-. Unreleased NO is then reduced to N_2O by nitric oxide reductase (*norB*, *P450nor*) enzymes. N_2O that does not escape to the atmosphere is subsequently reduced by nitrous oxide reductase (*nosZ*) to N_2 gas, completing the cycle. While considered to be an anaerobic process, denitrification has been shown to continue after soils have shifted to aerobic conditions where all denitrification enzymes except nitrous oxide reductase remain active under exposure to O_2 (Baggs, 2011). This

agrees with the findings of Banerjee et al. (2016) who found that N_2O emissions in soils drying from 80% water-filled pore space (WFPS) were several times larger than soils maintained at or wetted to 80% WFPS.

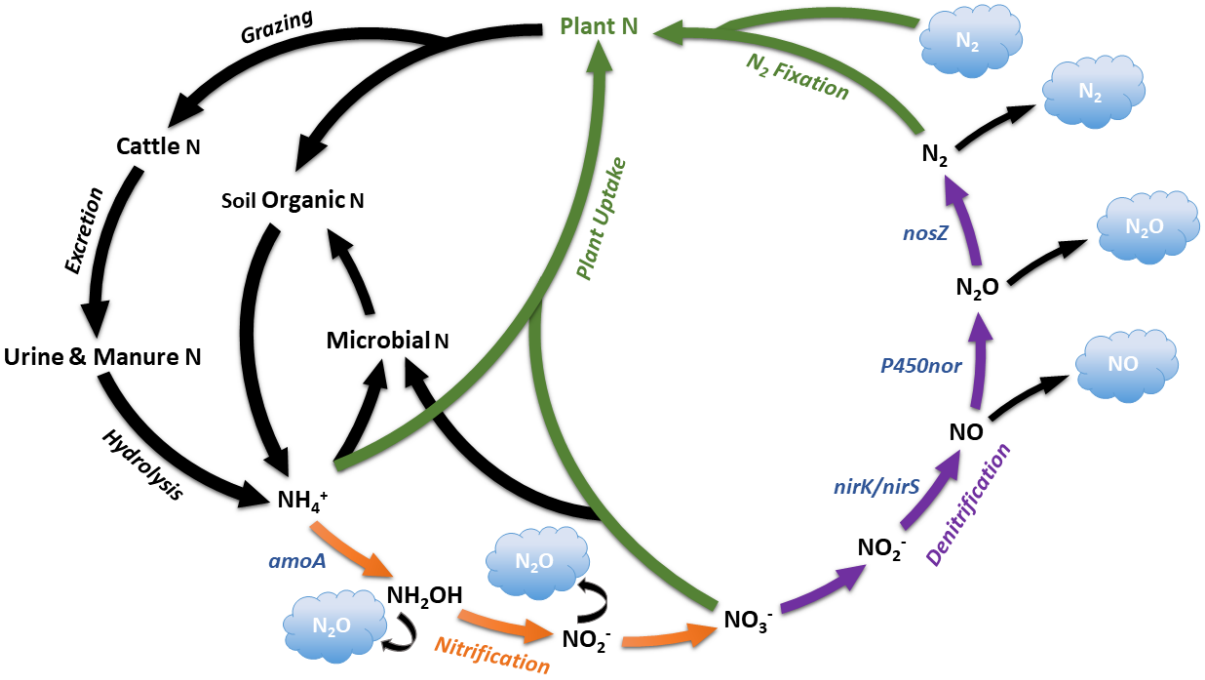

Figure 2.1: The primary components of the N cycle in a pasture grazing system. Potential N_2O-producing and reducing gene targets are shown in blue.

While nitrification and denitrification are the two primary mechanisms of N transformation to gaseous N forms in soils, alternate pathways exist within the cycle. Nitrifier-denitrification encompasses both nitrification and denitrification. This process involves the oxidation of NH_4^+ to NO_2^- which is then reduced to N_2O and N_2, providing a significant source of N_2O emissions in certain nutrient-poor soils (Gregorich et al., 2015). Ammonia oxidizing bacteria (AOB), but not archaea (AOA), are responsible for carrying out this process under increasingly anaerobic conditions, differentiating this process from nitrification-denitrification, which is carried out by multiple co-existing organisms (Gregorich et al., 2015). However, Bakken and Frostegård (2017) point out that the term "nitrifier-denitrification" may be a misnomer when considering the work of Hink et al. (2017), who demonstrated that during this process, >99% of all electron flow was directed to terminal oxidases at any oxygen concentration, that denitrification played no role in sustaining respiratory metabolism, and that electron flow to denitrification increased with NH_4^+

concentration. Rather than being a metabolic process, this AOB-mediated process was interpreted to ensure redox balance at high NH_4^+ concentrations. The contentious nature of this pathway highlights the need for further study of microbial N_2O-producing processes.

Another variation on denitrification is codenitrification, a process whereby NO combines with a co-substrate, such as an amino acid or ammonia, to form a hybrid product. The fungal denitrifying gene *P450nor* will facilitate codenitrification reactions (Shoun, Fushinobu, Jiang, Kim, & Wakagi, 2012). The product of codenitrification depends on the redox state of the N electron donor, with N_2 forming from amines and N_2O from imines or azides (Shoun et al., 2012). This process, found in both fungi and bacteria through different reduction mechanisms, has the potential to produce two N_2O for every NO_3^- reduced, compared to conventional denitrification, which produces just one N_2O for each NO_3^- reduced (Baggs, 2011). However, the occurrence of denitrification and codenitrification in a single organism are not mutually exclusive (Baggs, 2011). Differences in substrate preferences have been demonstrated between fungi (Baggs, 2011), which will have implications on quantities of N_2O produced. Rex et al. (2018) determined that codenitrification contributed >33% of total N_2O emissions in a urine-amended pasture soil, demonstrating that codenitrification can contribute significantly to total pasture N_2O emissions.

Some N_2O-producing shortcuts exist within the soil N cycle. The dissimilatory reduction of nitrate to ammonia (DRNA) was once thought to occur only in highly-reducing environments with high C:N ratios, but has increasingly been found in a wide range of soil environments (Baggs, 2011). Baggs suggests that high-C, transient high-O_2 and high NO_3^- demand conditions may exist within the root rhizosphere, contributing to the production of N_2O through DRNA in terrestrial systems. Annamox, the anaerobic oxidation of ammonia, produces N_2O in wastewater systems. While these processes are not known to be widespread in soil environments, they are nonetheless important sources of N_2O within the N cycle. The discovery of DRNA processes in arable soils (Schmidt, Richardson, & Baggs, 2011) indicates that the potential exists for these processes to be contributors of N_2O in soil systems.

2.2 Pasture System Influences on Soil Microbial Communities

Providing cattle with a diet of non-bloat legumes can increase protein uptake, reduce methane emissions, and in the case of sainfoin and cicer milkvetch, prevent pasture bloat (Dewhurst, Delaby, Moloney, Boland, & Lewis, 2009). Depending on the digestibility of individual legume species, high protein content could lead to inefficient protein utilization and subsequently, high urinary N soil inputs in the form of urea (Dewhurst et al., 2009; Powell & Broderick, 2011). Such differences in digestibility have been described in alfalfa, sainfoin, and cicer milkvetch (Brinkhaus, Bee, Silacci, Kreuzer, & Dohme-Meier, 2016; Loeppky, Hiltz, Bittman, & Frick, 1996), the pasture treatments in this study. The variability in protein utilization and efficiency between forage legumes is further pronounced by unbalanced diets. Garg et al. (2013) report that N use efficiency in cattle increased following ration balancing, resulting in a lower proportion of N excreted in urine and feces. These dietary factors combine to produce differences in urea-N excreted into pasture systems, altering microbial activity and subsequent GHG fluxes from each pasture's soil microbial community.

Pasture plant communities are a primary controller of soil microbial community composition, particularly forage legumes. The presence of legumes in a grass mixture enhanced the bacterial and fungal biomass in the soil compared to a grass monoculture (Chen, Chen, & Marschner, 2008), demonstrating the strong influence of legumes in shaping soil microbial communities. In a microcosm study, the presence of legumes in grass-forb mixtures tended to decrease microbial C:N ratios (Niklaus, Wardle, & Tate, 2006). Consequently, rates of microbial processes such as nutrient cycling and GHG emissions are affected. Soil NH_4^+ concentration, NO_3^- concentration, and potential nitrification rates all significantly increased in the presence of legumes in grass-forb mixtures, as did N_2O emissions (Niklaus et al., 2006). The study's models found that while moisture levels had a significant effect, NO_3^- concentration always explained more variance in N_2O emissions than soil water content. In a grassland study, increasing plant species richness decreased soil N_2O emissions, while N fertilization and an increase in the fraction of legumes present in the plant community increased emissions (Niklaus et al., 2016). Similarly, Bowatte et al. (2018) found legumes in a pasture had higher N_2O emissions compared to plants with high N uptake, such as grasses. However, after urine application, soil mineral N was in excess of this high

plant N demand, creating large N_2O fluxes. As such, the authors attribute the reduced N_2O emissions associated with high plant demand not to simple removal of N from microbial processes by the plant, but to more complex mechanisms such as inhibition of nitrification after application of urine. These studies demonstrate how differing legume pasture compositions can affect the fundamental biological processes responsible for soil GHG fluxes.

Additionally, land treatment alters microbial community abundance. A lack of physical disruption allows greater growth of both bacteria and fungi in soils. Long-term no-till management resulted in the vast majority of fungal biomass accumulating in surface soils (Sipilä, Yrjälä, Alakukku, & Palojärvi, 2012); soils which will have the greatest exposure to urea-N inputs. Likewise, Helgason, Walley, and Germida (2009) report that both fungal and bacterial biomass are higher in surface soils under no-till management regimes. Furthermore, land management practices that disrupt fungal communities, such as tillage, can significantly reduce fungal diversity (Wu, Chellemi, Martin, Graham, & Rosskopf, 2007): fungal diversity and richness remained highest in pasture grass compared to tilled and planted systems. Certain soil fungi are active denitrifiers that lack the ability to fully reduce NO_2^- to N_2, producing N_2O as an end product of denitrification (Higgins et al., 2016; Novinscak et al., 2016). Due to the expected increased presence and diversity of fungi in this pasture system, studying this group of denitrifying and N_2O-producing organisms could be key to understanding GHG fluxes. In addition, tillage can select for specific bacterial denitrifier groups. Domeignoz-Horta et al. (2017) reported that no-till increased the abundance of *nosZ* clade I, which is associated with higher N_2O fluxes than clade II, while inversion tillage increased the diversity of clade II. As such, a pasture system not exposed to tillage may harbor more clade I organisms, providing another biotic explanation for increasing N_2O emissions.

Addition of urea to a soil can cause acidification following nitrification, with long-term, field-scale effects estimated to occur after a decade of exposure (Black, 1992). Many Saskatchewan soils are rich in carbonates, making any such acidification unlikely. However, depending on diet and hydration level of cattle, urea concentration within urine patches may be high enough to create low-pH hotspots following nitrification, resulting in microbial stresses and community shifts. This effect would be especially pronounced in landscape positions where carbonates have been leached out of surface soils by net-downward groundwater flow, such as in

midslope and recharge depression positions. Orwin et al. (2010) found urine application had a significant effect on altering surface soil pH in a 44 d experiment, with the strongest effects occurring in wet soils. The high pH of urine resulted in a drastic range of pH, initially increasing to 8.7 then decreasing to 4.2 (in wet soils) – a net decrease of 1.2 when compared to untreated controls. Soil pH plays a significant part in shaping soil bacterial communities (Lauber, Strickland, Bradford, & Fierer, 2008). Generally, fungi prefer lower pH while bacteria dominate at higher pH through competitive inhibition in arable soils (Rousk, Brookes, & Bååth, 2010). Lower soil pH may favor fungal denitrifier communities over bacterial denitrifiers, increasing rates of N_2O production. A similar relationship exists between AOA and AOB, where AOA gene and transcript abundances decrease with increasing pH while those of AOB increase with pH, creating distinct populations of ammonia oxidizers in acid and neutral soils (Nicol, Leininger, Schleper, & Prosser, 2008). When considering differences in both nitrification kinetics and N_2O production between AOA and AOB, as well as relative contributions of fungal and bacterial denitrification to N_2O production, pH changes from urine deposition can have a significant effect on GHG fluxes.

Nicol et al. (2008) demonstrated that AOA and AOB are selected for by soil pH. Changes in community structure reflected different contributions to ammonia oxidation activity in the form of *amoA* transcripts. While bacterial *amoA* gene copies remained relatively constant across a range of pH 4.5-7.5, archaeal *amoA* gene copies decreased with increasing pH. Archaeal *amoA* transcript abundance decreased with increasing pH, while that of AOB increased. Both bacterial *amoA* gene and transcript abundance were a small portion of AOA (< 3% of gene and 0.03-8.9% of transcript abundance). These findings suggest that AOA and AOB subgroups have distinct physiological characteristics and ecological niches, affecting soil nitrification as a function of pH. However, it remains unknown whether these shifts are a direct function of pH, or due to indirect effects of low pH such as reduced NH_4^+ availability, increased metal toxicities, and element deficiencies (He, Hu, & Zhang, 2012).

In addition to shifting pH, urine addition can influence microbial communities through N supply rate and high NH_4^+ concentrations causing osmotic stress. Urea comprises 52-94% of total cattle urine N (Dijkstra et al., 2013) and is rapidly hydrolyzed into NH_4^+. Urine also contains N as metabolic products, hippuric and uric acids, ammonia, and amino acids (Dijkstra et al., 2013). High NH_4^+ concentrations are known to cause stress-induced metabolism in microbes and inhibit

nitrification activity (Dijkstra et al., 2013; Petersen, Roslev, & Bol, 2004). Monaghan and Barraclough (1992) found that as urinary-N concentrations increased, nitrification was retarded by ammonia toxicity. Orwin et al. (2010) state that the high concentrations of N and/or mixture of chemicals found in urine are much more likely to have faster and stronger effects upon AOB community structure than those found in fertilizers. In this study, the authors found that the degree to which urine affected soil microbes depended upon pre-existing moisture conditions, with the stronger effect in wet soils being attributed to the toxic effects of persistent NO_2^-, and the possibility of interactive effects between NO_2^- and urine with high salt content. Osmotic stresses from salts were conversely strongest in dry soils. While soil dehydrogenase activity was enhanced by urine through the addition of dissolved organic carbon, overall, the application of urine had a negative effect on microbial biomass. This was attributed to a lower activity of N cycling microbes allowing the buildup of toxic N compounds. Further PLFA analysis of these samples by Bertram et al. (2012) confirmed the decrease in microbial biomass. They found urine addition caused an immediate increase in bacterial PLFAs but a decrease in fungal PLFAs. In addition, Gram+:Gram- PLFA ratios decreased, stress PLFA indicators increased, and stress-induced metabolic responses increased. These effects were most pronounced in wet compared to dry soils. Phosphate release attributed to cell lysis in the urine treatments was also observed. Petersen, Roslev, et al. (2004) observed an increase in PLFA stress indicators due to osmotic stresses caused by urine as well. In a meta-analysis of ammonia oxidizer responses to N addition, AOB respond more strongly than AOA and with a few exceptions, AOA did not respond significantly to N fertilization at all (Carey, Dove, Beman, Hart, & Aronson, 2016).

Urine-N concentration was not found to affect N_2O fluxes from a Danish agricultural soil (van Groenigen, Kuikman, de Groot, & Velthof, 2005; van Groenigen, Velthof, van der Bolt, Vos, & Kuikman, 2005). However, increasing levels of ammonia, which is formed from the rapid hydrolization of urea in soils by urease, resulted in a significant increase in nitrification-derived N_2O emissions from German soils (Avrahami, Conrad, & Braker, 2002). In addition, *nirK* denitrifier community composition shifted in conjunction with this increase in N_2O emissions. When soils were treated with dual heavy-isotope labeled urea ($^{15}N^{13}C$) and $^{15}NH_4^+$, N_2O fluxes from urea-treated soils were nearly twice as large as those from NH_4^+-treated soils containing equivalent amounts of N (Ambus, Petersen, & Soussana, 2007). Both high and low concentration urea-N treatments had higher emission factors than the high NH_4^+-N treatment, with high urea-N

being twice that of the high NH_4^+ treatment. Due to unclear isotopic signals prior to day 12, the authors propose that the peaks of N_2O prior to day 12 were due to nitrification of NH_4^+ stimulated by organic constituents in the urine, followed by denitrification becoming the sole source of N_2O after 12 d. Considering the results of Avrahami et al. (2002), it is likely that Ambus et al. (2007) did observe nitrification-derived N_2O emissions in all treatments. This highlights the importance of determining interactions between properties such as water content and urine concentration on individual soils, and how these interactions can result in variable N_2O fluxes between sites. Orwin et al. (2010) found that the addition of urine had a significant effect in increasing the concentrations of dissolved organic carbon (DOC) in both wet and dry soils for 15 d, increasing carbon substrates available to microbes. This coincided with a significant increase in soil NH_4^+, NO_2^-, and NO_3^- concentrations, and subsequently, N_2O emissions, when compared to untreated soils. Nitrite build-up was largest and most persistent in wet, treated soils, possibly due to the combined effects of a high pH and NH_4^+ concentration causing a buildup of toxic ammonia and limiting NO_2^- reduction. Dijkstra et al. (2013) point out that reducing N output from cattle is critical to reducing N_2O emissions and that nutritional experiments affecting urine composition should be integrated with determination of N_2O emissions from urine following deposition on soil. Soil microbial responses to urine are likely to be context-dependent and as such, studying these responses in diverse soil systems is essential to understanding GHG production in sustainable agroecosystems.

In addition to microbial communities being affected by ammonia and NO_2^- toxicity, these communities and their N_2O emissions are strongly affected by WFPS. Van Groenigen, Velthof, et al. (2005) found N_2O emissions were maximized at a WFPS of 65% in a field experiment involving urine application regardless of season or timing of application, with either an increase or decrease 10% WFPS significantly decreasing emissions. This corresponds with the findings of Gleeson et al. (2010), who found gross and net nitrification rates significantly decreased past 65% WFPS. The authors observed a trend of bacterial *amoA* gene abundance increasing around 65% WFPS, an effect that did not exist for archaea, whose *amoA* gene abundance remained steady across all WFPS levels. However, it was found that while both archaeal and bacterial *amoA* community structures shifted with WFPS, only AOB community structure was significantly correlated with nitrification rates. Bacterial nitrifiers play a significant role in controlling nitrification rates in response to changing environmental variables, while AOA numbers remain constant across a wide range of conditions (Carey et al., 2016).

In the above studies analyzing the effects of WFPS on N cycling, WFPS conditions were maintained and hence static. However, in real-world environmental scenarios, soil moisture conditions often fluctuate. Banerjee et al. (2016) conducted a study with the hypothesis that bacterial communities respond to historical WFPS conditions and that the direction of moisture change, rather than just WFPS, is related to community structure, richness, and N_2O emissions. The authors found that under drying conditions, low WFPS resulted in less bacterial richness and greater evenness. Conversely, static, low WFPS resulted in greater richness and diversity. Drying conditions created heterogeneous communities comprised of fewer species; wetting conditions increased community evenness and diversity until 100% WFPS where they dropped substantially. Substrate availabilities and N-cycle transcript abundances of the communities were affected as well, with the greatest differences observed at ~80% WFPS. Abundances of *nosZ*, *norB*, and *hao* transcripts were significantly lower in wetting compared to static and drying treatments, with *nosZ* showing the strongest response to moisture regime although it was not more abundant than *amoA*. This demonstrates the effect of previous soil moisture conditions on nitrifier and denitrifier activity, resulting in substantially larger N_2O fluxes from drying than wetting and static moisture regimes at 80% WFPS.

The effects of shifting WFPS on denitrifier activity may be explained by the observations of Morley, Baggs, Dörsch, and Bakken (2008). In an experiment, soil bacteria cultures were exposed to anaerobic conditions where denitrification was active with reductases (NIR, NOR, and NOS) in a state of equilibrium. When the system was changed to aerobic conditions, all denitrification enzymes remained active, however NOS was more severely inhibited by the presence of oxygen than all other denitrifying enzymes. Under these oxic conditions, N_2O was emitted as the main product of denitrification, rather than N_2 under anoxic conditions. Activity levels of NOS recovered once again as oxygen was depleted. Since the sensitivity of NOS to oxygen appears to be organism-dependent (Morley et al., 2008), the impact of transient WFPS conditions on N_2O production will likely vary from pasture system to pasture system. Additionally, with exception to proteins regulated or degraded following the dissipation of an environmental signal, proteins can outlive the mRNA that signaled their synthesis (Moran et al., 2013). This may explain the larger N_2O fluxes from prokaryotes under drying rather than wetting regimes observed by Banerjee et al. (2016); proteins synthesized under wet conditions conducive to denitrification

would still be active as the soil dries, while microbes exposed to increasing WFPS would have yet to synthesize these enzymes, leading to the observed legacy effects.

Areas of high cattle traffic may result in compaction, which in turn will increase WFPS by evacuating air-filled pores and increasing the proportion of pore space comprised of micropores that are filled with water. Such areas may be near water troughs, or near manmade objects that pique a cow's curiosity. In an incubation study, a strong interactive effect was observed between urine addition and compaction, resulting in a five-fold increase in urine-N N_2O emission factors compared to non-compacted soils 25 d after application (van Groenigen, Kuikman, et al., 2005). Compaction increased bulk density from 1.07 to 1.22 g cm^{-3}, resulting in a final WFPS of 100%. In the corresponding field study (van Groenigen, Velthof, et al., 2005), compaction and urine application had an effect on WFPS similar to doubling the amount of urine applied, with an average increase in WFPS of 4% over 13 d. Soil N_2O emissions increased on average by a factor of 2.2 in compacted vs. non-compacted soils. Although the compaction effect was smaller in the field than in the incubation study, the increase in emission factor was still significant.

2.3 Role of Soil Microbial Communities in Altering Greenhouse Gas Fluxes

Microbial community structure plays a key role in the regulation of soil GHG emissions. Nitrifying archaea have much higher affinities for NH_4^+ in solution at lower concentration, which separates them from AOB in terms of nitrification kinetics (Martens-Habbena, Berube, Urakawa, de la Torre, & Stahl, 2009), giving AOA a competitive advantage in low NH_4^+ environments. Conversely, this provides rapid-growing AOB the advantage at higher NH_4^+ concentrations. Di et al. (2009) found a significant positive correlation between bacterial *amoA* gene copy number and NO_3^- concentration in soils treated with a high urine-N substrate. Bacterial *amoA* transcripts increased 177 times compared to the control upon urine addition, whereas archaeal *amoA* transcription remained unchanged. As a result, it appears that AOB will dominate over AOA in N-rich systems and increase nitrification rates if communities are not influenced by other environmental factors, such as pH or ammonia toxicity. Varying abundances between AOA and AOB populations will therefore alter NO_3^- supply, subsequently also controlling rates of denitrification and N_2O production. Nitrification mediated by AOA has been shown to produce half the N_2O emissions per unit NO_2^- produced by AOB (Hink, Nicol, & Prosser, 2017).

Additionally, the study found AOB dominated N_2O production in NH_4^+-amended soils, contributing 81-86% of the total emissions, while the contribution of AOA was negligible. In unamended soils, AOA contributed half of total N_2O emissions via mineralization of organic-N while AOB did not contribute to the flux. However, the total N_2O produced by the AOA dominated system was 10-14% that of the AOB emissions. The relative contributions of AOA and AOB to nitrification under changing conditions, despite the larger abundance of AOA, are therefore of great interest when analyzing N_2O fluxes from pastures.

In a study assessing N_2O emissions across arable soils, Domeignoz-Horta et al. (2017) found that while abiotic soil properties best explained basal N_2O fluxes, biotic factors best explained variation of high fluxes. Up to 68% of the variation causing high N_2O fluxes was explained by the diversity of *nosZ* and abundance of nitrifying and denitrifying microbial communities and their interactions. The study showed that the higher diversity of clade II *nosZ* organisms, rather than clade I, was concomitant with lower N_2O fluxes. Higher clade II abundance enhances a soil's N_2O sink capabilities due to a higher proportion of *nosZ-II* organisms being nondenitrifying N_2O reducers (Graf, Jones, & Hallin, 2014; Hallin, Philippot, Löffler, Sanford, & Jones, 2018). Since clade II organisms are more sensitive to environmental conditions than clade I (Domeignoz-Horta et al., 2017), relative abundances of each clade are important to consider when comparing N_2O fluxes between soils. Fluxes of N_2O are negatively correlated with *nosZ* transcripts (Németh, Wagner-Riddle, & Dunfield, 2014), showing that expression of this gene plays a key role in reducing N_2O emissions in soil systems. Likewise, Domeignoz-Horta et al. (2017) reason that *nosZ* clade II is a strong predictor of N_2O:N_2 ratios since 51% of observed clade II organisms lack either *nirK* or *nirS*, thereby only contributing to N_2O consumption but not production through denitrification (Graf et al., 2014; Hallin et al., 2018). Additionally, *nirS* has a higher co-occurrence with *nosZ* than *nirK* (Graf et al., 2014; Hallin et al., 2018), and studies have found *nirK* but not *nirS* correlates positively with N_2O production (Clark, Buchkina, Jhurreea, Goulding, & Hirsch, 2012; Di, Cameron, Podolyan, & Robinson, 2014). Bacteria which possess both *nir* genes exhibited differential expression patterns, suggesting different ecological roles for each of these genes (Wittorf, Jones, Bonilla-Rosso, & Hallin, 2018).

While denitrification is commonly thought of as a bacterial process, fungi are also capable of denitrification and can be a significant source of N_2O in grassland soils (Laughlin & Stevens,

2002; Rex et al., 2018). Many fungi produce the N_2O-producing, codenitrifying enzyme P450nor but lack the ability to reduce N_2O to N_2 gas (Novinscak et al., 2016). Higgins et al. (2016) detected *P450nor* in all fungal isolates producing N_2O, but failed to consistently detect fungal nitrite reductase (*nirK*, a common indicator gene in denitrification activity) in the same isolates. By contrast, Novinscak et al. (2016) detected *nirK* in all N_2O-producing isolates. In a study analyzing the contributions of codenitrification in a urea-amended grassland soil, Rex et al. (2018) demonstrated that fungi play a significant role in N_2O production in urea-rich soil environments, such as urine patches. Chemical inhibition of fungi reduced total N_2O emissions by at least 66% and codenitrification-derived N_2O emissions by 42%. Soils treated with fungal inhibitors showed a general trend of lower total N_2O and codenitrification-derived N_2O emissions compared to control soils and soils containing only bacterial inhibitors.

2.4 Review of Methods in Environmental Microbiology

Phospholipid fatty acid (PLFA) analysis is a widely used, highly useful tool for estimating microbial abundance and community structure changes in soil. As major constituents of bacterial and fungal cell membranes, variations in fatty acid synthesis between microbial groups can be used to establish community fingerprints in conjunction with multivariate statistical analysis (Drenovsky, Elliott, Graham, & Scow, 2004). Analysis of PLFAs is highly reliable due to PLFA specificity to living organisms, high consistency among replicates, and strong differentiation between sample treatments (Drenovsky et al., 2004). Community fingerprints based on extracted phospholipid biomarkers are established by comparing gas chromatograph (GC) peaks to a library of retention times for known fatty acids. Ratios of known PLFA biomarkers can be used to estimate community composition of broad microbial functional groups, measure community shifts in response to a change in soil conditions, and provide a proxy for estimation of microbial biomass (Willers, Jansen van Rensburg, & Claassens, 2015). However, several precautions must be considered. Conversion factors of biomarker PLFAs to microbial biomass vary widely (Willers et al., 2015). Although PLFAs degrade rapidly upon cell death, making them a high resolution indicator of temporal changes in microbial activity, rates of degradation can shift under varying environmental variables, including enzyme inhibition and changing temperatures (Frostegård, Tunlid, & Bååth, 2011). In addition, biomarkers used to identify specific groups may belong to

multiple microbial taxa due to known biomarker libraries being compiled from pure laboratory cultures (Frostegård et al., 2011). As a result, environmental samples can contain multiple groups that possess a biomarker thought to belong to a single broad functional group, introducing the potential for misidentification (Willers et al., 2015). However, of the 67 biomarkers commonly used, only eight are known to belong to multiple taxa, and this overlap can usually be eliminated based on environmental context (Willers et al., 2015). The detection of stress indicators may equally be caused by community shifts. This is due to having no way at present of differentiating between altered membrane compositions and altered species compositions (Frostegård et al., 2011). As a result, the presence of environmental stressors and the concentrations of biomarkers relative to other known biomarkers of the same functional group must be considered when interpreting PLFA results (Frostegård et al., 2011).

Extracellular enzyme assays are used as a measure of soil nutrient cycling capabilities and microbial metabolic activity. The activity of the exoenzyme β-glucosidase (βG) is correlated with microbial metabolism and rates of mass loss from plant litter in terrestrial ecosystems (Sinsabaugh & Follstad Shah, 2012). This cellulolytic enzyme is involved in the hydrolysis of cellulose, playing a major role in the degradation of soil carbohydrates (Eivazi & Tabatabai, 1988) where most new carbon is introduced as plant tissue. The glucose derivatives released by βG are believed to be an important energy source for soil microorganisms (Eivazi & Tabatabai, 1988). As such, βG makes a good indicator of heterotrophic soil microbial metabolism, respiration, and C cycling activity.

N-acetyl-β-D-glucosaminidase (NAG) is involved in C and N cycling in soils. It hydrolyzes amino sugars from chitin, a major structural component found in insects and fungal mycelia (Ekenler & Tabatabai, 2002). Amino sugars are one of the major sources of mineralizable N in soils and constitute 5-10% of the organic N in most surface soils (Ekenler & Tabatabai, 2002). Chitin is considered one of the most abundant biopolymers in nature, making it an important organic C and N pool in soils (Ekenler & Tabatabai, 2002). Total NAG activity reflects C and N mineralization rates through transformations of organic molecules to bioavailable nutrients.

Phosphatases are a broad group of phosphorus (P) cycling enzymes which release phosphates from organic phosphoesters, anhydrides, and P-N bonds (Eivazi & Tabatabai, 1977). Among the phosphomonoesterases, there are two broad groups: acid and alkaline phosphatases.

These groups vary in their optimum pH and therefore their predominance in acid and alkaline soils, with optimum pHs of approximately 6.5 and 11 for acid and alkaline phosphatase, respectively (Eivazi & Tabatabai, 1977). Phosphatase activity generally has an inverse relationship with environmental P availability (Sinsabaugh & Follstad Shah, 2012). Plants, in addition to microbes, possess the ability to synthesize acid phosphatase, releasing it to the environment through root exudation and mobilizing environmental P for uptake (Duff, Sarath, & Plaxton, 1994). The release of organic phosphates by phosphatase provides a key ecosystem function through the cycling of organic P into a readily available form.

Substrates labeled with a stable isotope are used to track metabolites through a biological system. This approach is known as stable isotope probing (SIP). Relative contributions of the substrate to metabolites can be determined by comparing the initial isotope abundance in the substrate to the abundance in the recovered target analyte (Ambus et al., 2007; Cabral, Capanema, Gebert, Moreira, & Jugnia, 2010). Target analytes include respired gases, such as CO_2 and N_2O, and biomolecules, such as PLFAs and deoxyribonucleic acid (DNA).

Source partitioning of N_2O isotopomers is used to quantify relative contributions of N_2O flux sources. This method can quantify ratios of total N_2O from bacterial denitrification and nitrification or fungal denitrification sources based on the location of the ^{15}N isotope on the N_2O molecule at natural abundance levels. This is achieved by comparing site preference (SP) with sample $\delta^{18}O$, where SP is the abundance of $\beta^{15}N_2O$ (^{15}N-N-O) subtracted from $\alpha^{15}N_2O$ (N-^{15}N-O). The principle is based on the observation that N_2O produced by hydroxylamine oxidation has a higher SP than N_2O produced by NO_2^- reduction in laboratory studies of model organisms, allowing for quantitative allocation of nitrifier and denitrifier fluxes (Sutka et al., 2006). The site mapping approach attempts to simultaneously quantify N_2O fractionation and mixing processes based on SP and $\delta^{18}O$ (Lewicka-Szczebak, Augustin, Giesemann, & Well, 2017). Two context-dependent models are used to estimate N_2O sources: the reduction-mixing model, where bacterial denitrifier N_2O is partially reduced then mixed with unreduced nitrifier and fungal denitrifier N_2O; and, the mixing-reduction model, where bacterial denitrifier and nitrifier/fungal denitrifier N_2O mixes, then the mixture is partially reduced (Lewicka-Szczebak et al., 2017). Nitrifier and fungal denitrifier N_2O overlap using the SP-$\delta^{18}O$ mapping approach, resulting in context-dependent interpretations. For example, nitrifier N_2O would only be present in an oxic environment, and

fungal denitrifier N_2O would likely outweigh nitrifier N_2O in a low NH_4^+, high NO_3^- environment (Lewicka-Szczebak et al., 2017). As a result, differentiating between these two sources is difficult in a medium with transitioning oxic and anoxic conditions, such as soils.

Organism DNA is commonly targeted when determining the functional diversity of a system through real-time quantitative polymerase chain reaction (qPCR). Whereas phylogenetic diversity deals with evolutionary lineages and relationships between microorganisms (genetic diversity), functional diversity deals with microbial physiology and ecology (Madigan, Martinko, Bender, Buckley, & Stahl, 2015, p. 434). Functionally similar organisms can exist between phylogenetically diverse groups due to convergent evolution and horizontal gene transfer (Madigan et al., 2015, p. 435). One such example is AOA and AOB, which are in two separate domains and therefore phylogenetically diverse, but share the same ecological function as nitrifiers. The 16S rRNA gene is the most commonly used target gene for phylogenetic diversity in archaea and bacteria. 16S gene sequences are used to construct phylogenetic trees and establish community diversity. In contrast, functional gene markers are used to quantify key ecological enzymes and can be useful in revealing important microbial guilds that are not dominant in number and are difficult to detect using 16S sequencing methods (Junier et al., 2010). An example of a functional gene marker is *amoA*, which encodes the enzyme that oxidizes ammonia to hydroxylamine, but is carried between two phylogenetically distinct groups: AOA and AOB (Junier et al., 2010).

The persistence of extracellular DNA in soils can decrease temporal resolution of active populations by harboring DNA from organisms that are no longer viable in that environment. Upon entry into the environment, DNA can persist by binding to soil minerals and humic substances through cation bridging (Levy-Booth et al., 2007). For example, DNA protected by humic acids required 100 times more DNase to inhibit transformation than free DNA (Crecchio & Stotzky, 1998). This study demonstrated one soil mechanism protecting DNA against nucleases in soils, thereby preserving DNA from dead organisms. Measuring functional gene abundance therefore might not accurately represent the genetic potential of a soil community. Furthermore, the detected presence of a gene does not necessarily represent its activity since the organism could be dormant or growing, but not carrying out the targeted genetic function.

Messenger ribonucleic acid (mRNA) provides an alternative to measuring functional gene abundance. Strands of mRNA serve as copies of the genetic DNA blueprint to a functional protein and indicate the need for an organism to carry out a function. It has a very rapid turnover rate, providing high temporal resolution. Since mRNA is only expressed when a microbe needs to synthesize an enzyme in response to stimuli, it is indicative of organism activity. However, the use of this nucleic acid as an indicator of microbial activity also has some limitations. Post-translational modifications of proteins synthesized from mRNA "alter the structure/function relationship and impact protein complex formation, enzyme catalysis, and other biomolecule interactions" (Cain, Solis, & Cordwell, 2014), as well as regulate protein functions by altering protein activity and cellular location (Seo & Lee, 2004). Such modifications include phosphorylation, acetylation, methylation, and many other transformations of amino acids carried out by both prokaryotes and eukaryotes. Modifications occur in response to metabolic and environmental stimuli, with fast switching regulatory systems allowing much faster adjustment to external stimuli than gene expression (Cain et al., 2014). As an example, Lycus et al. (2017) found a mismatch between genetic potential and N_2O reduction in 23% of denitrifying isolates, which was attributed to transcriptional and metabolic regulation. Under dynamic environmental conditions, mismatches between protein and mRNA levels can occur due to proteins outliving the mRNA molecule that signaled their synthesis; the half-life of bacterial protein is about two orders of magnitude longer than that of mRNA (Moran et al., 2013).

An organism may use post-translational regulation or targeted degradation of the protein to prevent the protein from functioning after the environmental signal has dissipated (Moran et al., 2013); this creates a disconnect between mRNA and enzyme activity that must be considered. Environmental conditions can directly affect the synthesis of an enzyme as well, such as the inhibitory effect of low pH on the synthesis of functional NOS enzymes, even though synthesized NOS is functional at low pH (Bakken & Frostegård, 2017). Therefore, mRNA is not necessarily a direct indicator of microbial activity, but rather a good indicator the direction of community responses to environmental stimuli. In order to quantify samples in the lab, mRNA extracts are transcribed to complementary DNA (cDNA) by reverse transcriptase which is then used for qPCR analysis (Thies, 2015). Although more challenging, mRNA quantification measures the responses and anticipated activity of microbial communities and supplements the community potential measured by DNA analysis.

3. A Survey of Microbial Controls on Soil N_2O Emissions in a Legume Pasture Grazing System

3.1 Preface

Cattle producers may introduce non-bloat legumes to grass pastures to increase cattle protein uptake, reduce pasture bloat, and improve soil quality. How non-bloat legume introduction affects the community composition, nutrient cycling activities, and greenhouse gas (GHG) emissions by soil microbes remains unclear. An understanding of how new non-bloat legume plant cover and the subsequent increase of nitrogen (N) in pasture soils influences microbial community structure, activity, and respiration will improve efforts to minimize GHGs derived from pasture soils. This chapter surveys the microbial composition and activity of pasture soils containing non-bloat legumes over two grazing seasons. Environmental and biological factors which influence soil microbial abundance, community structure, and activity within non-bloat legume pastures were determined and compared to soil GHG emissions. By analyzing how microbial communities relate to GHG emissions in non-bloat legume pastures, this study improves the understanding of practices which can limit net GHG emissions from pasture systems.

3.2 Abstract

Non-bloat legumes are grown in grass pastures to increase the protein uptake and decrease the enteric methane emissions of grazing cattle. The presence of these N-fixing legumes can also improve soil quality through the addition of N directly from plant exudates and residues, and indirectly through animal excretions. However, the effect of non-bloat legumes on soil microbial populations and their role in GHG emissions in legume-grass pastures remains unclear. The objective of this study was to determine whether the presence of non-bloat legumes alters the soil microbial structure found in a grass pasture, and whether these potential changes translate to an increase in soil GHG emissions. To answer this, soil microbial abundance and community

structure, nutrient cycling activities, and GHG fluxes were measured throughout two grazing seasons in two non-bloat legume-grass and one grass-alfalfa pasture treatments. Pastures containing mostly meadow brome (*Bromus biebersteinii*) with some alfalfa (*Medicago sativa*) were sod-seeded with common sainfoin (*Onobrychis viciifolia*) and Veldt cicer milkvetch (*Astragalus cicer*) treatments, while a control treatment of dominantly grass plus some alfalfa was not sod-seeded with non-bloat legumes. While discernible differences in microbial community composition between non-bloat legume and grass pasture control soils were found, the majority of observed community differences were due to seasonal changes in environmental conditions. Structural equation modeling (SEM) suggested potential links between cicer milkvetch pastures, AMF abundance and nitrous oxide (N_2O) in 2017. Microbial community structure was distinct between plant treatments and was correlated with soil nitrate (NO_3^-) content, but seasonal and spatial variability accounted for most observed differences within microbial communities. While no differences in mean daily N_2O emissions were found between pastures, cicer milkvetch tended to have the largest N_2O fluxes. However, this potential for higher soil N_2O emissions in cicer milkvetch pastures must be weighed against the expected reductions in enteric methane emissions from cattle grazing these pastures to fully understand the net effects of using cicer milkvetch.

3.3 Introduction

Non-bloat legumes are known to reduce enteric methane emissions by reducing pasture bloat in cattle. Increased protein content and digestibility of non-bloat legumes can also benefit cattle by increasing protein uptake. However, the presence of non-bloat legumes in a grazing system has the potential to increase N_2O emissions through multiple routes. First, the increased protein in non-bloat legumes may increase cattle urinary N content. Excretion of N-rich urine provides readily-available N to soil microorganisms and increases the potential for soil N_2O emissions from nitrifiers and denitrifiers in urine patches. The concentration of cattle urinary N has a positive linear relationship with dietary N intake (Dijkstra et al., 2013), increasing the likelihood of enhanced N_2O emissions due to the high N content of the forage in non-bloat legume pastures. Second, in a study analyzing soils in grass and legume mixed communities, the presence of legumes within the plant community shifted soil microbial community structure and increased bacterial, fungal, and total microbial biomass (Chen et al., 2008). Third, biological N-fixation by legumes decreases soil carbon:nitrogen (C:N) ratios which can lead to increased N_2O emissions

from mineralized N. Combined with lower C:N ratios, urine deposition events on pastures containing legumes resulted in larger N_2O fluxes than grass pastures (Bowatte et al., 2018). As such, understanding the cumulative impacts of non-bloat legumes on soil microbial communities improves strategies for mitigating the contribution of soil GHG emissions to net grazing system emissions.

Legume introduction to plant communities alters soil N dynamics and soil microbial community composition. Legumes form symbiotic relationships with *Rhizobia* bacteria to fix atmospheric N_2 into plant-available NO_3^-. Through biological N-fixation, legumes increase soil NO_3^-, nitrification rates, and N_2O emissions, but this effect is mitigated by the presence of non-legume species in mixed communities (Niklaus et al., 2006). Where legumes are present alongside grass species, N_2O emissions increase with the fraction of legume biomass (Niklaus et al., 2016). In addition to soil N, legumes can have a dominant effect on soil microbial community composition in mixed legume-grass plant communities. Plant communities containing legumes have been shown to increase microbial biomass. For example, bacterial and fungal biomass in legume-grass mixed communities was higher than in grass communities (Chen et al., 2008). Additionally, legumes played a dominant role in shaping soil microbial community structure since legume-grass communities had a microbial community composition similar to legume monocultures (Chen et al., 2008). In pasture systems, where urine deposition from cattle is expected, N_2O emissions may be further exacerbated under legume-containing vs. grass-only forage stands. For example, soils under pasture legumes treated with urine applications emitted higher rates of N_2O than grass, possibly due to the lower soil N uptake of N-fixing legumes compared to grasses (Bowatte et al., 2018). Thus, legumes have a strong influence on both soil microbial community composition in mixed plant communities and net N_2O emissions, particularly in pastures where N-rich urine is excreted into the soil.

Phospholipid fatty acid (PLFA) analysis is used to evaluate soil microbial community structure and abundances by quantifying the phospholipids present in the cell membranes of bacteria and fungi. Unique PLFA biomarkers belonging to Gram-positive bacteria (G+), Gram-negative bacteria (G-), actinobacteria, arbuscular mycorrhizal fungi (AMF), and saprotrophic fungi (Willers et al., 2015) are used to identify broad functional groups. Stress indices are calculated based on the ratio of known stress-induced PLFA biomarkers to their precursor phospholipid in

G- bacteria (Grogan & Cronan, 1997). Differences in functional group biomass and abundances can be compared to identify treatment effects. Identified PLFAs also provide a proxy of microbial community structure when PLFA abundances are converted to a dissimilarity matrix and compared using multivariate ordination methods. This allows comparison of microbial community structures between treatments which may provide insights into pasture GHG emissions. The rapid decomposition and turnover of PLFAs in soil means that only viable microbial biomass is measured. However, PLFA turnover rates vary between soil environments and changes should be interpreted with this consideration of temporal resolution (Frostegård et al., 2011).

Microbial extracellular enzyme analyses can be used to quantify nutrient cycling of soil C, N, and phosphorus (P). They provide indication of the potential soil nutrient turnover rates under ideal conditions, and can indicate microbial nutrient demands. Since extracellular enzyme production has a high energy and material cost, and control is lost once the enzyme is secreted from the cell, enzyme transcription is closely regulated at the cellular level (Sinsabaugh & Follstad Shah, 2012). Transcription is linked to environmental signals, such as consumption of substrate by the cell, indicators of toxicity, or detection of quorum signals from other cells (Sinsabaugh & Follstad Shah, 2012). Once secreted into the soil environment, extracellular enzymes degrade organic-bound materials into forms viable for cellular uptake. Thus, soil enzymatic activities can provide an indication of microbial nutrient demand and comparisons between treatments may be made. Potential correlations between microbial nutrient cycling activity and GHG emissions might be observed, providing explanatory power for possible treatment differences in GHG emissions.

Structural equation models (SEMs) provide a powerful statistical approach for analyzing complex datasets with multiple intercorrelated variables (Lamb, Shirtliffe, & May, 2011), such as interactions between plant treatments, soil microbial communities, and environmental conditions. Since SEMs seek to examine networks of causal relationships rather than focusing on net effects, SEMs allow deeper insights into ecological patterns and processes (Grace, 2006). In SEM, an initial path model based on theoretical knowledge implies variances and covariances which are then compared to actual data variances and covariances. In the case of an inadequate model fit, additional pathways are suggested that could improve model fit. By adding new pathways, SEM becomes more exploratory than confirmatory and can lead to novel biological hypotheses for future exploration (Lamb et al., 2011).

The goal of this study was to determine whether the introduction of non-bloat legumes to a grass-alfalfa pasture affects soil microbial community structure and activity, and whether these potential effects influence GHG emissions. It was hypothesized that introducing non-bloat legumes to a grass-alfalfa pasture would shift soil microbial community composition and extracellular enzyme activity. To answer this, a grass-alfalfa pasture was divided into paddocks and sod-seeded in triplicate with two non-bloat legume treatments and a grass-alfalfa control. The paddocks were surveyed for PLFA abundances, enzyme activities, and GHG emissions throughout two grazing seasons. Enzyme, GHG, and PLFA data were analyzed against soil nutrient and environmental data to find potential net influences resulting from non-bloat legume introduction to grass-alfalfa grazing systems.

3.4 Materials and Methods

3.4.1 Pasture layout and field sampling design

Non-bloat legumes were introduced to an existing grass-alfalfa pasture near Lanigan, SK (51.863, -104.893) to investigate their effects on soil microbial communities and GHG emissions. The site features Black Chernozemic soils which developed on glacial till. The existing pasture consisted mostly of *Bromus biebersteinii* (meadow brome) grass and small amounts of *Medicago sativa* (alfalfa). Two non-bloat legumes, *Onobrychis viciifolia* (common sainfoin) and *Astragalus cicer* (Veldt cicer milkvetch) were sod-seeded into each of three replicate 300x75 m (2 ha) paddocks in 2015 (Fig. A1). Control paddocks without sod-seeded non-bloat legumes were established in triplicate. Based on site topography (Fig. A1), mid-slope positions were chosen as the representative sampling position for the soil microbial community present within each paddock. Four steers were introduced to each paddock in late June and grazed for 21 consecutive days in 2017 and 49 consecutive days in 2018 (Fig. 3.1). Pasture plant production was lower in 2017 due to low precipitation throughout the year, resulting in a shorter grazing period than 2018. Pasture weather conditions, forage yield, and forage composition data are available in Tables A1-A3.

3.4.2 Soil sample collection and analysis

In order to capture seasonal variation in pasture conditions, soil samples were collected five times throughout the season coinciding with GHG sampling (Fig. 3.1). The first sampling date

of each year occurred before cattle were introduced to the paddocks. A shorter grazing period in 2017 meant that only one sampling date fell within the grazing period, whereas two sampling dates fell within the 2018 grazing period. Three soil cores were sampled 30 cm from each mid-slope GHG sampling chamber in a triangular pattern around the chamber using an ethanol-sterilized, 3.2 cm diameter JMC Backsaver soil probe (JMC Soil Samplers, Newton, IA). The top 10 cm of the three cores was combined and stored on ice in a cooler for transport to the lab and stored at 4 °C overnight. The following morning, samples were sieved using sterilized 2 mm sieves and stored at -20 °C awaiting further analysis.

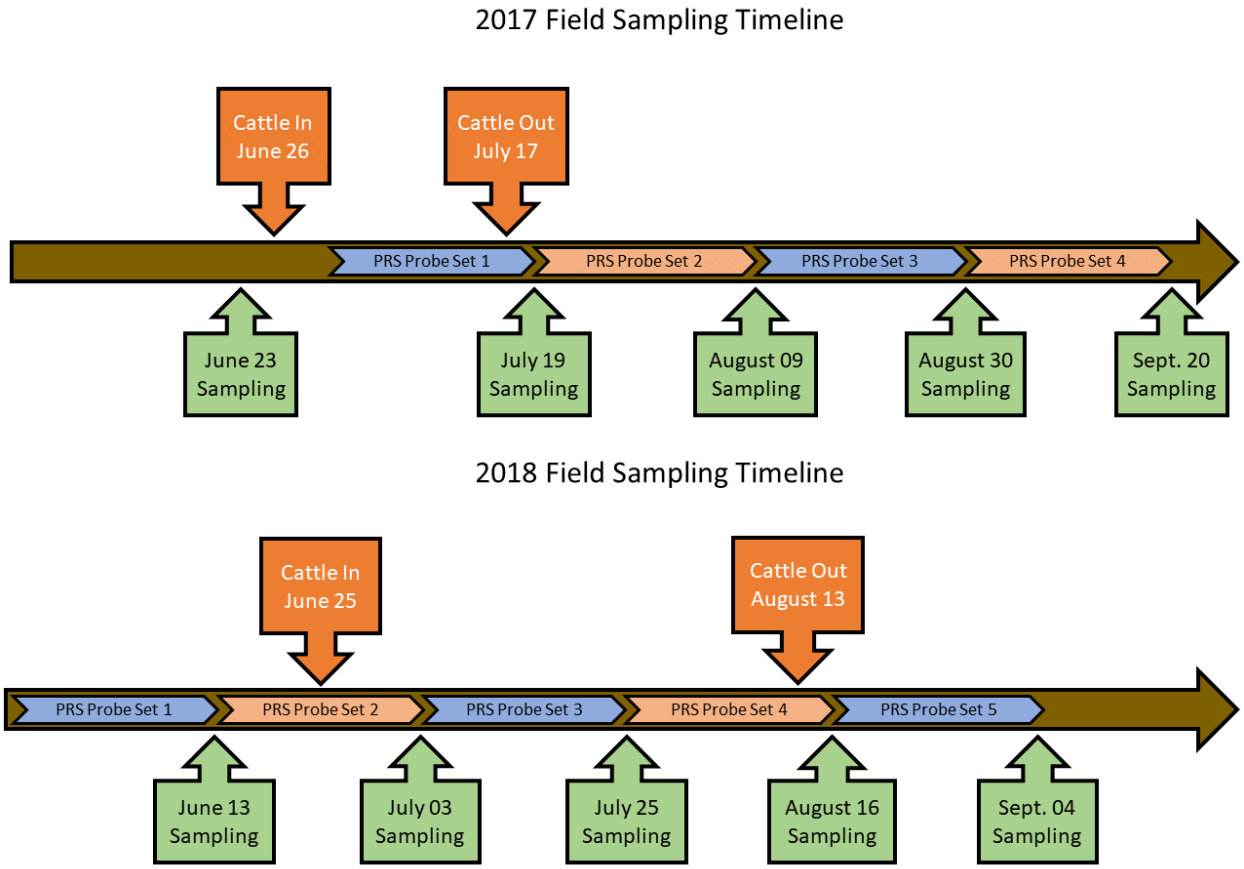

Figure 3.1: Timeline of 2017 and 2018 field microbial and greenhouse gas (GHG) sampling events and PRS (plant root simulator) probe burial.

3.4.2.1 Soil biological, chemical, and physical properties

Microbial extracellular enzyme activity was quantified to determine rates of soil nutrient cycling. β-glucosidase (βG), N-acetyl-β-D-glucosaminidase (NAG), and acid phosphatase (AP) were chosen to represent C (cellulose), C and N (chitin), and monophosphate cycling rates, respectively. A combination of tube incubation and microplate readings of sample 4-methylumbelliferone (4-MUB) fluorescence as described by Hargreaves and Hofmockel (2015) and Bell et al. (2013) was used. Briefly, 1.0 g of soil was blended on high with 125 mL maleate buffer (pH = 7.0) for 30 s to form a slurry then transferred to a beaker on a stir plate. While slurry homogeneity was maintained by a magnetic stir bar, 1.8 mL of slurry was transferred to a 5 mL tube. 450 μL of either 4-methylumbelliferyl-α-D-glucopyranoside for βG; 4-methylumbelliferyl N-acetyl-glucosaminide for NAG, or; 4-methylumbelliferyl phosphate salt for AP (Sigma-Aldrich Corp., St. Louis, MO) was added to respective assay tubes. Tubes were shaken laterally at 142 rpm on a rotary shaker for 3 h at 28 °C. Following centrifugation at 2000 rpm for 5 min, 4-MUB fluorescence was measured on a FilterMax F5 microplate reader (Molecular Devices LLC, San Jose, CA) at 360 nm excitation and 465 nm emission wavelengths.

Soil inorganic nitrogen, in-situ soil inorganic N fluxes, dissolved organic carbon (DOC), total dissolved nitrogen (TDN), pH, and soil moisture were measured to provide potential explanatory power for microbial data. Soil NH_4^+ and NO_3^- was extracted using 2 mol L^{-1} KCl solution (Maynard, Kalra, & Crumbaugh, 2008) and quantified using an AA3 autoanalyzer (SEAL Analytical Inc, Mequon, WI). In-situ soil NH_4^+ and NO_3^- fluxes were measured using plant root simulator probes (PRS probes, Western Ag, Saskatoon, SK). Two cation and two anion exchange probes were buried alongside GHG chamber collars for the three-week period prior to microbial sampling dates (Fig. 3.1). Probe-bound NH_4^+ and NO_3^- was eluted and quantified by Western Ag. Soil DOC and TDN was extracted using the methods of Chantigny and Angers (2008) with slight modifications. Soil slurry was shaken in in 50 mL plastic tubes rather than stirred with glass rods in beakers to minimize the disruption of soil colloids. Slurries were vacuum filtered through 0.45 μm filters. Filtrate DOC and TDN was quantified using a Shimadzu TOC-V CPN (Shimadzu Corporation, Tokyo, Japan). Soil pH was determined by shaking 20 mL of 0.01 mol L^{-1} $CaCl_2$ with 10 g of air-dried soil for 30 min. Solution pH was measured after shaken samples stood for 1 h.

3.4.2.2 Microbial community structure and abundance

Soil PLFAs were identified and quantified to determine microbial community composition and functional group abundance within each treatment using methods described by Helgason, Walley, and Germida (2010). First, frozen soils were freeze-dried for 48 h, then 4.0 g of freeze-dried soil was shaken with 19 mL of modified Bligh and Dyer (1959) extractant solution described by White et al. (1979) containing 50 mmol L^{-1} phosphate buffer. Phospholipids were isolated using 500 mg silicon fractionation columns (Bond Elut, Agilent Technologies, Santa Clara, CA) then methylated for gas chromatograph (GC) analysis. The resulting fatty acid methyl-esters (FAMEs) were quantified on a Bruker 436 GC flame ionization detector (FID) (Bruker Corporation, Billerica, MA) then identified by comparing retention times against a library of known FAME retention indices. Known PLFA biomarkers were used to identify G+ and G- bacteria, actinobacteria, fungi, AMF, and two stress indices (Helgason et al., 2010; Willers et al., 2015). G+ biomarkers consisted of 14:0 iso, 15:0 iso, 15:0 anteiso, 16:0 iso, 17:0 iso, and 17:0 anteiso. G- biomarkers consisted of 16:1 ω9c, 16:1 ω7c, 17:0 cyclo ω7c, 18:1 ω9c, 18:1 ω7c, 19:0 cyclo ω7c, and 19:0 cyclo ω9c. Soil AMF abundance was determined by the presence of 16:1 ω5c. Actinobacteria were evaluated based on 16:0 10-methyl and 18:0 10-methyl abundance. Fungal abundance was determined by 18:2 ω6c abundance. Two G- stress indices, Stress 1 and Stress 2, were determined by the ratio of 17:0 cyclo ω7c to 16:1 ω7c and of 19:0 cyclo ω7c to 18:1 ω7c, respectively. The ratio of fungi to bacteria (Fungi:Bacteria ratio) was calculated by comparing total 18:2 ω6c to the sum of G+, G-, and actinobacterial PLFAs.

3.4.3 Soil greenhouse gas fluxes

Pasture GHG fluxes were sampled and quantified by the Prairie Environmental Agriculture Research Laboratory (PEARL, University of Saskatchewan, Saskatoon, SK). At the start of gas sampling, chamber lids were sealed onto chamber collars. Chamber headspace was sampled in ten-minute intervals over a 30 min period. Gas samples were drawn using 20 mL syringes and transferred immediately to evacuated 12mL Exetainers. Gases were identified and quantified on a SCION 456 GC (SCION Instruments, Livingston, Scotland) with multiple detectors: CO_2 using a thermal conductivity detector (TCD) and N_2O using an electron capture detector (ECD). The sampling date soil GHG flux rate was then determined by using R package 'HMR' (Pedersen, 2017) to calculate changes in chamber gas concentration.

3.4.4 Statistical analyses

All statistical analyses were performed using R v3.6.0 (R Core Team, 2019). A general linear mixed effects model (Bates, Maechler, Bolker, & Walker, 2015) was fit to test for treatment differences in GHG fluxes, PLFA, enzyme activity, and soil nutrients, followed by Type-III ANOVA F tests (Fox & Weisberg, 2019) and contrasts of estimated marginal means (Lenth, 2020) using the Tukey adjustment for family-wise error. Time and treatment were defined as fixed effects, while treatment paddock was defined as a random effect. Due to high spatial variability within pastures, effects were declared significant if $p < 0.1$.

Microbial PLFA compositional data were ln-transformed to increase sensitivity to low-abundance PLFAs then transformed into a Bray-Curtis dissimilarity matrix. Multivariate analyses were then used to assess influences on soil microbial structure using R package 'vegan' (Oksanen et al., 2018). Non-metric multidimensional scaling (NMDS) was used to visualize microbial community structure and the factors influencing structural variation. Spearman rank correlations were used to support visual correlations between NMDS vectors. Permutational multivariate analysis of variance (PerMANOVA) was used to determine the significance of environmental and treatment effects on microbial community structure. Distance-based redundancy analysis (dbRDA) was used to determine the relationships of microbial communities to specific factors, specifically plant treatment, soil NO_3^- and DOC content, and N_2O flux.

Potential microbial-environmental interactions indicated by NMDS vector correlations were used to build a structural equation model (SEM) to represent a hypothetical model for observed data. Analysis was performed using R package 'lavaan' (Rosseel, 2012). This analysis was not a hypothesis-testing use of SEMs, where a hypothetical framework of interactions is constructed prior to data gathering then the unmodified model is tested against data. This SEM analysis was exploratory, rather than confirmatory, and hypothesis-generating in that a model was built based on data observations then modified to best fit the data through the addition of logical pathways and the removal of insignificant pathways.

The SEMs were constructed to avoid overfitting by having five observations for every fitted pathway. Treatments were binarily dummy-coded to determine treatment effects relative to the control. Since the non-bloat legume treatments were sod-seeded into pre-existing grass-alfalfa

pastures, the control treatment was coded to be the baseline which the effects of each legume were compared against in each SEM. A microbial community structure term was created using a 1-dimensional NMDS solution of PLFA data. Satorra-Bentler scaling was used to correct for data non-normality, which is effective in data with small to moderate sample sizes (Rosseel, 2012). A model with a Chi-square (χ^2) $p > 0.05$ was considered to be statistically significant. In SEM, the alternative hypothesis is rejected if the data variance is not statistically different from the implied model variance, therefore models with a $p > 0.05$ are significant. The ideal model fit would have the highest χ^2 p-value, the lowest root mean square error of approximation (RMSEA) but at least < 0.08 with a 90% confidence interval between 0.00 and 0.08, and a square root mean residual (SRMR) of < 0.08.

3.5 Results

Daily soil N_2O fluxes did not differ between treatments on microbial sampling dates. However, fluxes did vary with time (Fig. 3.2), with sampling date influencing daily N_2O fluxes in both 2017 and 2018 ($p < 0.001$ and $p = 0.033$, respectively). Similarly, treatment did not explain differences in enzyme activity. Soil βG activity varied with time in 2017 ($p = 0.081$) but not 2018, while NAG activity varied with time in 2018 ($p = 0.006$) but not 2017. No differences in AP between treatments or sampling events were found. Activity rates of all enzymes tended to be higher in 2018 compared to 2017 (Figs. B3-B5), which coincides with a numerical increase in total PLFA abundance (Table B1) and a large drop in CO_2 respiration (Fig. B1).

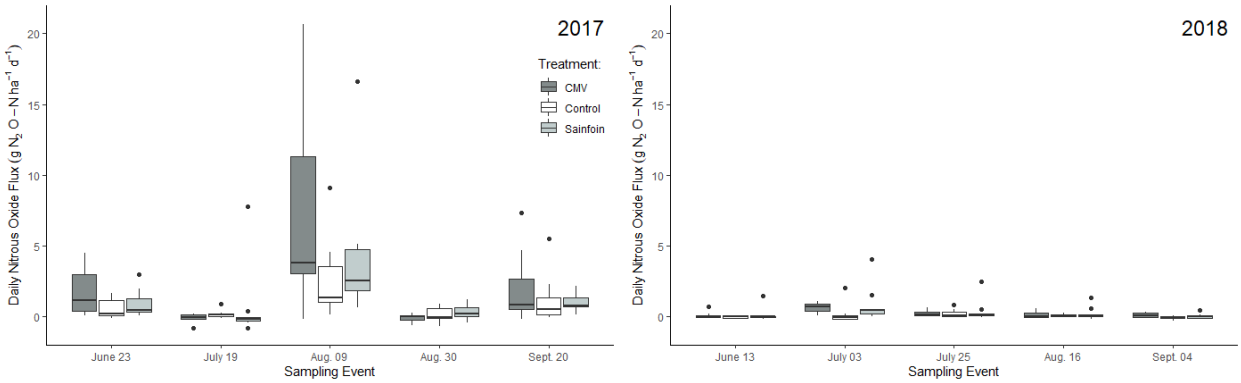

Figure 3.2: Daily soil N_2O fluxes on sampling dates between cicer milkvetch (CMV), sainfoin, and control plant treatments.

Time influenced total PLFA quantity in 2018 ($p = 0.077$) while the interaction between treatment and time was significant in 2017 ($p = 0.026$). In 2017, total PLFA was lower in cicer milkvetch than control pastures at the July 19th sampling event ($p = 0.038$), and lower than both control ($p = 0.028$) and sainfoin pastures ($p = 0.053$) at the August 30th sampling event. These dates coincided with low soil moisture (Fig. B2). Relative PLFA abundances and stress indices varied in response to treatment and time (Figs. B6-B13). Time influenced G+, G-, actinobacteria, and Stress 1 PLFA relative abundances in both 2017 and 2018 (Tables C1 and C2). Additionally, actinobacteria PLFA relative abundance was influenced by treatment in 2017 ($p = 0.06$) and had an interaction between treatment and time in 2018 ($p = 0.097$). Treatment and time affected 2017 relative fungal PLFA abundance in 2017 ($p = 0.075$ and 0.078, respectively), while an interaction between the two factors had an effect in 2018 ($p = 0.041$). This interaction in 2018 was the result of higher relative fungal abundances in cicer milkvetch ($p < 0.001$) and sainfoin ($p = 0.022$) pastures compared to the control pastures at the final sampling event. Stress 2 had an interaction between treatment and time in 2017 ($p = 0.0175$) while only time affected this ratio in 2018 ($p < 0.001$).

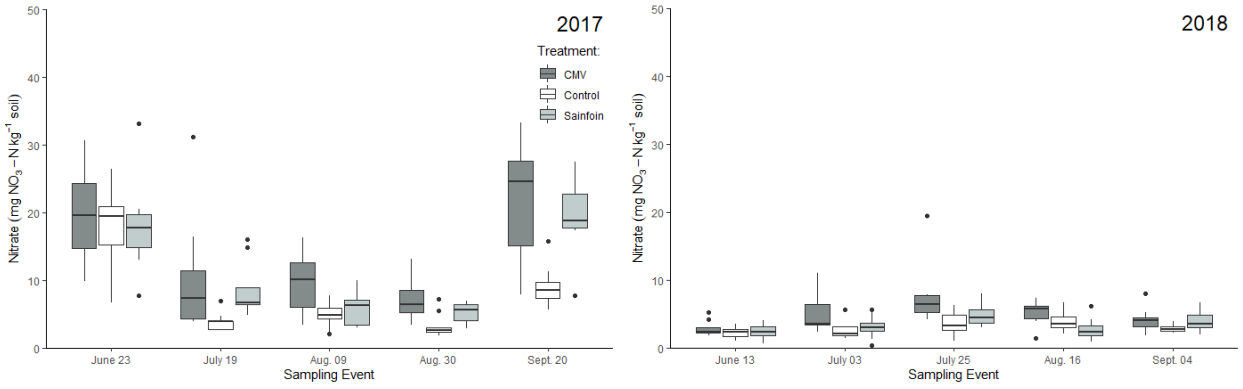

Figure 3.3: Soil NO_3^- content on sampling dates between cicer milkvetch (CMV), sainfoin, and control plant treatments.

Soil NO_3^- varied throughout 2017 but less so in 2018 (Fig. 3.3). An interaction was found between treatment and time in 2017 ($p = 0.013$), while only time had an effect on NO_3^- content in 2018 ($p < 0.001$). In 2017, cicer milkvetch and sainfoin had higher soil NO_3^- than the control on the final sampling date of the year ($p = 0.002$ and 0.010, respectively). Soil NH_4^+ followed a similar trend (Fig. B14), however an interaction between treatment and time was found in both 2017 ($p =$

0.030) and 2018 ($p = 0.040$). On the final sampling day of 2017, sainfoin soils were found to have higher soil NH_4^+ than cicer milkvetch ($p = 0.003$) and control soils ($p = 0.028$). In 2018, however, NH_4^+ was lower in sainfoin than control soils for 3 sampling events ($p = 0.052$, 0.043, and 0.060 for June 13th, July 25th, and August 16th, respectively). Soil NH_4^+ was lower in cicer milkvetch than control pastures in 2018 at the June 13th ($p = 0.086$) and July 25th ($p = 0.072$) sampling events. Soil DOC (Fig. B15) had an interaction between treatment and time in both years ($p = 0.002$ and 0.042 in 2017 and 2018, respectively). The quantity of DOC differed at the end of each study year, with sainfoin soils containing more than cicer milkvetch and the control in 2017 ($p = 0.003$ and 0.050) and 2018 ($p = 0.060$ and 0.034). Soil DOC was also higher in the control plots than cicer milkvetch on August 30th, 2017 ($p = 0.038$), which coincides with a low soil moisture day.

3.5.1 Pasture soil microbial community composition

Microbial PLFA data grouped strongly by year and strong seasonal gradients were apparent (Fig. 3.4). Community structure shifts progressed along a similar trajectory from June to September, but this shift was longer in 2018 than in 2017. Communities were less similar between study years in June and became more similar as the season progressed, becoming most similar in September. Based on ANOSIM, within-treatment variation was comparable to between treatment variation throughout both seasons (2017: $R = 0.055$, $p < 0.001$; 2018: $R = 0.054$, $p = 0.002$). By comparison, between-timepoint was much higher than within-timepoint variation of soil microbial communities in both years, indicating that temporal changes in pasture conditions had a much larger influence on soil microbial community composition than forage legume. Between-timepoint variation was highest in 2018 ($R = 0.656$, $p < 0.001$), with slightly lower between-timepoint variation in 2017 ($R = 0.503$, $p < 0.001$).

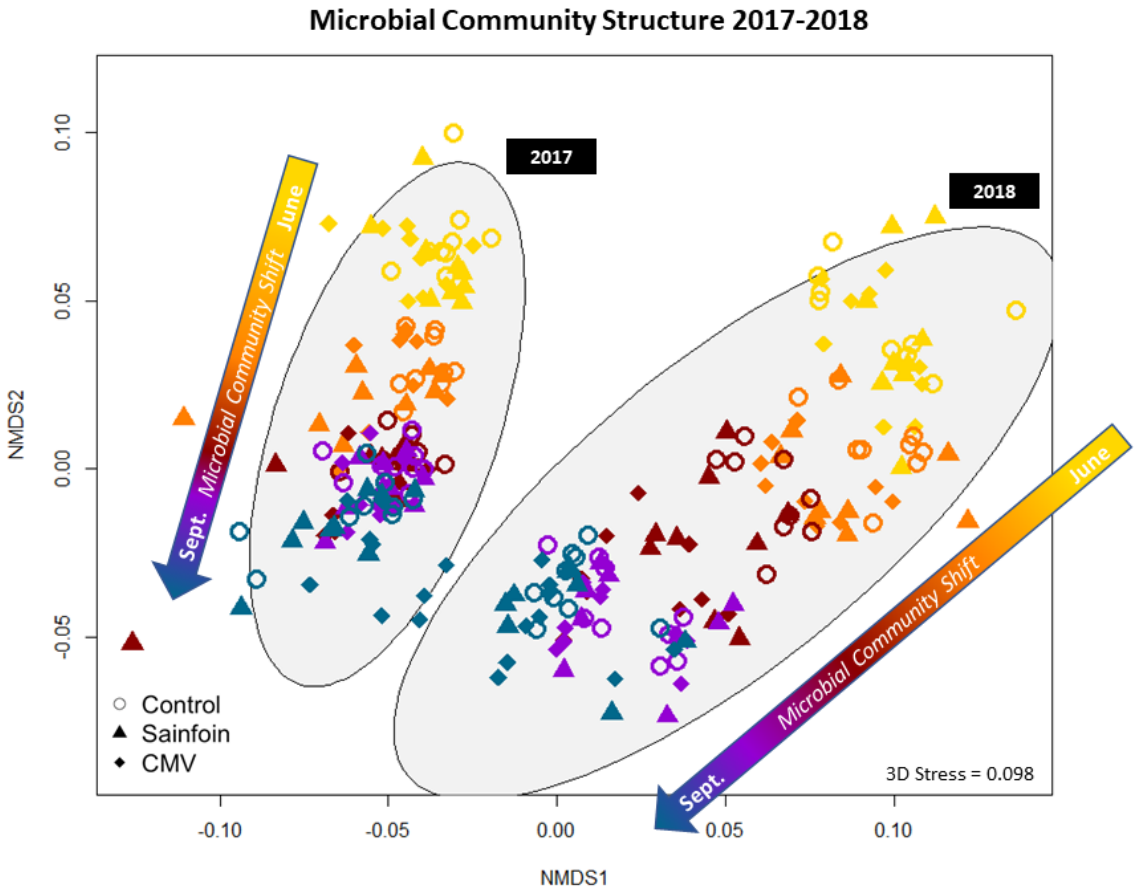

Figure 3.4: NMDS plots of 2017 and 2018 PLFA community compositions. Ellipses represent 95% confidence intervals of study year communities.

Within each study year, the largest community shift was observed along the seasonal gradient, with sampling dates clustering according to temporal proximity (Fig. 3.5). More precipitation variability prior to sampling dates occurred in 2017 than in 2018, resulting in larger differences in soil moisture between 2017 sampling dates (Fig. B2). Specifically, extended dry periods occurred in 2017 prior to July 19th and August 30th sampling dates, and rainfall occurred the day prior to August 9th and September 20th sampling dates, resulting in an average of 0.18 g g^{-1} and SD of 0.07. In contrast, soil moisture was much more consistent across 2018 sampling dates, with an average of 0.14 g g^{-1} and SD of 0.04. As a result, both time of year and timing of precipitation relative to sampling date had a large influence on microbial community composition throughout both years. In 2017, microbial communities grouped due to drought conditions on July 19th and August 30th, while communities grouped due to increased soil moisture on August 9th and

September 20th (Fig. 3.5). Due to this moisture variability in 2017, microbial community shift along the temporal gradient was less smooth and more irregular than in 2018.

Soil microbial community structure correlated with a combination of microbial abundances, enzyme activities, and stress indices (Fig. 3.5). The magnitude of some of the effects differed between years. In both years, there were positive associations among stress indices, G+ bacterial abundance, and AP activity, and negative associations between all of these vectors and relative G- bacterial abundance (Fig. 3.5; Table 3.1). Relative G- abundance was positively associated with relative fungal abundance in 2017, as well as with relative AMF abundance in 2018. Stress indices are partially explained by an association with soil moisture in 2017 (Spearman R Stress 1 = -0.36, Stress 2 = -0.69; $p < 0.001$). Relative G- abundance had an association with NH_4^+ ($R = 0.49$, $p < 0.001$) and moisture content ($R = 0.58$, $p < 0.001$) in 2017, whereas relative G- abundance was associated with pH in 2018 ($R = 0.44$, $p < 0.001$). Relative actinobacterial abundance was associated with early-season June communities in 2017, but in 2018, relative actinobacterial abundance was associated with late-season September communities along with increasing soil DOC ($R = 0.36$, $p < 0.001$). Late-season microbial communities were associated with increasing βG activity in 2017. In comparison, the activity of all three βG, NAG, and AP enzymes was associated with increasing stress indices and relative G+ abundance in 2018.

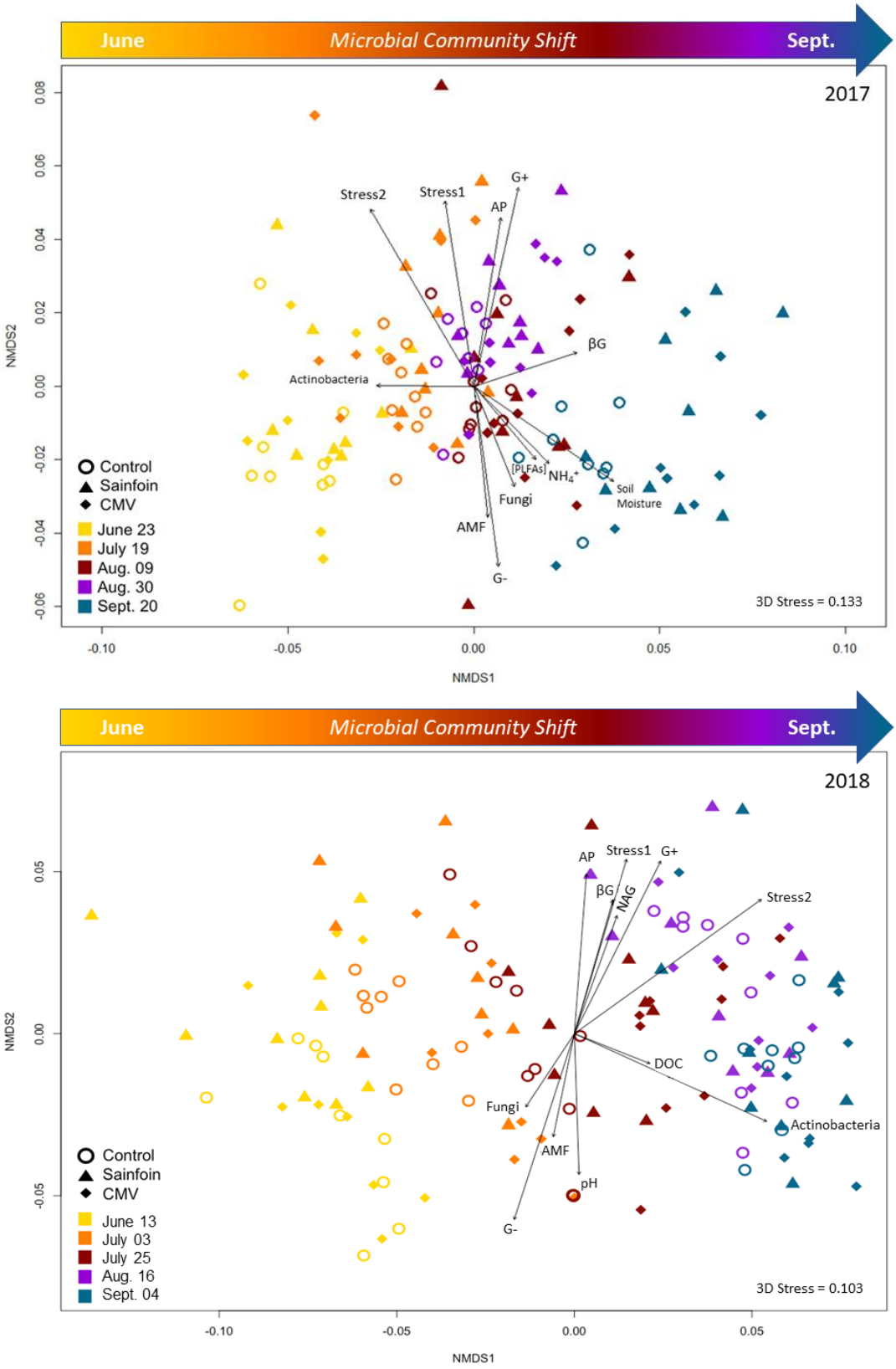

Figure 3.5: NMDS plots of 2017 and 2018 PLFA Bray-Curtis dissimilarity matrices. Vectors represent linear gradients associated with the ordination; non-linear vectors removed.

Table 3.1: Spearman rank correlations between NMDS vectors.

	G-	G+	Stress1	Stress2
		2017		
G+	-0.70 ***	---		
Stress1	-0.63 ***	0.56 ***	---	
Stress2	-0.66 ***	0.40 ***	0.61 ***	---
AP	-0.37 ***	0.55 ***	0.61 ***	0.14 ns
AMF	0.14 ns	---	---	---
Fungi	0.22 **	---	---	---
		2018		
G+	-0.76 ***	---		
Stress1	-0.70 ***	0.68 ***	---	
Stress2	-0.66 ***	0.64 ***	0.54 ***	---
AP	-0.55 ***	0.67 ***	0.68 ***	0.30 ***
AMF	0.31 ***	---	---	---
Fungi	0.34 ***	---	---	---
βG	-0.46 ***	0.55 ***	0.36 ***	0.40 ***
NAG	-0.40 ***	0.51 ***	0.34 ***	0.42 ***

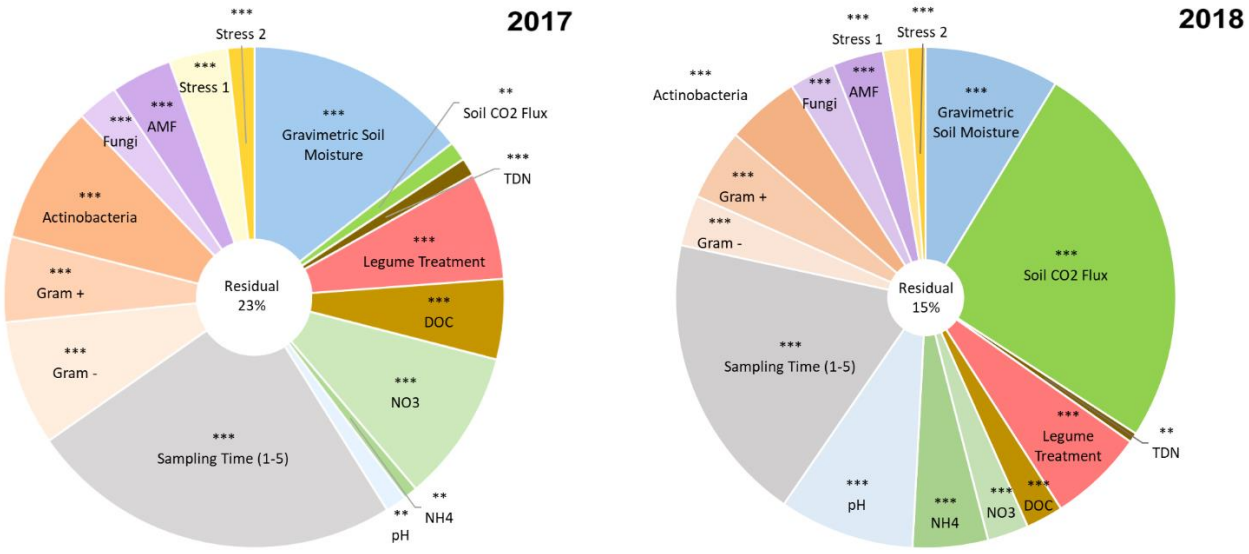

Figure 3.6: PerMANOVA models showing the proportional correlation of factors with microbial community structure in each study year. Models explain 77% of 2017 and 85% of 2018 variation in community structure. Each model is significant at p = 0.001 (n = 135, residual df = 114).

Forage legume treatment had a small but significant effect on microbial community composition in each study year model (Fig. 3.6). Models revealed that legume treatment explained roughly the same amount of community variation within each study year (r^2 = 0.052, 0.053 in 2017, 2018, respectively; p = 0.001). In 2017, seasonal pasture progression had the most sizeable impact on community structure variation (r^2 = 0.19, p = 0.001). Soil moisture (r^2 = 0.11, p = 0.001) and soil NO_3^- (r^2 = 0.08, p = 0.001) contributed strongly to community variation as well. Changes in microbial PLFA abundances cumulatively explained more community variation than legume treatment, with G- and actinobacteria individually being higher (r^2 = 0.06, 0.07 respectively; p = 0.001). In 2018, seasonal progression was also a significant contributor to community change (r^2 = 0.16, p = 0.001). Despite much lower CO_2 respiration than 2017 (Fig. B1), this minimal amount of plant and microbial respiration explained the largest amount of 2018 community variation (r^2 = 0.22, p = 0.001). While moisture was less variable in 2018, it still contributed to community variation (r^2 = 0.07, p = 0.001). Both soil pH (r^2 = 0.07, p = 0.001) and NH_4^+ (r^2 = 0.04, p = 0.001) explained more community variation than NO_3^- (r^2 = 0.02, p = 0.001). Microbial PLFA abundance cumulatively contributed to more variation than legume treatment again in 2018, but not individually.

3.5.2 Temporal and spatial variation of pasture microbial communities

Throughout both study years, variation in soil conditions, plant cover composition between paddocks and sampling sites, and seasonal growth conditions may have outweighed any potential influences of legumes on the soil microbial community. This spatial and temporal variability is reflected in the results of the ANOSIM previously discussed, with large within-treatment and between-timepoint variability. Distance-based redundancy analysis (dbRDA) was used to constrain the effect of temporal and spatial variation in environmental conditions on PLFA community ordinations. Within each model, soil moisture (Fig. B2), TDN (Fig. B16), and pH were included as continuous conditional factors, and sampling timepoint was included as a categorical conditional factor. This resulted in 40.7% and 58.9% of total model inertia attributed to conditional factors in 2017 and 2018, respectively, reinforcing the strong influence of temporal and spatial variation on microbial community composition in these pastures. Legume treatment, NO_3^-, DOC, and daily N_2O emissions were used as model constraints to visualize the relationships between these factors of interest and microbial community structure.

With seasonal and spatial environmental variability included as conditional factors as previously defined, soil microbial communities grouped according to legume treatment more clearly but still had some overlap (Fig. 3.7). In 2017, NO_3^- content influenced legume pasture communities, with cicer milkvetch communities generally displaying the strongest association with NO_3^- content (Fig. 3.7). The daily N_2O emissions vector was nearly parallel with the NO_3^- vector. Both these vectors were most associated with cicer milkvetch microbial communities. Sainfoin microbial communities were less associated with the soil NO_3^- vector than cicer milkvetch communities, but more associated than control microbial communities. Control pasture communities were more associated with higher soil DOC content compared to legume pasture communities.

Community overlap increased in 2018 but treatment groupings were still visible (Fig. 3.7). Trends in NO_3^- were similar to 2017 with legumes being associated with increasing soil NO_3^- levels. Cicer milkvetch microbial communities were once again most strongly associated with increasing soil NO_3^-, but were ordinated in much closer proximity to control treatment community structure than in 2017. Sainfoin pastures had a larger overlap with control pasture communities in 2018. Of the microbial communities most strongly associated with higher soil NO_3^- , the majority still belong to cicer milkvetch pastures with more overlap with sainfoin communities. Model N_2O and NO_3^- vectors were more perpendicular than parallel in 2018. The association of control communities with increasing DOC was less apparent in 2018, with many legume communities positioning as high as or higher than the controls.

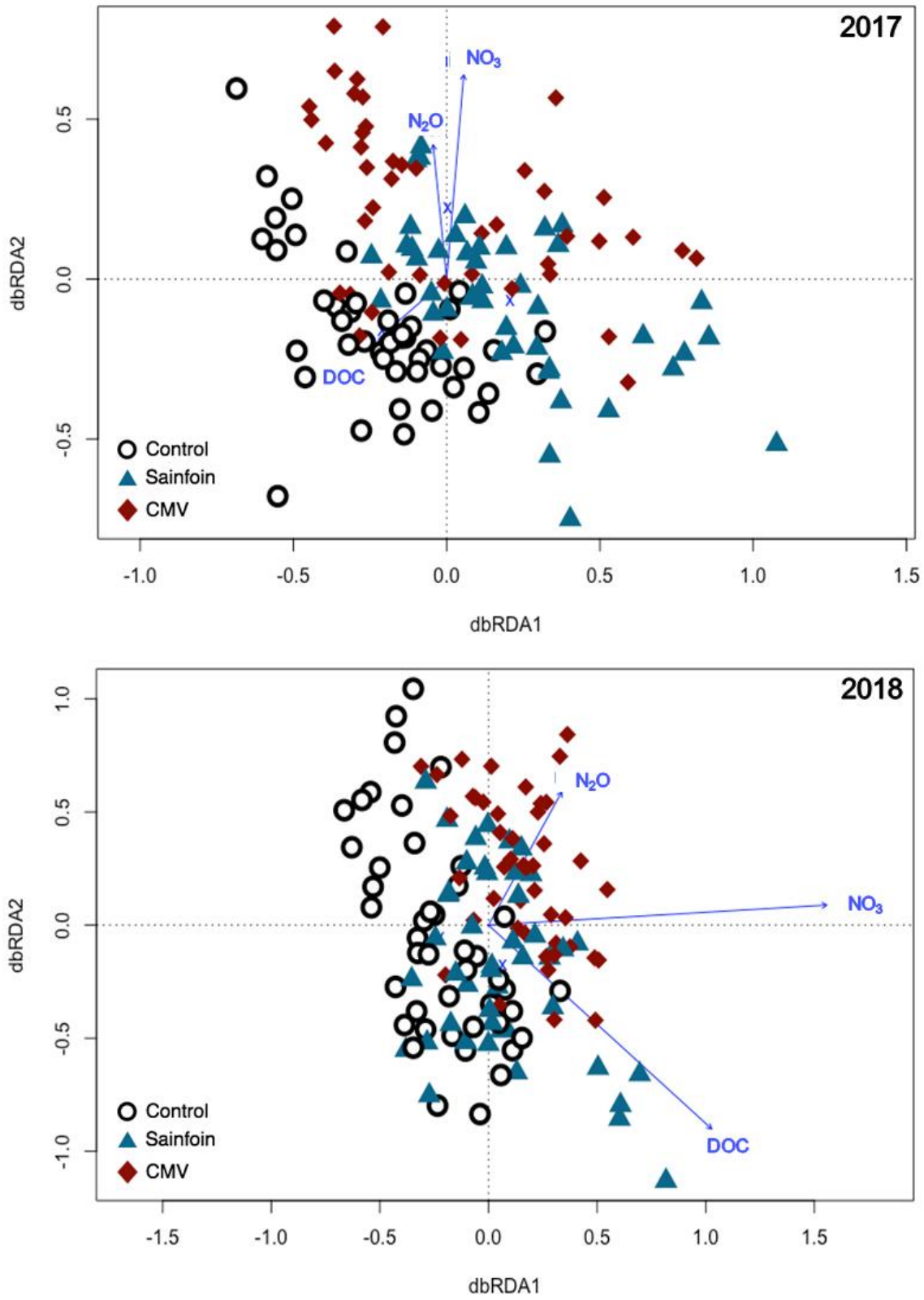

Figure 3.7: Distance-based redundancy analysis (dbRDA) models of 2017 and 2018 PLFA data ($p = 0.001$). Vectors represent linear gradients within the data ($p < 0.1$).

3.5.3 Structural equation modeling of interactions between legume treatment, soil microbes, and N_2O fluxes

Spatial and temporal variation may have obscured any potential effects of forage legumes on daily GHG fluxes in this pasture. Legume treatments tended to have higher, wider ranges of soil NO_3^- fluxes and daily N_2O emissions, but these ranges overlapped with control values. The degree of heterogeneity in soil conditions within paddocks combined with minute daily N_2O fluxes resulted in unclear interpretations and insignificant results when using general linear mixed effects models. The use of SEMs indicated significant interactions between legume treatment, soil nutrient fluxes, microbial community structure, enzyme activity, and daily N_2O fluxes under differing environmental conditions in 2017. Fitting 2017 SEMs to 2018 data and combined, multi-year data resulted in a poor model fit (χ^2 p = 0.000). Alternative modeling attempts for 2018 and combined data also resulted in a poor fit. The first study year (2017) had higher precipitation variability than 2018, which may have accentuated the observed differences between treatments.

Structural equation modeling of daily 2017 N_2O fluxes revealed a network of possible interactions between plant treatment, microbial nutrient cycling, microbial community structure, and environmental conditions (Fig. 3.8). Including a negative, two-way interaction between soil NO_3^- and daily N_2O flux improved overall model fit. Daily pasture N_2O fluxes were likely primarily controlled by soil moisture content, which was correlated not only with increased emissions but soil nitrogen as well. Cicer milkvetch and sainfoin were positively associated with soil NO_3^- relative to the control. Cicer milkvetch and sainfoin altered microbial community structure compared to the grass pastures. In addition to these interactions, other mechanisms influencing soil N cycling are associated with the presence of cicer milkvetch in the pastures, whereas sainfoin had weaker interactions with soil resource availability.

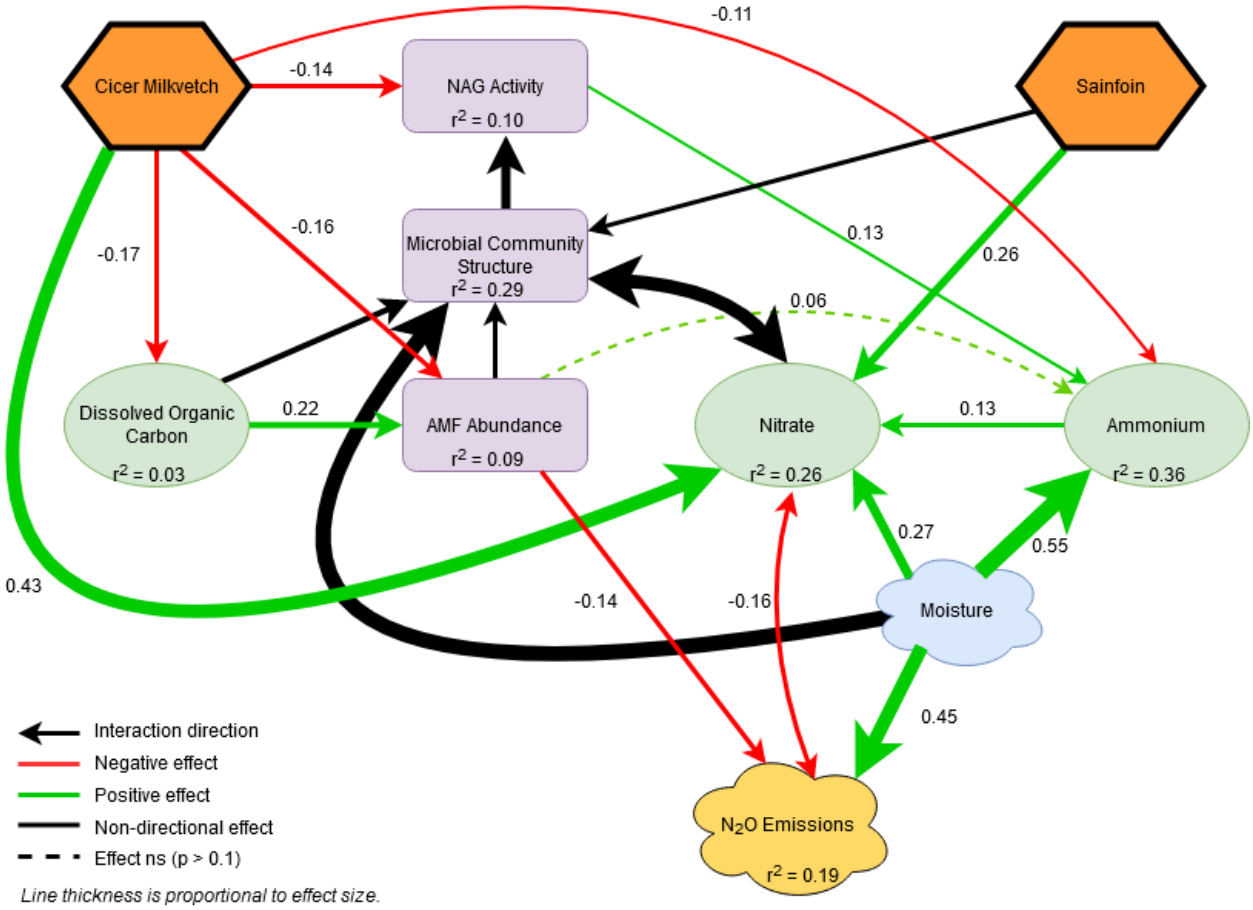

Figure 3.8: Structural equation model of daily 2017 pasture N_2O emissions. Lines and standardized regression coefficients (next to lines) are proportional to effect size. Dotted lines are marginally insignificant at $p > 0.1$. r^2 represents total explanatory power of pathways leading into term. Satorra-Bentler χ^2 p = 0.233; RMSEA = 0.037; SRMR = 0.057).

Structural equation modelling indicated that the presence of cicer milkvetch in a pasture could potentially influence soil N content both directly through inputs and also indirectly by influencing microbial mechanisms mediating pasture soil N levels. Cicer milkvetch was negatively correlated to soil DOC and NH_4^+ content. The model suggests a potential reduction in relative AMF abundance in cicer milkvetch pastures, which was partially associated with a decrease in DOC content. Through this suggested negative association with AMF, cicer milkvetch can affect microbial community structure, which has further potential to influence soil NO_3^- content. Relative AMF abundance was negatively correlated to daily pasture N_2O emissions. The SEM also suggests a negative association of cicer milkvetch pastures with NAG activity, potentially further reducing soil NH_4^+ content. Cumulatively, although the SEM suggests cicer milkvetch may have decreased

soil NH_4^+ relative to grass pastures, both non-bloat legumes had positive associations with soil NO_3^- levels.

3.6 Discussion

Understanding the responses of soil microbes to non-bloat legume introduction in cattle pastures can improve GHG mitigation practices. This study aimed to determine whether introducing non-bloat legumes would alter pasture soil microbial community structure, nutrient cycling rates, and daily N_2O emissions. This study demonstrated that while plant treatment was not the most influential factor on microbial community structure, it did have an effect nonetheless. Differences in mean daily N_2O emissions were not observed between treatments on microbial sampling dates, however a tendency for larger N_2O fluxes in cicer milkvetch pastures was observed. Soil enzyme activity was not affected by non-bloat legume introduction in this study. Seasonal progression within the pasture was found to have a large influence on both microbial community structure and enzyme activity. Legume soil NO_3^- was only higher than the controls at the end of 2017, but tended to be higher throughout the 2017 season as reflected by SEM (Fig. 3.8) and the generally larger range of legume soil NO_3^- values relative to the controls (Fig. 3.3).

Microbial community composition was most affected by seasonal gradients in both 2017 and 2018 (Figs. 3.4 and 3.5), a result of changing pasture growth stage. Nonetheless, both PerMANOVA and constrained ordination (Figs. 3.6 and 3.7) demonstrated some effect of non-bloat legumes on pasture soil microbial communities. Pasture PLFA composition not only differed in magnitude of seasonal shift between years but was also different between seasons, grouping according to year (Fig. 3.4). These differences in community structure between grazing seasons might result from the recency of non-bloat legume introduction. Pasture soil communities may still be adjusting to this management change. Soil microbial communities in established Canadian grassland soils are resistant to changes in plant functional group composition and may not respond to changes within five years (Marshall et al., 2011). Seasonal shifts and annual distinctions between microbial PLFA composition were observed following the establishment of a pasture, with differences in total PLFA biomass increasing with year of pasture rotation (Lin, McCulley, Nelson, Jacobsen, & Zhang, 2020). Since the legumes in this study were sod-seeded into existing perennial grass two years prior to the study, observed treatment differences may be reduced due

to ongoing community shift. Drought in 2017, which stunted community progression, may have also stunted plant effects on microbial community shifts (Fig. 3.4).

The observed seasonal shifts were likely caused by pasture growth stage. Edwards et al. (2018) found that seasonal community shifts in a grass root microbiome were correlated with plant life cycle stage. Stevenson, Hunter, and Rhodes (2014) found a similar shift in seasonal pasture soil PLFA composition, which was speculated to be the result of seasonal changes in plant root exudates. Seasonal patterns in N-cycling microbial communities were associated with changes in substrate availability related to plant growth stage in a grassland (Regan et al., 2017). Additionally, increased denitrification enzyme activity was associated with the appearance of legumes in a grassland (Regan et al., 2017). In this study, legume soil microbial communities diverged from the controls throughout June and July, with maximum community dispersion occurring in late July to early August (Fig. 3.5). This may be due to changing plant litter and root inputs into the soil and plants altering their interactions with microbes as their needs change with the season. Plant die-off at the end of season resulted in similar microbial communities despite initial shifts between years (Fig. 3.4).

Soil moisture provided additional influence on microbial community development, particularly in 2017 when droughts occurred, disrupting the seasonal gradient (Fig. 3.5). A drought-stressed grass was shown to have a developmentally immature rhizosphere soil microbiota compared to unstressed plants (Edwards et al., 2018). Hammerl et al. (2019) observed that in a grassland, the responses of soil microbial communities following a drought were strongly dependent upon plant growth stage. Observed differences in microbial response were thought to be the result of differing plant development stages, root community composition, and root exudate quantity and quality (Hammerl et al., 2019). Combined, this suggests potential interactions between drought and pasture growth stage. Additionally, low moisture may have influenced microbial communities indirectly by diminishing grazing effects. A grazing tolerant grass has been observed to provide additional C root exudates to stimulate soil microbial activity in exchange for inorganic N following a grazing event (Hamilton & Frank, 2001). Therefore, the direct effects of moisture limitation on microbial growth as well as the indirect effects of a reduced grazing period due to drought may have limited seasonal pasture plant growth progression, with consequences for microbial community temporal dynamics in 2017 relative to 2018 (Fig. 3.4).

A large amount of microbial community variation was correlated with differences in relative G+ and G- bacterial abundances, which coincided with shifts in G- environmental stress indices and shifts in relative fungal abundance (Table 3.1, Fig. 3.5). In 2017, these shifts were mostly regulated by soil moisture correlating positively with G- abundance and negatively with stress indices. Throughout the season, G+ populations remained steady, with their abundance increasing as G- decreased during droughts, indicating a stronger resilience of G+ bacteria during droughts. Multiple studies have demonstrated soil G+ bacterial abundances to increase and G- to decrease following induced droughts, suggesting an advantage of slow-growing, drought-adapted G+ bacteria over the rapid growing G- in drought conditions (Chodak, Gołębiewski, Morawska-Płoskonka, Kuduk, & Niklińska, 2015; Fuchslueger, Bahn, Fritz, Hasibeder, & Richter, 2014; Sun et al., 2020; Xi, Chu, & Bloor, 2018).

Pasture heterogeneity and temporal shifts may have obscured potential microbial community responses to non-bloat legume introduction. Pastures are active, living systems with factors which are difficult to control for, such as burrowing animals bioturbating the soil prior to and throughout this study, increasing heterogeneity. Unconstrained NMDS ordinations showed overlap between treatment communities with grass microbial communities showing less within treatment variability than legumes (Fig. 3.5). Soil microbial community structure has been shown to be more variable under legume treatments than grass, with legumes showing higher bacterial diversity (Zhou, Zhu, Fu, & Yao, 2017). Additionally, microbial enzyme activities have been observed to vary both spatially and seasonally within a grassland soil (Regan et al., 2017). However, constrained ordination was effective in constraining pasture variability and revealing the effects of non-bloat legumes on soil microbial communities.

Plant treatment had a minimal direct effect on microbial community structure, but indirect effects related to legume presence had further influence. Non-bloat legumes were associated with increasing soil NO_3^- (Figs. 3.3 and 3.8). Differences in soil NO_3^- inputs and uptake between treatments had a large effect on community structure in 2017 (Fig. 3.6). Non-bloat legume communities were positively associated with soil NO_3^- and daily N_2O emissions (Fig. 3.7), providing context for potentially larger N_2O fluxes. Niklaus et al. (2016) observed larger N_2O emissions in grass pastures containing legumes due to soil N increasing. While this study did not find significant differences between daily treatment N_2O fluxes on microbial sampling dates, a

tendency towards a larger range of N_2O fluxes was observed in legume treatments, particularly cicer milkvetch (Fig. 3.2).

Relationships between plant treatment, soil microorganisms, environmental conditions, and GHG emissions are complex and interwoven in active pasture systems. Applying SEM to dynamic systems with complex relationships, such as pastures, can indicate potential interactions and net effects on ecosystem services of interest. A study used SEM to study interactions between grasses, legumes, and weeds with the net effect on biomass yield in Canadian grasslands (McLeod, Banerjee, Bork, Hall, & Hare, 2015). Here, SEM was used to investigate interactions between plant treatment, soil microbes, environmental conditions, and the net effect on daily GHG emissions.

Interactions between legumes, soil N, microbial community structure, and daily soil N_2O emissions in 2017 were explored using SEM (Fig. 3.7), while modeling attempts of 2018 data were not informative. The presence of AMF in soils has been demonstrated to reduce N_2O emissions (Storer, Coggan, Ineson, & Hodge, 2018), thought to be the result of AMF outcompeting slow-growing nitrifiers for soil NH_4^+ (Storer et al., 2018; Teutscherova et al., 2019), or that perhaps increased N_2O reduction occurs in the presence of AMF (Teutscherova et al., 2019). While no differences in relative AMF abundance were found using mixed effects models, the SEM suggests possible negative associations between cicer milkvetch and AMF abundance. The negative association of cicer milkvetch with NAG activity and AMF abundance may suggest reduced competition for soil NH_4^+ in cicer milkvetch pastures. However, this association may equally be the result of lower total AMF necromass reducing NAG levels since there is less chitin to degrade. Soil NO_3^- was positively associated directly with both plant species, and more strongly with cicer milkvetch, which implies reduced soil NO_3^- uptake (and not increased NO_3^- production through nitrification), leaving more NO_3^- to be denitrified to N_2O under wet conditions, increasing N_2O emissions.

One unexpected result of the SEM was a two-way negative interaction between NO_3^- and daily N_2O emissions, which may be explained by variable moisture in 2017. Nitrification would still occur at a reduced capacity during dry conditions while plant uptake is limited, increasing soil NO_3^-. Following rainfall, plant uptake and denitrification would deplete soil NO_3^- content as denitrification produced N_2O. Conversely, nitrification rates would increase during higher

moisture conditions, as would plant uptake, leaving less soil NO_3^- than during dry conditions. This interaction may additionally be explained by the lack of an expected N_2O flux in September of 2017, which had high moisture, NO_3^-, and DOC. These conditions should favor denitrification events. Regan et al. (2017) report that potential nitrifier and denitrifier activities correspond to periods of rapid plant growth in grassland soils. By the September 2017 rainfall event, the pasture plants had largely died off. This would result in low N_2O production, causing a negative interaction between high NO_3^- and low N_2O. This unexpected negative interaction highlights the challenge present in predicting and capturing soil N_2O emissions, particularly in systems with highly interdependent processes such as pastures. In this context, SEM has been effective in exploring potential relationships not captured by other modeling methods.

3.7 Conclusion

Seasonal pasture progression, soil heterogeneity, and moisture variability had dominant effects on microbial structure and activity in pasture soils. This variability in pasture conditions created difficulty in modeling and discerning the effect of non-bloat legume introduction on soil microbes and GHG emissions. Some microbial activity was affected by time but not treatment. For example, legumes did not influence mean microbial enzyme activity levels, but seasonal progression did affect βG and NAG activity in 2017 and 2018, respectively. However, non-bloat legume introduction to this established grass pasture did influence soil microbial community structure and appeared to be strongly influenced by the resulting N availability. Treatment differences in microbial community structure are apparent when isolated from seasonal, soil, and moisture variability in models. Even with a proportionately smaller influence, introducing new non-bloat forage legumes created soil microbial communities that were distinct from grass-alfalfa pastures but did not influence GHG emissions. Legume pasture communities were associated with increased soil NO_3^- content. No differences in mean daily N_2O flux were observed between pasture treatments, however cicer milkvetch had a tendency for larger daily N_2O fluxes. Potential links between cicer milkvetch pastures, AMF abundance and daily N_2O fluxes were suggested by SEM in 2017. This study finds that non-bloat legume introduction to a grass pasture will shift microbial community composition, but not in a way which conclusively increases average daily N_2O emissions. The scale of any N_2O increase must be considered when implementing best

management practices given the expected reduction in GHG emissions from cattle. The global warming potentials of each must be weighed to determine the net benefit of a change in management practice and to find the best environmental outcome.

4. TEMPORAL CHANGES IN N_2O PRODUCTION AND ACTIVITY BY NITRIFIER AND DENITRIFIER POPULATIONS IN URINE-AMENDED SOILS

4.1 Preface

Non-bloat legumes can provide benefits to cattle producers through improved pasture soil nitrogen (N) inputs, increased cattle protein uptake, and reduced enteric methane emissions compared to conventional grass-alfalfa pastures. Depending on legume protein content and digestibility, excess protein intake can increase the N content of excreted urine in the form of urea. Once excreted to the soil, urea is rapidly hydrolyzed to carbon dioxide (CO_2) and ammonium (NH_4^+), providing fresh N substrate to soil nitrifiers and subsequently denitrifiers. This increase in soil N tends to increase soil nitrous oxide (N_2O) emissions through nitrification and denitrification pathways. While influences on N-cycling microbes and increases in N_2O emissions in urine patches have been observed, it remains unclear how urine deposition affects the activities and abundances of N_2O-producing soil microbes. The contribution and relation of urine urea to total N_2O and CO_2 emissions remains ambiguous as well. The goal of this study was to determine the effect of urine deposition on soil nitrifier and denitrifier populations and determine any relationships with N_2O emissions. Additionally, this study sought to determine the relative contributions of nitrifiers and denitrifiers to total N_2O emissions, and the urea-derived contributions to N_2O and CO_2 emissions.

4.2 Abstract

Changes in cattle dietary protein intake, such as those resulting from the incorporation of non-bloat legumes into grass pastures, can alter urinary N output, primarily in the form of urea. How these potential changes alter the soil N-cycling microbial community and ultimately N_2O production in the urine patch remains unclear. This study was designed to determine how varying urine urea content affects soil CO_2 and N_2O emissions, nitrifier and denitrifier activities and abundances, and the contributions of urea to CO_2 and N_2O emissions in the urine patch. Two

concentrations of urea in urine: low urea (3.5 g L^{-1}) and high urea (7.0 g L^{-1}); and a water control were added to microcosms containing pasture soils. Gases were sampled over a period of 240 h and analyzed for total CO_2 and N_2O, ^{15}N-N_2O abundance, and N_2O isotopomer abundances. Soil samples were collected to measure N-cycling mRNA and DNA abundances. The high urea urine increased N_2O cumulative flux relative to the control, while low urea had no significant effect. Doubling urine urea content doubled urea-derived CO_2 and N_2O but not total N_2O, likely due to increased urine toxicity and N_2O reduction capacity in high urea soils. Isotopomer ratios indicate that denitrifiers contributed much of the N_2O in the urine patch, while nitrifiers and denitrifiers contributed near equally in the controls. Despite higher AOA gene abundance, AOB responded to urine addition and were the dominant nitrifiers, increasing both transcripts and population size. The dominant denitrifier group shifted during the experiment, with *nirK* denitrifiers responding immediately during an N_2O peak and *nirS* denitrifiers responding slower but more strongly during a secondary peak. Urine addition resulted in a larger clade II vs clade I *nosZ* transcription increase, improving soil N_2O reduction capacity. The observed population dynamics between nitrifier and denitrifier groups adds to the understanding of urine patch N_2O sinks and sources. This study finds that an increase in urine urea content that may arise from adding non-bloat legumes to cattle forage will not increase cumulative N_2O emissions in the urine patch.

4.3 Introduction

Cattle urine deposition onto soil can affect the soil microbes responsible for N_2O emissions by increasing available N concentration and altering soil physical and chemical conditions, ultimately impacting N_2O emissions. The degree to which these effects occur is largely dependent on urine-N concentrations, which is a function of dietary N intake. Urea is the primary constituent of cattle urine N, comprising 52-94% of total urine N, which also contains N as metabolic products, hippuric and uric acids, ammonia, and amino acids (Dijkstra et al., 2013). Increases in dietary N intake can increase urine-N content more rapidly than fecal-N and exhibit an exponential relationship in some cases (Dijkstra et al., 2013). As such, variation in cattle urine-N would primarily occur in the form of urea content, and excess N would be excreted into soil as urea. This increase in soil N has the potential to increase the activity of N-cycling microbes, and subsequently N_2O emissions released through nitrification and denitrification.

Urine deposition affects soil microbial communities in multiple ways, including decreasing pH and increasing osmotic stresses, depending on soil moisture content (Orwin et al., 2010). Urea hydrolysis and subsequent nitrification have the potential to increase soil H^+ concentration and to lower soil pH. Osmotic stresses from high urine-N concentrations can inhibit nitrifier activity, particularly in dry soils (Monaghan & Barraclough, 1992). Soil nitrifiers have exhibited increased stress responses from osmotic pressures following deposition of urine with high urea content (Petersen, Roslev, et al., 2004). High urea-N concentrations initially inhibited denitrifying and nitrifying bacteria, delaying N_2O production (Petersen, Roslev, et al., 2004). Initial inhibitory effects of urine deposition subsequently subsided and were followed by increased microbial activity and net growth (Petersen, Roslev, et al., 2004; Petersen, Stamatiadis, & Christofides, 2004). High urea N_2O emission rates were less than low urea emission rates until 9 d had passed. As such, increases in urine-N content can alter N_2O production rates by inhibiting microbial community activity, especially in dry soils.

Stable isotopes, such as ^{15}N and ^{13}C, can be used to quantify the microbial transformations of a labeled substrate of interest into a target GHG. This allows differentiation of target CO_2 and N_2O gas fluxes from those derived from other C and N sources. For example, $^{15}N^{13}C$ urea can be added to urine to elucidate urea-derived GHG fluxes from those derived from soil C and N and other urine C and N compounds. Since urea is the primary form of cattle N excretion, excess protein-N would be excreted as urea, and the majority of N_2O emissions would hypothetically come from urea sources. The ability to differentiate urea from non-urea derived fluxes could assist with defining urine patch GHG fluxes and provide potential targets for GHG mitigation.

Genes and gene transcripts of N-cycling soil microorganisms can be targeted to better understand processes responsible for observed soil N_2O fluxes. Ammonia oxidizing archaea (AOA) and ammonia oxidizing bacteria (AOB) are responsible for soil nitrification, which is the transformation of soil NH_4^+ to hydroxylamine and eventually NO_3^- (Fig. 4.1), producing N_2O as metabolic by-products of hydroxylamine and NO_2^- oxidation in the process. In terrestrial environments, AOB exceed AOA activity and produce more N_2O despite AOA usually having higher gene abundances than AOB. For example, AOB produced the majority of N_2O emissions following NH_4^+ addition to soil and produced more N_2O per unit nitrite than AOA (Hink, Nicol, et al., 2017). The same trend was found when animal urine was deposited on pasture soils.

Following deposition, total N_2O emissions were significantly related to bacterial *amoA* gene copy numbers and soil NO_3^- levels, but not archaeal *amoA* abundance (Di, Cameron, Sherlock, et al., 2010). In grazed grassland soils, topsoils had higher AOB than AOA abundances prior to urine deposition; AOB grew substantially following urine addition, whereas AOA only grew in the controls (Di, Cameron, Shen, et al., 2010). Additionally, nitrification rates in these grassland soils were related to AOB but not AOA abundances. Abundances of AOB increased following urine deposition on a pasture soil and were strongly correlated with N_2O emissions (Di, Cameron, Podolyan, & Robinson, 2014). The relative abundances and activities of AOA and particularly AOB are therefore of interest when targeting N_2O emissions.

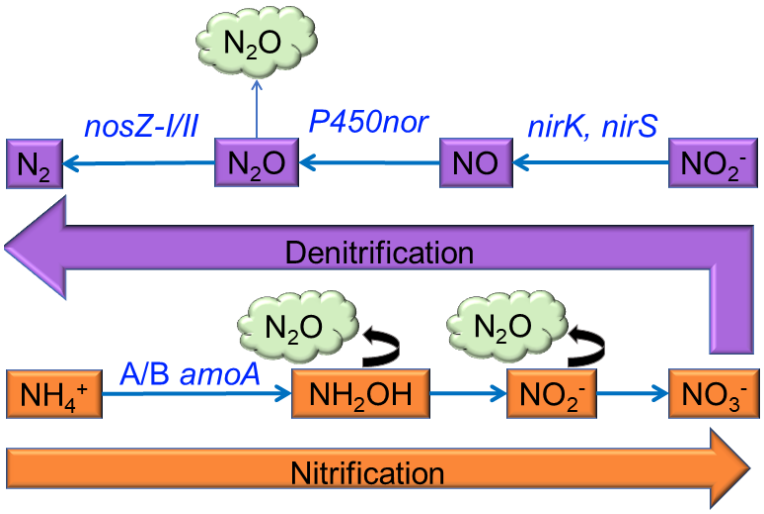

Figure 4.1: Depiction of a partial N cycle and potential N-cycling gene targets.

Bacterial denitrifiers can carry the *nirS* or *nirK* gene, producing N_2O during denitrification (Fig. 4.1). Organisms carrying *nirS* have a higher rate of co-occurrence with *nosZ* genes than *nirK* organisms (Graf et al., 2014; Hallin et al., 2018). Additionally, half of clade II *nosZ* organisms lack denitrifying *nir* genes, while 83% of clade I also possesses *nir* (Graf et al., 2014; Hallin et al., 2018). Therefore, differences in the relative abundances of these genes can explain differences in the quantities of denitrifier N_2O which escape the soil into the atmosphere. Abundances of these denitrifying genes can be related to N_2O production. However, responses of bacteria carrying either gene to urine deposition may vary. While urea application to a pasture soil increased *nirK*, *nirS*, and *nosZ* abundances within a day of application, no relation was found between these denitrifier gene abundances and soil N, N_2O, and N_2 dynamics (Hamonts et al., 2013). However,

the results suggested that in ruminant urine patches, shifts in denitrifier population sizes may influence N fluxes in the long-term. Other studies have found similar effects. For example, urine application on a grazed pasture soil significantly increased *nirK*, *nirS*, and clade I and II *nosZ* gene abundances, particularly in soils with higher moisture content (Di et al., 2014). The abundance of *nirK*, but not the other denitrifier genes studied, was found to be significantly correlated with N_2O emissions (Di et al., 2014). The responses of these bacterial denitrifier genes are likely to differ following urine deposition and are of particular interest when studying N_2O emissions.

Fungal P450nor produces N_2O directly and fungal denitrifiers carrying this gene do not possess the ability to reduce it (Shoun et al., 2012). Fungal denitrification has been shown to be a primary source of N_2O in pastures after simulated urine deposition (Rex et al., 2018). A study has shown a stronger relationship between *P450nor* detection and fungal N_2O production than fungal *nirK* detection and N_2O production (Higgins et al., 2016). Therefore, quantification of *P450nor* may provide explanatory power for N_2O emissions in a pasture soil, where fungi are expected to be prevalent. Fungal abundance may be higher in pasture soils where tillage does not disrupt hyphal growth. However, relative fungal abundance to bacteria may remain unchanged in no-till systems due to the proportional disruption of tillage to both fungal and bacterial communities (Helgason et al., 2009).

Differentiating between nitrifier- and denitrifier-derived N_2O in the urine patch can aid with targeted GHG mitigation by identifying N_2O sources and reinforce the inferences provided by nitrifier and denitrifier gene abundances and activities. The reduction-mixing model described by Lewicka-Szczebak et al. (2017) uses differences in site preferences of N_2O-producing organisms to distinguish between nitrifier- and denitrifier-derived N_2O fluxes. Site preference is calculated based on the difference between α and β $^{15}N_2O$ abundances, where α $^{15}N_2O$ has the ^{15}N atom located on the middle N, and β $^{15}N_2O$ has the ^{15}N atom located on the outermost N. The model assumes partial reduction of bacterial denitrifier N_2O before mixing with unreduced nitrifier and fungal denitrifier N_2O. Reduction of bacterial N_2O is modeled using $^{18}O_{N2O}$ abundances. Using this model, the relative contributions of nitrification and denitrification to N_2O production can be inferred.

The goals of this study were to determine the microbial sources of N_2O in urine-affected soils, quantify the effect of increasing urea content on N_2O emissions, and determine how urine deposition would affect the abundances and activities of N_2O-producing microbial communities. It was hypothesized that increasing urine urea content would result in higher N_2O emissions and increase the growth and activity of both nitrifiers and denitrifiers. To achieve the study goals, a factorial time-series laboratory incubation experiment was conducted. Soil microcosms were injected with two concentrations of urea urine containing $^{15}N^{13}C$ dual isotope-labeled or natural abundance urea. Gas fluxes were sampled periodically and isotope abundances were quantified. Soils were destructively sampled and N-cycling gene and gene transcript abundances were measured.

4.4 Materials and Methods

4.4.1 Soil collection and microcosm preparation

To evaluate the effects of urine on N-cycling microbial abundance, activity, and N_2O emission rates, a microcosm incubation study was designed (Fig. 4.2). Soil cores from a study field site near Lanigan, SK (51.863, -104.893, see Ch. 3) were collected for the incubation experiments. Briefly, a pre-existing grass-alfalfa (*Bromus biebersteinii, Medicago sativa*) pasture was divided into triplicate paddocks and sod seeded with sainfoin (*Onobrychis viciifolia*) or cicer milkvetch (*Astragalus cicer*) treatments. The site features Black Chernozemic soils formed on glacial till. For this study, soil cores were randomly collected from each cicer milkvetch paddock, divided into 0-5 cm and 5-10 cm depths, then sieved through 2 mm ethanol-sterilized sieves and stored at 4 °C. Collected soil was a loam texture, with a pH of 7.2, NO_3^--N content of 190 mg kg^{-1}, and NH_4^+-N content of 5.6 mg kg^{-1}. Soils were uniformly wetted to 80% field capacity and packed into size 40 dram vials at field bulk densities of 0.85 g cm^{-3} for the surface and 1.20 g cm^{-3} for the subsurface layers, resulting in 38% and 54% water-filled pore space (WFPS) for surface and subsurface layers, respectively. This moisture level was chosen to represent realistic field conditions and to not exceed 100% field capacity following urine injection. Each soil layer was 4 cm for a total depth of 8 cm. Microcosms were covered with perforated parafilm to allow gas exchange but maintain soil moisture levels. Microcosms were then pre-incubated at 24 °C to allow biological activity to stabilize.

Following pre-incubation, microcosms were randomized with four microcosms per group and treated with either natural abundance urine, $^{15}N^{13}C$-urea urine, or H_2O (control) (Fig. 4.2). Beef cattle urine was used to mimic the chemistry of a real-world deposition event. To determine the rates of urine application, urine from cattle that grazed in the field study was collected. This urine was analyzed for urea content and found to contain 3.5 g urea L^{-1} (Prairie Diagnostic Services, Saskatoon, SK). The first concentration of urea treatment was set at this level of 3.5 g L^{-1} (low urea) and the second concentration was set at 7.0 g L^{-1} (high urea). Both treatment concentrations are consistent with reported cattle urea concentrations of 2.1-19.2 g urea L^{-1} and within the proportion of urea in total urine N (Dijkstra et al., 2013). Additionally, the high urea treatment is comparable to average beef cattle urine N concentrations (Selbie, Buckthought, & Shepherd, 2015).

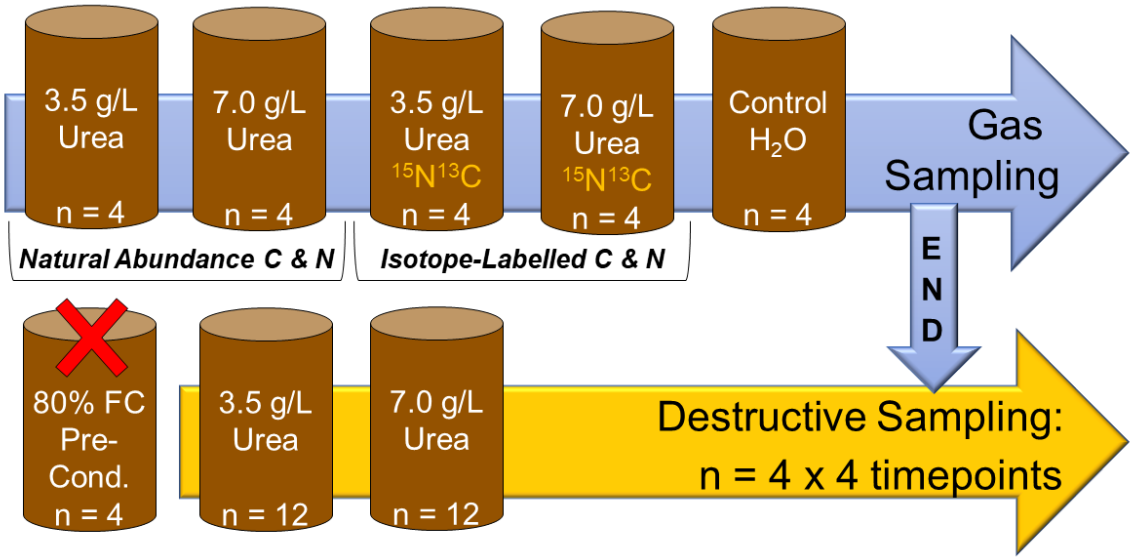

Figure 4.2: Incubation experiment design and sampling layout. Unlabeled soils were destructively sampled immediately prior to urine injection (0 h), then at 8 h, 36 h, and 168 h. All samples (i.e. natural abundance and $^{13}C^{15}N$ labeled) were destructively sampled at 240 h.

Urine collected from beef cattle for soil application had a urea concentration of 19.2 g L^{-1} (Prairie Diagnostic Services) and was subsequently diluted with artificial urine saline solution as described by van Groenigen, Kuikman, et al. (2005) to concentrations slightly below the targeted 3.5 and 7.0 g urea L^{-1} (Table 4.1). Urine was brought up to the final urea concentrations of 3.5 and 7.0 g L^{-1} through the addition of either $^{15}N^{13}C$-labeled or unlabeled natural abundance urea. Dual-

isotope labeled urine was made by adding $^{15}N^{13}C$-urea to urine to achieve 4X natural abundance levels of urea-C and urea-N (4.4 atom% urea-^{13}C; 1.6 atom% urea-^{15}N). An equivalent amount of unlabeled urea was added to natural abundance sample urine. Total urine C and N was determined using a TOC-V CPN (Shimadzu Corporation, Tokyo, Japan).

Table 4.1: Microcosm experiment urine composition.

Treatment	Urea-N	Urea-C	Total N	Total C	Proportion as Urea	
	g L^{-1}				% urea-N	% urea-C
3.5 g L^{-1} urea	1.6	0.7	2.4	4.8	68.5	14.5
7.0 g L^{-1} urea	3.3	1.4	4.8	8.6	68.5	16.3

A urine application of 8 mL per microcosm at the above concentrations was selected to be consistent with cattle urine patch loading rates of 5 L m^{-2} (Boon, Robinson, Chadwick, & Cardenas, 2014; Williams & Haynes, 1994) and 50 mL kg^{-1} soil used in previous microcosm studies (van Groenigen, Kuikman, et al., 2005). One set of microcosm groups designated for GHG sampling and final destructive sampling at 240 h received either $^{15}N^{13}C$-urea or natural abundance urea urine (Fig. 4.2). A second set of microcosm groups designated for destructive soil sampling at 8, 36 and 168 h likewise received natural abundance urine while control microcosms received an equivalent amount of distilled H_2O. Treatment urine was injected into the microcosms using dual-port 25 G Whitacre spinal needles from 0-8 cm at a rate of 1 mL cm^{-1}. This was done to avoid preferential flow down the sides of the microcosms which would cause accumulation of urine at the bottom. Following urine or H_2O injection, microcosms had a surface and subsurface layer WFPS of 47% and 65%, respectively. To minimize temporal variation between treatment groups, treatment groups were injected simultaneously. For example, the first replicates of the 3.5 g L^{-1} natural abundance gas, 3.5 g L^{-1} isotope-labeled gas, and 3.5 g L^{-1} 8 h destructive sampling microcosms were injected at the same time, followed by the subsequent replicates. Injection of treatment group destructive samples (i.e. 36 h and onward) occurred soon afterward.

Following urine injection, GHG sampling microcosms were sealed in 1 L canning jars and flushed with ultra-zero air at a rate of 1 L min^{-1} for 7 min. Destructive sampling microcosms were covered with parafilm. Samples were then incubated in a dark chamber at 24 °C over the next 240 h. Pre-condition (time zero) samples were sealed, flushed, and incubated for 8 h prior to urine injection, then headspace gases were sampled and soils destructively sampled.

4.4.2 Greenhouse gas and soil sampling

Experiment length and sampling timing were determined through a pre-experiment. Peak N_2O emission periods were targeted for destructive sampling and increased gas sampling to improve GHG flux resolution in the main experiment based on the results of this pre-experiment. Immediately following urine injection, microcosm headspace gases were sampled in regular intervals, initially with higher frequency (every 2 h for 12 h), then every 4 h for 24 h around the expected 36 h peak and every 24 h after 72 h. Headspace gases were mixed with a 35 mL syringe through the septa then 35 mL withdrawn and transferred to an evacuated 8 mL Exetainer. Immediately following sampling, jars were flushed with ultra-zero gas for 7 min at 1 L min^{-1}.

Destructive soil samples were taken at 8 h, 36 h, and 168 h time points from natural abundance urine microcosms, with all labeled and natural abundance microcosms destructively sampled immediately following the final 240 h gas sampling event. At the time of sampling, soil microcosms were emptied into a sterilized beaker, homogenized, transferred into sterile 1.5 mL microcentrifuge tubes, and immediately flash frozen in liquid N_2 before being transferred into storage at -80 °C awaiting extraction. Small soil core samples from control gas microcosms were collected with sterilized metal straws (5 mm diameter), homogenized in sterile beakers, and immediately flash frozen in liquid N_2. Reductions in control soil weight from coring were recorded to normalize control gas fluxes.

4.4.3 Quantification of greenhouse gases, isotope abundances, and isotopomer ratios

All GHG quantification and isotope measurements were performed at the Prairie Environmental Agriculture Research Laboratory (PEARL, University of Saskatchewan, Saskatoon, SK). Gases were quantified on a SCION 456 GC (SCION Instruments, Livingston, Scotland) fitted with a thermal conductivity detector (TCD) for CO_2 and an electron capture detector (ECD) for N_2O abundances. Isotope gas samples were diluted then analyzed on a range of Picarro Cavity Ringdown Spectrometers (CRDS, Picarro, Inc., Santa Clara, CA). $\delta^{13}CO_2$ was determined using a Picarro G2201-I CRDS. Natural abundance $\delta^{15}N_2O\alpha$ and $\delta^{15}N_2O\beta$ isotopomers as well as total $\delta^{15}N_2O$ for isotope-labeled samples were performed on two separate Picarro G5131-I CRDS. Isotope-labeled N_2O concentrations were used to determine the contributions of urea-N and urea-C to observed N_2O and CO_2 fluxes using the atom fraction mixing model. Natural

abundance isotopomer ratios were used in the sample mapping reduction-mixing model described by Lewicka-Szczebak et al. (2017) to determine relative contributions of nitrifiers and denitrifiers to observed N_2O fluxes. Nitrifier and denitrifier ratios were adjusted to bring values within a range between zero and one. For each microcosm, the minimum and maximum values were found and set to a minimum value of zero and maximum of one to create a regression line. All other values were adjusted proportionally using the regression line for each microcosm. Unadjusted values are available in Fig. D4.

4.4.4 Quantification of nitrogen cycling genes and gene transcripts

Soil RNA and DNA was extracted using the RNeasy PowerSoil Total RNA Kit coupled with the RNeasy PowerSoil DNA Elution Kit according to the manufacturer protocols (QIAGEN, Hilden, Germany). To minimize RNA losses, extraction tubes were chilled on ice prior to the addition of frozen soil then immediately placed back on ice. All tools were sterilized and treated with RNase inhibitors (RNase AWAY, Molecular BioProducts, San Diego, CA). Soil RNA and DNA extracts were quantified using a Qubit 4 Fluorometer with the Qubit RNA HS Assay Kit and the Qubit dsDNA HS Assay Kit (Invitrogen, Waltham, MA). Samples yielding less than 5 ng ul^{-1} total RNA were re-extracted and eluted in a smaller volume of nuclease-free water. All DNA and RNA samples were stored at -80 °C awaiting further analysis.

A two-step quantitative reverse-transcription polymerase chain reaction (qRT-PCR) was used to quantify N-cycling gene transcripts. First, total RNA was standardized to 5 ng ul^{-1} on ice. Standardized samples were then treated with DNase to remove contaminating genomic DNA (gDNA), then reverse transcribed to complementary DNA (cDNA) for future qPCR analysis (SuperScript IV VILO Master Mix with ezDNase Enzyme, Invitrogen).

Prior to qPCR analysis, cDNA or gDNA concentration was optimized to mitigate inhibitor effects. qPCR master mix components and primers were also optimized to achieve a reaction efficiency between 90-110%. Once an acceptable reaction efficiency had been achieved, cDNA and gDNA samples were randomized across 5 plates for each gene being analyzed. Each plate contained a replicate standard curve as well as an internal control sample – one sample that was on another plate – to ensure reaction reproducibility. A combination of master mixes was used based on which polymerase enzyme performed best for the target gene. Platinum SYBR Green

qPCR SuperMix-UDG (Invitrogen) and PowerUp SYBR Green Master Mix (Applied Biosystems, Waltham, MA) were used with published primers (Table E1). Target gene and gene transcript abundances were then quantified on an Applied Biosystems Quantstudio 3 using published cycling settings (Table E2) and a seven-point descending log standard curve of 10^7 to 10 gene copies of cloned genes from a single gene target obtained from either a pure culture or a synthesized DNA fragment (Table E3). Clade II nosZ was constructed from 10 cloned environmental amplicons whose identity was confirmed by DNA sequencing (Table E3).

4.4.5 Statistical analyses

All statistical analyses were performed using R v3.6.3 (R Core Team, 2020). General linear mixed effects (GLME) models were used to test differences in hourly and cumulative gas flux rates (Bates et al., 2015). Due to gas fluxes from individual microcosms being measured multiple times throughout the experiment, a repeated measures design was used. Microcosm was designated as a random effect while treatment and time were fixed effects. Gene and gene transcript abundances were modeled using general linear models (GLM) with treatment and time as fixed effects. A natural log (ln) transformation was applied to some model response variables to bring model residuals to normality. A square root transformation was used on the hourly N_2O flux rate model when an ln transformation did not improve model residual normality. A Type-III analysis of variance (ANOVA) F test was used to determine the significance of each fixed term (Fox & Weisberg, 2019). If a significant interaction was found, post hoc testing was performed with estimated marginal means (EMM) (Lenth, 2020). Pairwise contrasts were performed to test differences between treatments within each time point using the Tukey adjustment for family-wise error.

4.5 Results

4.5.1 Greenhouse gas fluxes

The highest CO_2 flux rates were measured 2 h after the addition of urine or water to the microcosms followed by a rapid decline in flux rate (Fig. 4.3 A). The high urea soils had the largest initial CO_2 flux rate of the two urea application rates ($p = 0.033$). Low and high urea soils maintained larger CO_2 flux rates than the control ($p < 0.001$) until the 24 h measurement, where a

secondary peak in flux rate caused the control CO_2 emissions to increase to the same flux rate as the low urea soils ($p = 0.890$) but not the high urea soils ($p < 0.001$). A secondary peak was observed in both high and low urea soils after 28 h. From 28 h onward, both urea treatment CO_2 flux rates remained larger than the control ($p < 0.050$) until 192 h for the low urea soils and 240 h for the high urea soils. Cumulative CO_2 fluxes (Fig. 4.3 C) were greater than the controls for both low and high urea soils at all time points ($p < 0.001$). Cumulative CO_2 flux was greater in high vs low urea soils by 6 h ($p = 0.020$) until experiment end at 240 h ($p < 0.001$).

Rates of N_2O flux increased steadily for both high and low urine treatments following urine addition and peaked shortly after (Fig. 4.3 B). A large spike in control N_2O flux rate was measured at 24 h followed by a rapid decline. Secondary N_2O peaks appeared in both urine amended soils after 28 h coinciding with secondary CO_2 peaks. High and low urea soil flux rates did not differ until the 168 h measurement where the high urea soil flux was larger ($p = 0.050$). By 240 h, high urea soil N_2O flux rates declined and converged with the low urea soil flux rates ($p = 0.154$). By comparison, after 168 h, control N_2O flux rates increased to become larger than both high and low urea soils at 216 h (low urea: $p < 0.001$; high urea: $p = 0.049$) and 240 h ($p < 0.001$). At the end of the experiment, the cumulative N_2O flux (Fig. 4.3 D) of low urea soils was not different from the control ($p = 0.168$) or high urea soils ($p = 0.759$), while the high urea soil flux was larger than the control ($p = 0.047$).

Outliers in N_2O flux rate occurred in one individual microcosm from every replicate group of samples (one in four) in both natural abundance and isotope-labeled microcosms (Figs. D1-D3). Since microcosms were randomly assigned to treatment groups, it is highly unlikely that these outliers were the product of a biological pattern resulting from microcosm construction. These outlier samples had substantially larger initial or secondary N_2O flux rate peaks which resulted in cumulative fluxes four times larger than the treatment mean. These “hotspots” did not have an accompanying difference in CO_2 emissions or shift in N_2O isotopomer ratios. Isotope-labeled hotspots emitted less urea-N as N_2O initially before continually increasing emission rates of urea-N as N_2O, while treatment means of the other three replicates decreased. Due to cumulative N_2O fluxes four times larger than the treatment means, these samples were removed from both natural abundance and isotope-labeled low urea and high urea treatments ($n = 3$ for all treatments). No outliers were found in the control, therefore sample size remained at $n = 4$. While these samples

were treated as outliers, the differences in N_2O flux and urea-N conversion to N_2O remain an interesting anomaly, particularly at a consistent frequency of one out of four.

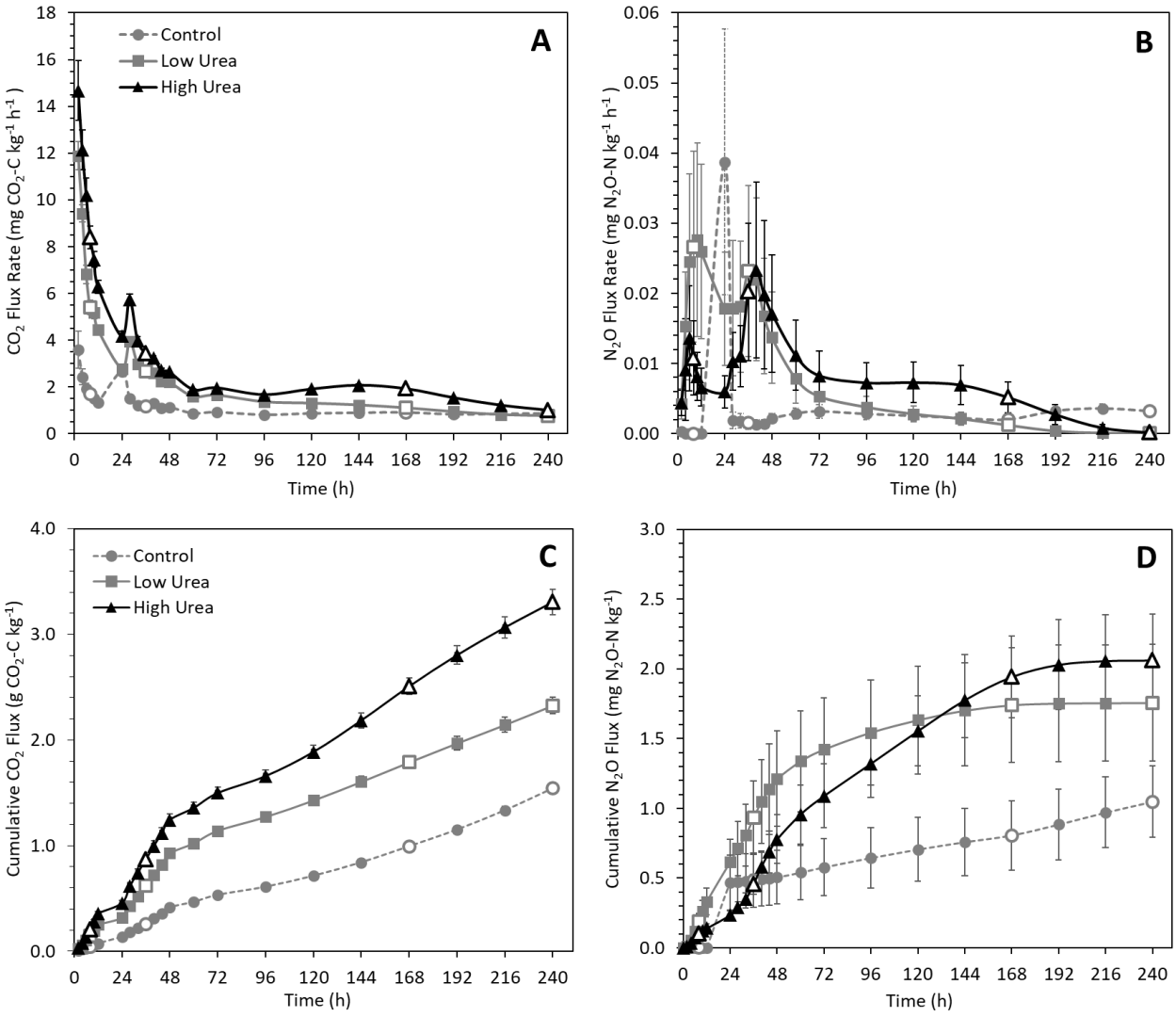

Figure 4.3: Hourly CO_2 (A) and N_2O (B) flux rates and cumulative CO_2 (C) and N_2O (D) fluxes of natural abundance microcosms. Hollow points are destructive sampling points. Error bars represent SE.

Using average urine patch size and number of urination events for a single cow in one day (Selbie et al., 2015), the 10 d flux of CO_2 and N_2O from one cattle's average daily urine output was calculated (Tables 4.2 and 4.3). For these extrapolations, an average wetted area of 0.24 m^2 and urination frequency of 10 events per day were used. While patch wetted area varies in size from 0.14 – 0.49 m^2 per event, the average was used to represent average patch area over 10 events.

Since microcosms were designed with edges constraining the flow of urine, projections were based on wetted area only. These projections are conservative since they do not include the diffusional area of the urine patch, which is a significant source of N_2O emissions in urine patches once urine-N diffuses from the wetted area into the surrounding soil (Marsden, Jones, & Chadwick, 2016).

Table 4.2: Cumulative CO_2 and urea-CO_2 fluxes over a 10 d period from a single cow's average daily urination.

Treatment	Total Flux	Avg. Patch	Daily Cow Avg.
	g CO_2-C m^{-2}	g CO_2-C	g CO_2-C d^{-1}
Control	17.4 a	4.17	41.7
Low Urea	27.9 b	6.70	67.0
High Urea	39.5 c	9.49	94.9
	---Urea-Derived Fluxes---		
Low Urea	1.82	0.44	4.37
High Urea	3.76	0.90	9.02

Cattle excreting twice as much urea on average would double the CO_2 derived from urea (Table 4.2). Considering the rapid hydrolyzation of urea to CO_2 by urease, this result is expected. Results suggest that doubling the urea concentration only slightly increases average N_2O emissions from the urine patch (Table 4.3). Considering the wide range of observed cattle urea-urine concentrations (1-20 g L^{-1}, Dijkstra et al., 2013), differences may be more pronounced in a wider range of urea treatments. If higher urea concentrations tend to create larger N_2O fluxes, the cumulative effect may substantially increase urine patch emissions over the lifetime of a cow.

Table 4.3: Cumulative N_2O and urea-N_2O fluxes over a 10 d period from a single cow's average daily urination.

Treatment	Total N_2O			Total Urea-N_2O		
	Flux	Avg. Patch	Daily Cow Avg.	Flux	Avg. Patch	Daily Cow Avg.
	mg N_2O-N m^{-2}	mg N_2O-N	mg N_2O-N d^{-1}	mg N_2O-N m^{-2}	mg N_2O-N	mg N_2O-N d^{-1}
Control	72.3 a	17.3	173	---	---	---
Low Urea	121 ab	29.1	291	18.7 a	4.48	44.8
High Urea	142 b	34.1	341	34.8 b	8.35	83.5
			---Outliers---			
Low Urea	377	90.5	905	42.4	10.2	102
High Urea	593	142.2	1422	113	27.2	272

Patches behaving similar to the N_2O flux outliers would emit approximately three to four times more N_2O emissions than mean experimental fluxes observed here (Table 4.3). Since outliers occurred once per treatment group, it was not possible to compare differences between outliers and the treatment means statistically.

4.5.1.1 Urea-derived greenhouse gas fluxes

Cumulative urea-derived CO_2 fluxes increased rapidly following urine addition (Fig. 4.4 A). The low urea soil cumulative flux leveled off while the high urea soil flux increased again after 96 h. The high urea soil urea-CO_2 flux rate was consistently larger than low urea soils throughout the study ($p < 0.05$), except for at 60 h (data not shown). Cumulative urea-CO_2 flux was largest in high urea soils at all measurements ($p < 0.05$). After 240 h, cumulative high urea soil urea-CO_2 was twice as large as that of low urea soils ($p < 0.001$).

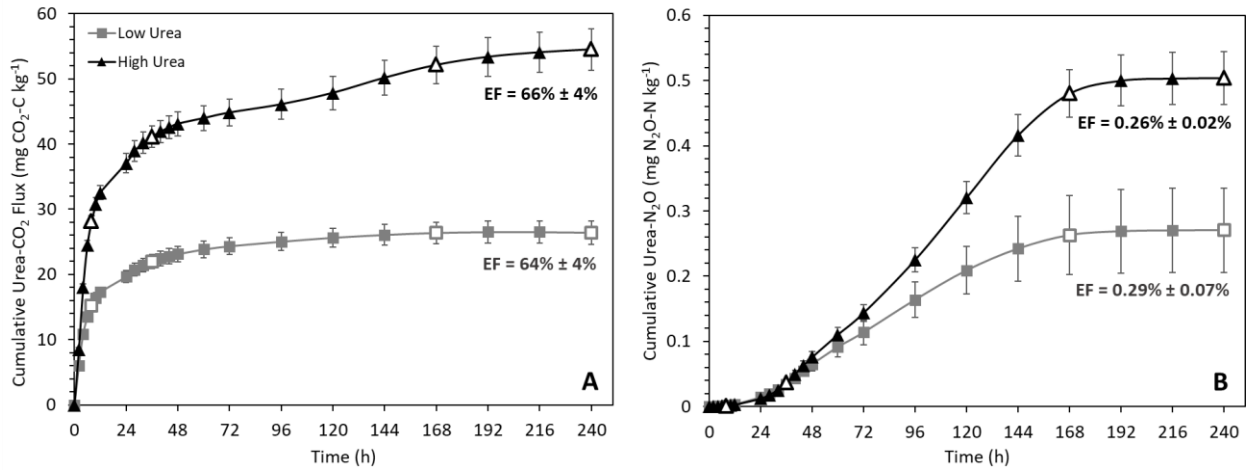

Figure 4.4: Cumulative urea-derived CO_2 (A) and N_2O (B) fluxes measured from microcosms treated with isotope-labeled $^{13}C^{15}N$ urea. Hollow points are destructive sampling points. Error bars represent SE. Cumulative emission factors (EF) are listed as mg urea-derived CO_2-C or N_2O-N produced per mg urea-C or urea-N added to soil.

Similar to the natural abundance microcosms, each treatment had one N_2O flux outlier that emitted large amounts of both total and urea-derived N_2O; these data points were removed. Urea-derived N_2O fluxes began increasing as of the 24 h measurement (Fig. 4.4 B). The urea-N_2O flux rate was larger in low urea soils at the 4 h and 6 h measurements ($p \leq 0.01$) and in high urea soils from 144 h to 216 h ($p < 0.05$; data not shown). This is mirrored by the cumulative urea-N_2O flux,

where low urea soil fluxes were larger from 4 h to 8 h ($p < 0.05$) and high urea soil fluxes were larger from 144 h to 240 h ($p < 0.05$). At the end of the experiment, the cumulative urea-derived N_2O flux was twice as large in high urea soils ($p = 0.007$). Despite larger urea-derived CO_2 and N_2O fluxes in high urea soils, emission factors were comparable between both treatments. While outlier hotspots had larger urea-N_2O fluxes, urea-N contributed a lower proportion of the total N_2O flux (Table 4.4).

Table 4.4: Proportion of GHG fluxes derived from urine-urea in $^{15}N^{13}C$ labeled urea soils.

Treatment	Urea Gas Flux		Gas Flux		Proportion of Flux	
	mg CO_2-C kg^{-1}	mg N_2O-N kg^{-1}	g CO_2-C kg^{-1}	mg N_2O-N kg^{-1}	% CO_2	% N_2O
Low Urea	26.4	0.27	2.33	1.32	1.1	20.5
High Urea	54.5	0.50	3.31	2.00	1.6	25.0
			---Outliers---			
Low Urea	---	0.61	---	5.91	---	10.3
High Urea	---	1.64	---	10.5	---	15.6

4.5.1.2 Nitrifier and denitrifier contributions to N_2O fluxes

Patterns in N_2O emission sources based on isotopomers differed between urine treatments and the controls, but with minimal differences between urine treatments. Bacterial denitrification composed the majority (64-99%) of initial N_2O emissions as nitrifier contributions increased in the urine treatments (Fig. 4.5 A). Nitrifiers provided an increasing proportion of N_2O emissions from treatment application until 12 h. Nitrifier contributions then decreased until 24 h before increasing and peaking at 28 h. High urea soils tended to have smaller denitrifier contributions at 12 h and 24 h ($p = 0.253$ and 0.187). After 28 h, nitrifier contributions declined and leveled off until 192 h. Bacterial denitrifier emissions decreased as low nitrifier contributions increased after 192 h. High urea soils sustained a longer bacterial denitrifier flux by 216 h and 240 h ($p < 0.001$). Control soil N_2O sources varied much in comparison to urine treated soils throughout the incubation (Fig. 4.5 B). The majority of the initial low N_2O flux in the controls was contributed by nitrifiers (64-86%) while bacterial denitrifiers contributed much less. However, the N_2O flux was near-zero in the controls during this time, indicating nitrifiers contributed the majority of this minimal flux. Bacterial denitrifier N_2O increased by 24 h as N_2O flux rate increased and by 60 h,

overtook nitrifier contributions holding a near-equal ratio of 45% nitrifier:55% denitrifier steady until the end of the incubation.

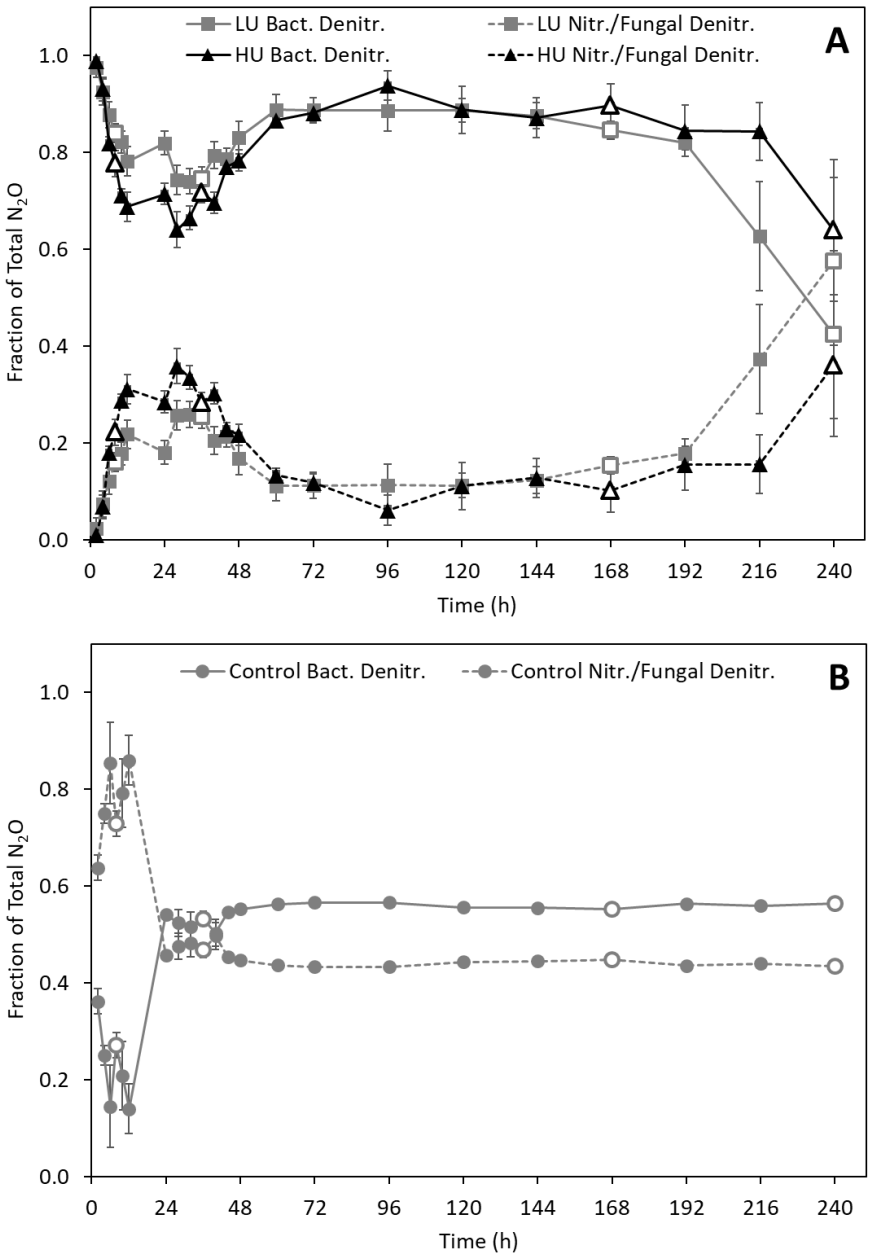

Figure 4.5: Fractions of total N_2O derived from bacterial denitrification and nitrification and/or fungal denitrification from low urea (LU) and high urea (HU) urine treatments (A) and controls (B). Hollow points are destructive sampling points. Error bars represent SE.

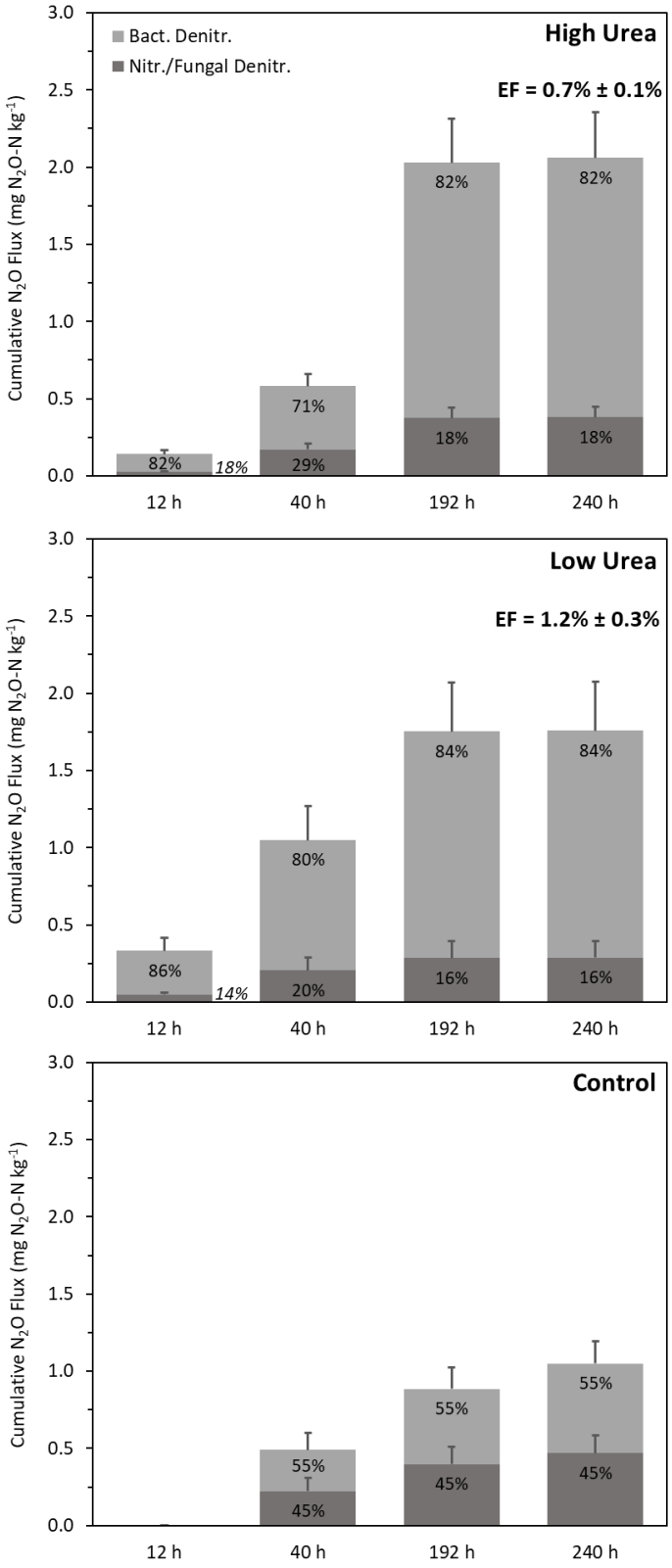

Figure 4.6: Relative contributions of nitrifiers and denitrifiers to total N_2O from soils after 12, 40, 192, and 240 h. Error bars represent SE. Cumulative emission factors (EF) are listed as mg N_2O-N produced per mg urine-N added to soil.

The relative contributions of nitrifiers and denitrifiers to cumulative N_2O fluxes shifted over the course of the experiment (Fig. 4.6). Denitrifier N_2O fluxes from soils treated with high rates of urea were initially delayed compared to low urea at 12 h and 40 h before increasing and reaching a similar cumulative flux at 192 h. The emission factor for high urea soils was smaller than low urea soils, indicating less urine and soil N was released as N_2O per unit urine-N added in high urea soils.

4.5.2 Nitrifier abundance and transcription activity

Archaeal and bacterial nitrifiers varied in growth responses to urine introduction and concentration. Populations of AOA were larger than AOB, but AOA gene copy number did not differ very much among treatments or with time throughout the experiment (Fig. 4.7 A). However, high urea soils had a larger AOA population than the control ($p = 0.012$) but not low urea soils ($p = 0.059$) by 36 h, and the low urea soil AOA population was 59% larger than the control by 240 h ($p = 0.003$). In contrast, AOB populations varied throughout the experiment and had increased in urine treatments by 240 h (Fig. 4.7 B). Urine addition initially diminished AOB populations in low urea soils to levels below the controls ($p = 0.003$), but the populations recovered to control levels in both urine treatments by 36 h. By the end of the incubation (240 h), AOB gene copy numbers were three and ten times higher than controls in low and high urea soils, respectively ($p < 0.001$).

Quantification of *amoA* gene transcripts revealed different responses in gene transcription between AOA and AOB; transcript counts of AOB were higher than AOA in both the high and low urea soils. Abundance of archaeal *amoA* transcripts were not significantly different between urea treatments and time points ($p = 0.085$). However, AOA transcript copies in low urea soils tended to be the highest of all treatments at 168 h, and control copies highest at 240 h. Many samples fell below the detection range of the AOA RT-qPCR standard curve, indicating minimal AOA activity in most microcosms. In contrast, bacterial nitrifier populations increased *amoA* transcription rates in response to urine addition (Fig. 4.7 D). Both high and low urea soils had higher bacterial *amoA* transcription rates than the control from 36 h to 240 h ($p < 0.001$) but were not significantly different from one another, with the highest observed activity at the 168 h sampling.

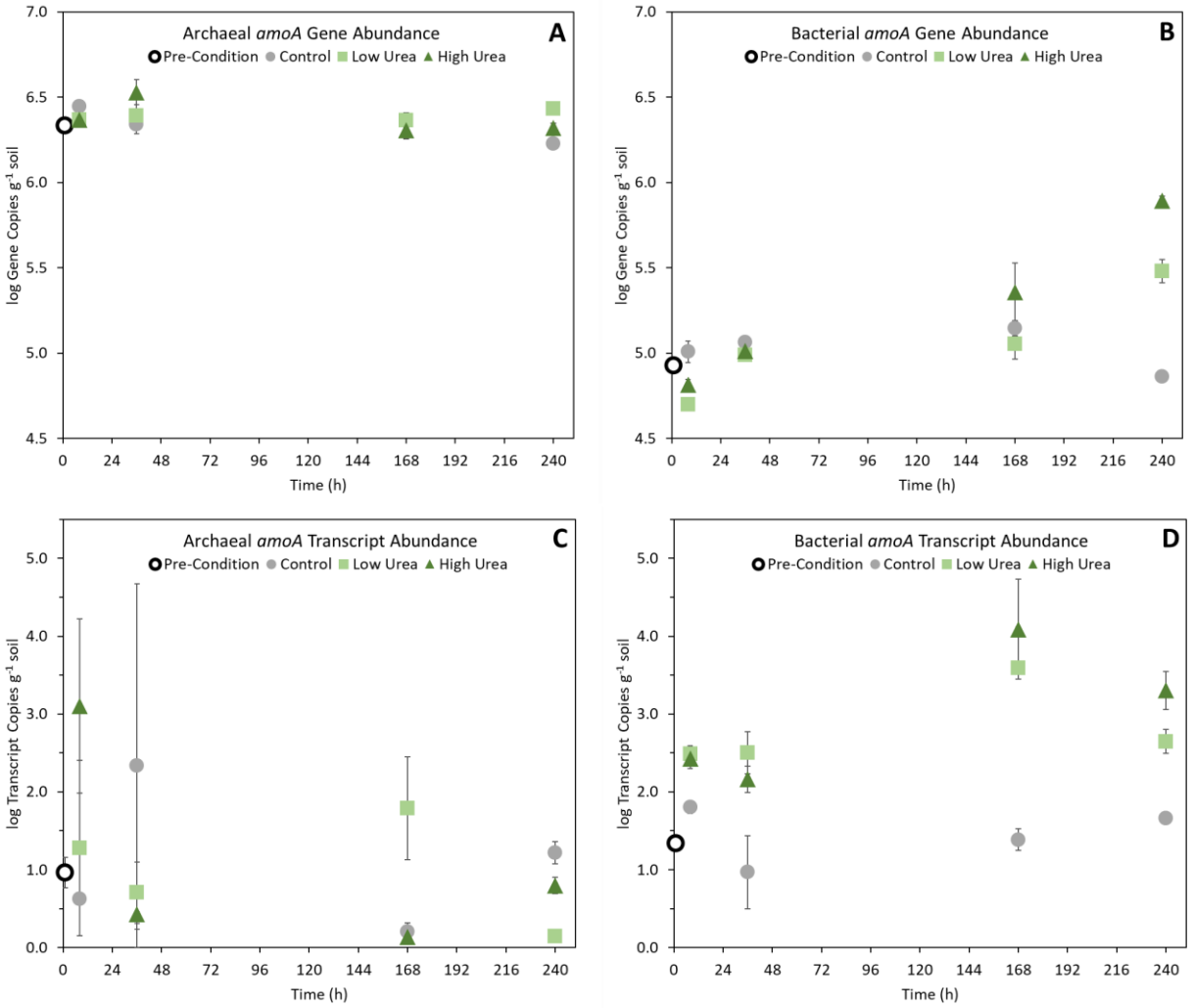

Figure 4.7: Archaeal (A) and bacterial (B) *amoA* gene copy abundances (DNA); archaeal (C) and bacterial (D) *amoA* gene transcript abundances (mRNA). Error bars represent SE.

4.5.3 Denitrifier abundance and transcription activity

Comparisons between organisms possessing nitrite reductase genes revealed differences in growth response to urine addition by the two groups, *nirK* and *nirS*. Denitrifiers possessing *nirK* displayed less dynamic growth responses (Fig. 4.8 A). Populations in urine treated soils decreased slightly in abundance as control soil communities increased by 168 h ($p < 0.01$); all treatments had converged by 240 h ($p > 0.05$). By comparison, *nirS* populations displayed more variation over time and between treatments at 8 h and 168 h (Fig. 4.8 B). Both high urea soils and the controls had larger *nirS* populations than low urea soils at 8 h ($p < 0.01$) before converging to similar sizes by 36 h. By 168 h, the high urea soils had a 8X and 18X larger *nirS* gene counts than the low urea

and control soils, respectively ($p < 0.001$), and decreased by 240 h. Populations of *nirK* were larger than *nirS* throughout the experiment in all treatments except for in high urea soils at 168 h.

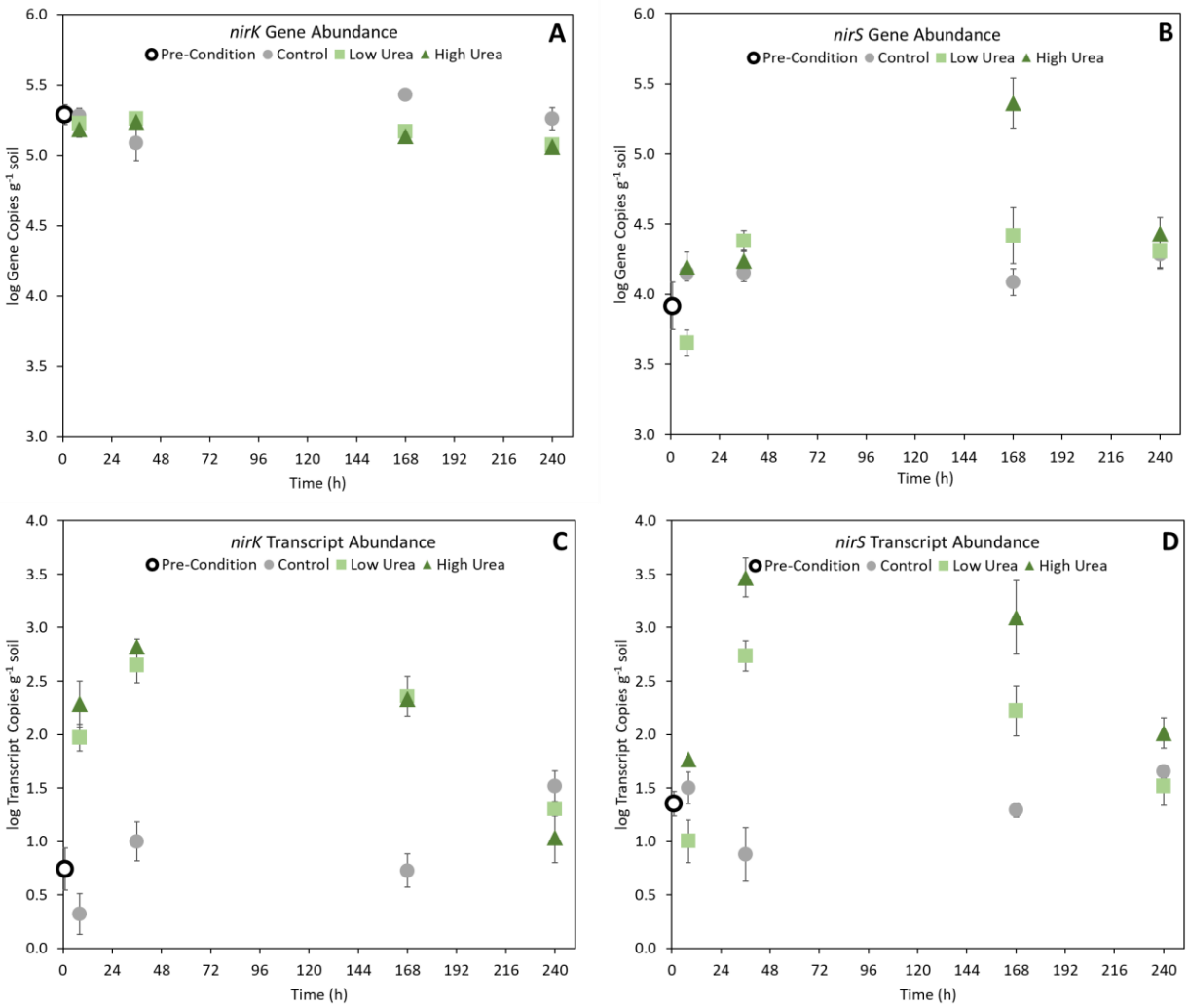

Figure 4.8: *nirK* (A) and *nirS* (B) gene copy abundances (DNA); *nirK* (C) and *nirS* (D) gene transcript abundances (mRNA). Error bars represent SE.

Transcript abundances increased in both *nir* groups following urine addition. Transcripts of *nirK* were higher in both treatments than the control soon after urine addition ($p < 0.001$), maintaining a higher abundance until declining by 240 h (Fig. 4.8 C). Production of *nirS* transcripts increased by 36 h and 168 h in urine treatments (Fig. 4.8 D). This was particularly true in high urea soils, which were 389X and 62X larger than the controls ($p < 0.001$), and four to seven times larger than low urea soils ($p < 0.01$), respectively. Low urea soils had lower transcript abundance

than high urea soils at 8 h ($p = 0.005$) but was greater than the control at 8 h and 168 h ($p < 0.01$). Transcript abundance of *nirS* was generally higher than *nirK* from 36 h onward in high urea soils.

Similar to the two *nir* genes, clades I and II of *nosZ* displayed differences in community growth. Clade II communities were 70X more abundant than clade I. Organisms possessing *nosZ-I* did not respond strongly to urine introduction (Fig. 4.9 A). While ANOVA revealed a significant interaction between treatment and time ($p = 0.007$), post-hoc EMM contrasts revealed few differences. High urea was soils had lower gene abundance than the control at 8 h ($p = 0.027$), and lower abundance than low urea soils at 240 h ($p = 0.034$). However, growth of *nosZ-II* organisms was more dynamic among treatments and over time (Fig. 4.9 B). Control and high urea soil communities were both greater than low urea at 8 h ($p = 0.038$ and $p = 0.007$). After 36 h, high urea soil communities were larger than both low urea soils and the control ($p < 0.001$). At 168 h, the control communities were larger than both treatments ($p < 0.001$), of which high urea was the largest ($p = 0.032$). All treatments returned to similar *nosZ-II* gene abundances after 240 h.

While *nosZ-I* organisms did not respond strongly in terms of population growth, transcript abundances indicated an increase in activity with urine addition (Fig. 4.9 C). Transcripts were consistently higher in urine soils than the controls from 8 h to 168 h ($p < 0.01$) before converging with control levels at 240 h. Urine soil transcripts differed at 36 h ($p = 0.004$). Control soil *nosZ-II* transcripts were often below the RT-qPCR assay detection limit (< 10 copies per well). However, both low urea and high urea soil transcription activities were higher than the controls at all time points ($p < 0.001$) before falling below the detection limit at 240 h (Fig. 4.9 D). High urea soil *nosZ-II* transcript counts were higher than low urea soils at 36 h ($p < 0.001$). Clade II transcript counts were higher than clade I throughout the incubation until 240 h, where clade I had higher transcription activity.

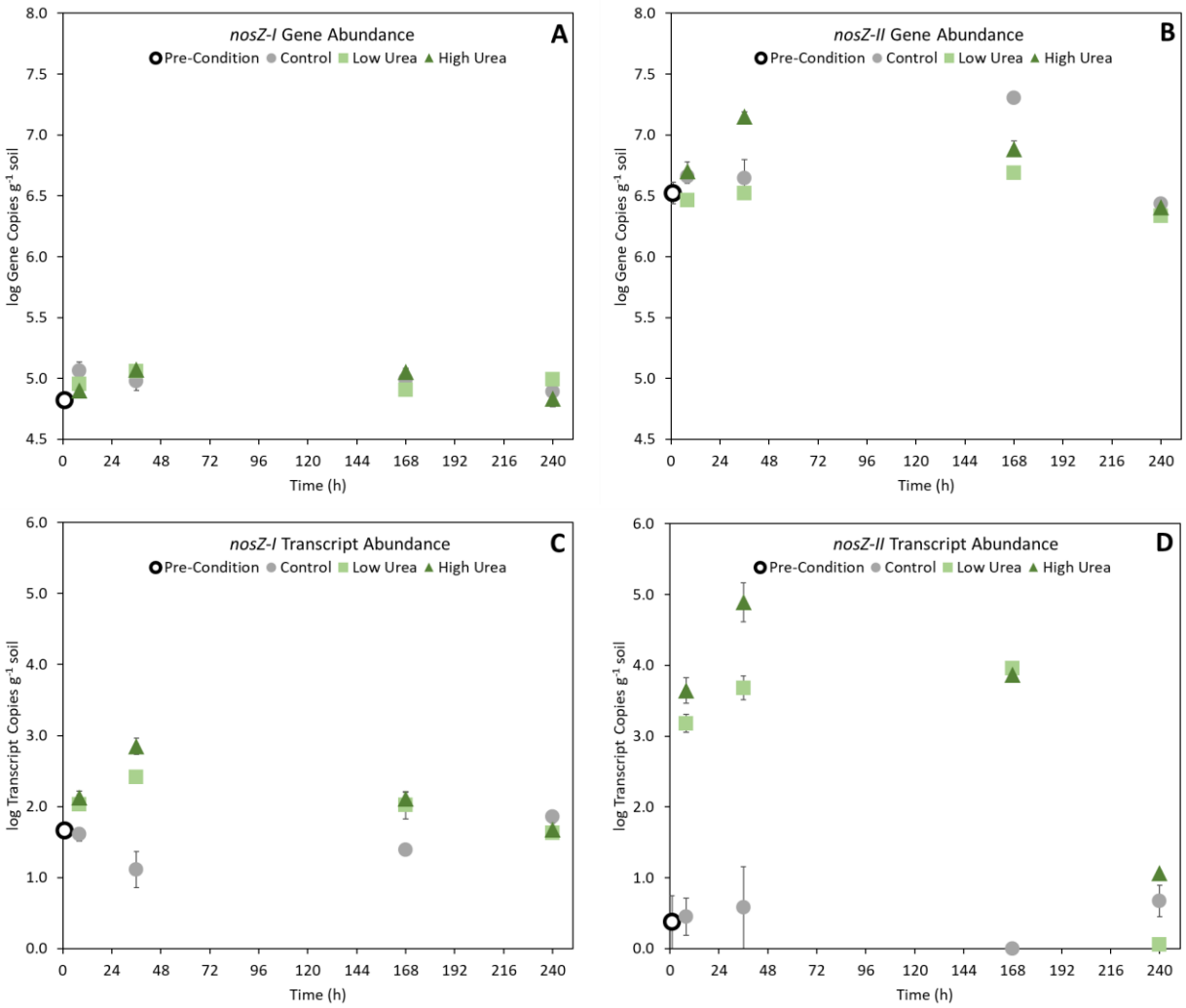

Figure 4.9: *nosZ-I* (A) and *nosZ-II* (B) gene copy abundances (DNA); *nosZ-I* (C) and *nosZ-II* (D) gene transcript abundances (mRNA). Error bars represent SE.

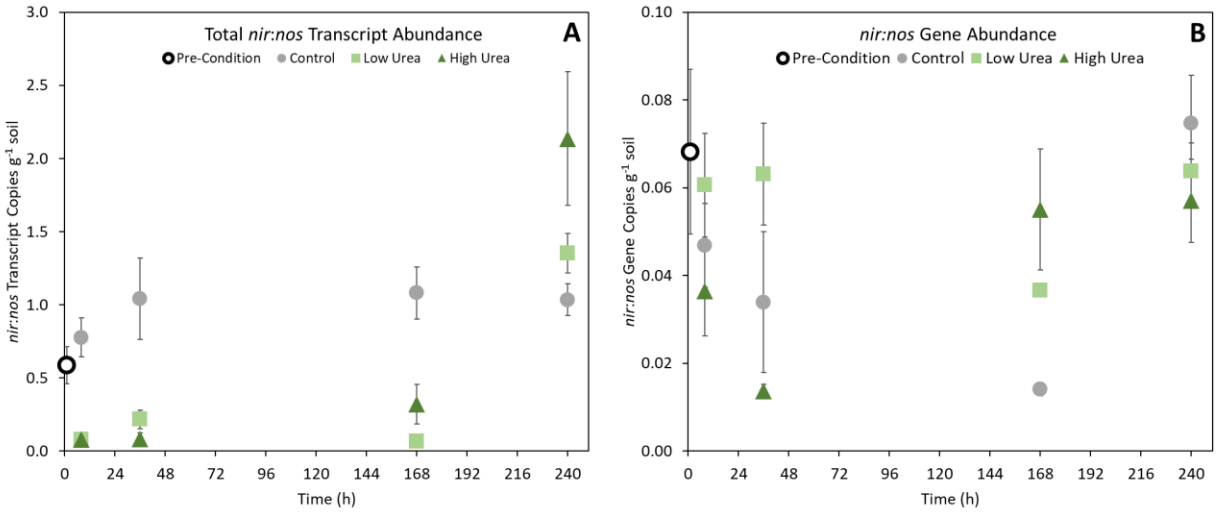

Figure 4.10: *nir:nos* ratios of mRNA transcripts (A) and DNA copies (B) calculated as total *nir* (*nirK* + *nirS*) relative to total *nosZ* (clades I + II). Error bars represent SE.

Ratios of *nir:nos* gene and transcript copies varied between treatments throughout the experiment ($p < 0.001$). Transcript *nir*:*nos* ratios were highest in control soils through 168 h ($p < 0.05$) due to urine deposition increasing *nosZ* transcription rates and decreasing *nir:nos* transcript ratios in urine treated but not control soils (Fig. 4.10 A). The magnitude of increase in *nosZ* transcription was larger than *nir* in urine treated soils, decreasing ratios until *nosZ* transcription activity slowed to control levels by 240 h. Gene *nir*:*nos* ratios tended to be higher in low urea than high urea soils ($p = 0.078$) but similar to controls. Low urea soils had the highest *nir:nos* gene ratio by 36 h ($p < 0.05$), and high urea soils by 168 h ($p < 0.001$). All treatments had similar *nir:nos* gene ratios by 240 h.

4.5.4 *P450nor* qPCR assay development

While PCR assays produced *P450nor* bands from DNA extracts of some cicer milkvetch field soils using published primers (Novinscak et al., 2016), no such bands were detected in the microcosm study soils. A qPCR method to reliably quantify *P450nor* was not achieved in this study. Optimization of SYBR mix and primer concentration was unsuccessful due to the persistence of multiple non-target qPCR products. Assays above 70% efficiency produced multiple melt curve peaks, which were verified for multiple bands on an agarose gel. Increased efficiency resulted in an increased occurrence of non-target qPCR products in both environmental and pure culture templates. Novinscak et al. (2016) found both fungal *nirK* and *P450nor* in all N_2O-

producing fungal isolates but Higgins et al. (2016) did not consistently detect *nirK*. Therefore, *P450nor* PCR primers remain suited for detection and diversity studies, while fungal *nirK* qPCR assays (Wei et al., 2015) are likely the most suitable method for quantifying fungal denitrification genes.

4.6 Discussion

The introduction of non-bloat legumes to cattle pastures may increase cattle urine urea-N concentration and provide additional N substrate for N_2O production by soil microorganisms following urine deposition. This study sought to determine whether an increase in cattle urine urea content would increase N_2O emissions and to identify the effects of urine deposition on nitrifier and denitrifier population size and activities. Stable isotope probing, N_2O isotopomer abundances, GHG measurement, and gene and transcript abundances of key functional genes in the nitrifier and denitrifier pathways were used to better understand N_2O emissions from urine treated soils in a controlled laboratory incubation. No difference in cumulative N_2O emissions was found between low and high urea soils. This study indicates that increased N intake from non-bloat legumes will not increase net N_2O emissions from urine deposition in pasture soil.

Urine addition to pasture soils stimulated N_2O emissions, but the magnitude of the emissions did not increase proportionally to N addition rates, resulting in a urine-N N_2O emission factor for the high urea soils smaller than the low urea soils. Although high urea soils emitted more urea-N as N_2O than low urea soils, this increase was proportional since urea-N N_2O emission factors were similar between low and high urea soils. Control soils were treated with H_2O and did not contain any urine C substrate; the lack of an immediate increase in control soil N_2O may be due to lack of available C. An influx of urine C likely increased oxygen consumption in urine soils, potentially reducing aerobic nitrifier activity and providing anaerobic conditions favorable to denitrifier N_2O production. Nitrifier and denitrifier contributions to total N_2O emissions followed different trends between high and low urea concentration soils, favoring stronger initial contribution of denitrification in the low vs. high urea treatments (Figs. 4.5 A and 4.6). Denitrifiers contributed most of the urine N_2O emissions throughout despite a delayed response in high urea soils. Urine deposition stimulated AOB but not AOA activity and growth. Following urine deposition, denitrifier *nirS* and *nosZ* clade II increased both gene and transcript abundances while

nirK and *nosZ-I* increased transcription only. Bacterial *amoA* transcript abundance tracked roughly with nitrifier N_2O emissions, and both *nirK* and *nirS* transcripts tracked with denitrifier N_2O emissions in urine treated soils. Denitrification contributed substantially to the larger urine-derived soil N_2O emissions. Initial suppression of denitrification and a large increase in clade II *nosZ* activity in high urea soils reduced net N_2O emissions and resulted in a urine-N emission factor of 0.7% compared to 1.2% in low urea soils, which is comparable to literature reported median emission factors of 1.3% (van Groenigen, Kuikman, et al., 2005).

The lower urine-N N_2O emission factor in high vs. low urea soils was partially due to a short-term toxicity effect from high concentration urea. Urine addition was demonstrated to affect the community structure of AOB and nitrite-reducing bacteria (Orwin et al., 2010) and induce stresses on microbial communities regardless of salt concentration (Bertram et al., 2012; Monaghan & Barraclough, 1992). These effects are particularly strong at higher urea concentrations (Petersen, Roslev, et al., 2004) and suggested to be the result of ammonia and nitrite toxicity. Other studies have reported a similar effect, with lower urine-N loading rates resulting in higher N_2O emissions (Clough et al., 2003). The toxicity effect in high urea soils was short-lived with apparent recovery by around 36 h; at the end of the 240 h incubation period N_2O flux rates were negligible in both urine treatments.

The lack of differences between urine treatment N_2O fluxes is similar to the findings of van Groenigen et al. (2005), who observed no difference in cumulative N_2O emissions relative to the amount of urine-N added to a pasture soil over a 103 d period. Total cumulative N_2O emissions from urine treated soils in this study were lower than literature reported values: 5 mg N_2O-N kg^{-1} dry soil in a 103 d field study (van Groenigen, Kuikman, et al., 2005); 0.84 – 2.77 g N_2O-N m^{-2} in a 25 d soil monolith study (Monaghan & Barraclough, 1993); and 326 mg N_2O-N m^{-2} in a 56 d field study (Boon et al., 2014). These differences are likely the result of the aforementioned studies featuring different soils with differing biological properties and responses, a wider range of urine-N loading rates, and longer measurement periods. However, the cumulative N_2O emissions observed in this study are comparable to the 169 mg N_2O-N m^{-2} over 30 d in a pasture observed by Barneze et al. (2014) who used similar cattle urine-N concentrations (5.5 g N L^{-1}).

Since urea-N_2O fluxes were largest in high urea, but total N_2O fluxes were not, the utilization of soil N or other N compounds in the urine was likely reduced in high urea soils where a delayed N_2O flux was observed (Fig. 4.3). This could be a result of toxicity from urine containing high concentrations of N (Orwin et al., 2010; Petersen, Roslev, et al., 2004) and a higher rate of complete reduction of urea-N to N_2. The observed differences in *nir* and *nos* gene and transcript patterns show different responses of denitrifier groups to urea-N concentration (Fig. 4.8 and 4.9). Similar to urea-N_2O emissions, doubling the urine urea application also doubled urea-CO_2. Carbonaceous urine components other than those derived from urea and soil-derived C account for most of the observed total CO_2 fluxes. However, doubling of urea and total urine C increased total CO_2 emissions by 110% of the urine-induced flux, indicating the potential for soil C loss as urea concentration increases.

The sample mapping method of analyzing N_2O isotopomers (Lewicka-Szczebak et al., 2017) revealed that denitrifiers produced most (82-84%) of the cumulative N_2O following urine deposition (Fig 4.6). The large initial denitrifier flux in urine treatments suggests that denitrifier groups utilize soil N in response to urine deposition (Figs. 4.5 A and 4.6). This is supported by the urea-N_2O flux data, which shows that urea-N was not emitted as N_2O until after 12 h (Fig. 4.4 B). In a urine deposition study, Ambus et al. (2007) suggest that organic urine N constituents stimulated a denitrifier N_2O peak preceding N_2O derived from urine-derived NH_4^+. Their work also indicated that denitrification was a key source of N_2O in urine-affected soils. Other urine deposition studies have observed immediate denitrifier activity following deposition with denitrification being the majority source of total N_2O emissions (Monaghan & Barraclough, 1993; Yamulki et al., 2000). Nitrifier N_2O emissions contributed an increasingly larger proportion of the initial N_2O peak (Fig. 4.5 A). Since PCR did not detect *P450nor* in microcosm samples, the nitrifier/fungal denitrifier flux is likely majority nitrifier-derived. The lack of urea-derived N_2O during this peak suggests that initial nitrifier N_2O fluxes were derived from soil N and other urine N compounds rather than urea-N. While nitrifiers exhibited some response in this study, denitrifiers appear to have contributed the majority of urine-derived N_2O.

Nitrification activity and nitrifier N_2O production have been shown to be dominated by soil AOB populations following urine or N additions (Carey et al., 2016; Di et al., 2014, 2009; Di, Cameron, Sherlock, et al., 2010; Hink, Nicol, et al., 2017; Meinhardt et al., 2018; Sterngren, Hallin,

& Bengtson, 2015). Furthermore, bacterial *amoA* transcripts increase in response to soil wetting (Banerjee et al., 2016) that would occur during urine deposition. In this study, less abundant AOB grew and increased nitrification activity in response to urine addition despite greater archaeal *amoA* gene abundance (Fig 4.7), similar to previous findings (Di et al., 2014; Di, Cameron, Shen, et al., 2010; Sterngren et al., 2015). However, unlike Di et al. (2010), this study did not find that AOA abundances increased in the controls. This study found further nuanced responses of AOB gene abundance to urine rates, where AOB initially decreased, particularly in the low urea soils, suggesting an initial suppression of AOB populations. It has been suggested that the high concentrations of N in urine and/or urine chemistry is likely to have quick and strong effects on AOB communities (Orwin et al., 2010). Elevated AOB transcription rates coincided with near-zero N_2O fluxes in urine treated soils at the end of the experiment, indicating nitrification was proceeding without N_2O production. This is supported by the increasing soil NO_3^- content observed in the urine treated microcosms (Table D1). The increase in AOB population at the end of this experiment calls into question what would happen to nitrifier N_2O emissions should a secondary urination event occur on a previous urine patch where AOB populations have increased up to tenfold from pre-urine levels (Fig. 4.7). A similar question could be asked about *nirS* and denitrifier N_2O since *nirS* gene abundances were elevated 240 h after urine deposition (Fig. 4.8). Repeated urination is likely to occur in high-traffic areas or crowded pastures and increases in likelihood with stocking rate and time, posing a potential risk for higher proportional losses of N_2O-N in subsequent urine deposition events.

Nitrite-reducing population dynamics differed in timing and scale due to differences in toxicity sensitivity or growth strategy. The response of *nirS* denitrifiers to urine addition was delayed, but stronger and more sustained than *nirK* populations (Fig. 4.8). This agrees with Orwin et al. (2010), which found *nirS* community structure displayed a much more permanent change in response to urine addition in wet soils compared to *nirK* denitrifiers. Unlike previous studies (Di et al., 2014; Hamonts et al., 2013), this study did not find an increase in *nirK* abundances following urine deposition, but did find an immediate increase in *nirK* transcription activity. While increases in *nirS* transcription rates were not as immediate, they were higher than *nirK* in high urea soils at 36 h and 168 h and increased with urea content. Increased growth and activity of *nirS* coincided with the second N_2O peak and an increase in urea-N_2O. The lag in *nirS* responses to urine suggests an increased sensitivity to urine toxicity and/or a difference in a growth strategy. Organisms

harboring *nirS* or *nirK* are suggested to differ in habitat selection, community responses to environmental conditions, and ecological niches (Enwall, Throbäck, Stenberg, Söderström, & Hallin, 2010; Jones & Hallin, 2010). This is supported by a field study that found *nirK* and *nirS* are likely subject to different selective pressures (Clark et al., 2012). Differential expression patterns in bacteria harboring both *nirS* and *nirK* suggests different roles between these two nitrite reductase genes (Wittorf et al., 2018). A higher co-occurrence of *nosZ* in *nirS* organisms increases the potential for complete denitrification since only 10-30% of observed *nirK* organisms possessed *nosZ* (Graf et al., 2014; Hallin et al., 2018).

The highly abundant clade II *nosZ* communities responded more strongly to urine addition than clade I, both in abundance and transcription rates (Fig. 4.9). A study has suggested that clade II communities should be more abundant in most environmental conditions, but also that clade I organisms are predicted to be the dominant N_2O consumers under conditions where N addition increases N_2O emissions for a prolonged period of time (Yoon, Nissen, Park, Sanford, & Löffler, 2016). Here, clade II organisms were the most abundant and active N_2O consumers following urine addition. Clade II communities temporarily increased in abundance in high urea soils but not low urea soils while clade I abundances did not respond to urine addition. These results contrast with Hamonts et al. (2013), where soil *nosZ* abundances increased following urea addition, as well as Di et al. (2014), where both *nosZ* clades increased abundances following urine addition. However, while *nosZ* clade I abundances did not increase in urine treatments, transcription rates did, indicating that clade I populations increased N_2O reducing activity. Urine treatments had a lower *nir:nos* transcript ratio than the controls due to increased *nosZ* transcription rates following urine deposition (Fig. 4.10). Bacteria in these soils may have needed to detoxify urine compounds since in addition to respiration, NosZ can detoxify cells (Hallin et al., 2018). The majority of the increase in urine treatment *nosZ* was accounted for by clade II organisms. Approximately half of *nosZ-II* organisms appear to be nondenitrifying N_2O reducers whereas most *nosZ-I* organisms possess *nir* (Graf et al., 2014; Hallin et al., 2018), resulting in a greater potential for clade II reduction of N_2O without producing it. The higher relative abundance and activity of clade II *nosZ* may therefore have minimized urine soil N_2O fluxes, particularly in high urea soils where clade II saw a large increase in activity. This may further explain the lower urine-N emission factor observed in high urea soils.

Denitrifier response to urine addition does not always relate to N_2O emissions. For example, Di et al. (2014) found that while abundance of *nirK*, *nirS*, and both clades of *nosZ* increased in response to urine addition, only *nirK* abundance correlated with N_2O emissions. *nosZ* has a higher rate of co-occurrence in denitrifiers possessing the *nirS* gene than the *nirK* gene, leading to a greater likelihood of complete denitrification to N_2 in *nirS* organisms (Graf et al., 2014; Hallin et al., 2018). In this study, denitrifier *nirK* populations exhibited a more immediate increase in transcription activity compared to *nirS* (Fig. 4.8), which corresponded with the initial denitrifier N_2O peak in urine treatments at 8 h. The second N_2O peak in urine soils coincided with the highest rate of *nirK* transcription at 36h. However, by this point, *nirS* abundances had grown and transcripts had increased to levels higher than *nirK*, providing increased competition for NO_2^- substrates. Increased *nirS* activity and a higher co-occurrence of *nirS* with *nosZ* suggests that by this point, microbial populations had an increased capacity for complete denitrification to N_2, reducing N_2O emissions.

Outlier N_2O microcosm hotspots may have been caused by ideal conditions for both nitrifier and denitrifier emissions. Nitrifier and denitrifier emissions increased proportionally in these hotspots. Across all treatments, AOA transcript abundance did increase in some microcosms, however the occurrence of this effect was inconsistent between replicates. This variation within treatments is unlikely to entirely explain the observed N_2O hotspot outliers since AOA are more efficient nitrifiers, generating half the N_2O per unit NO_2^- produced compared to AOB (Hink, Nicol, et al., 2017). Additionally, doubling urine N content corresponded with a near doubling of outlier N_2O fluxes, a trend which was not observed in treatment means. Hotspots also featured unique flux patterns. Hotspots are likely the effect of ideal soil conditions and warrant future study.

4.7 Conclusion

Increasing urine urea content did not significantly increase N_2O emissions in this study. Urine deposition mainly increases denitrifier emissions. While high urea soils emitted more urea-N as N_2O, urea-N emission factors were the same between both treatments. Urine-N emission factors were lower in high urea soils due to increased urine toxicity, resulting in no differences between urine treatment cumulative emissions. Application of urine was found to increase AOB abundance and activity, which were likely responsible for nitrifier N_2O emissions. Increases in

denitrifier emissions are likely due to increased *nirK* organism activity due to a lower co-occurrence with *nosZ* than *nirS*. Increases in *nosZ* activity and a higher abundance and activity of *nirS* and clade II *nosZ* improved soil N_2O-reducing capacity, particularly in high urea soils. The community dynamics of nitrifiers and denitrifiers in this study contributes to further understanding the responses of N_2O-producing microorganisms in the urine patch, an N_2O hotspot. This study finds that an increase in cattle urine-N content from non-bloat legumes in forage will not significantly increase cumulative N_2O fluxes from the urine patch in the short term.

5. SYNTHESIS AND CONCLUSIONS

Management of livestock N inputs is a key environmental issue of the 21st century. Globally, the livestock sector emits one third of total human-induced N emissions which have transgressed the planetary bounds for N, impacting the environment (Uwizeye et al., 2020). While N use efficiencies have increased over the last two decades of Canadian agriculture, so has the mass of N potentially lost to the environment, and increasing N inputs to agricultural systems has an exponential trend with increasing N_2O emissions (Karimi et al., 2020). Consumer demands for sustainable agricultural products and the predicted negative impacts of climate change on Western Canadian cattle production systems reliant upon grazing (Sloat et al., 2018) indicate the need for continual improvement in environmental sustainability. Western Canadian cattle producers have led the way in minimizing the environmental impacts of beef production systems. Using novel non-bloat legumes, producers aim to reduce enteric methane emissions while improving cattle value and pasture soil quality. Agricultural management changes can alter soil microbial communities at a landscape scale. Since microbial life has a sizeable impact on atmospheric composition, understanding the effects of such agricultural management decisions on GHG-respiring soil microbes will improve the efficacy of management decisions and outcomes.

The goal of this research was to understand how the introduction of non-bloat legumes to cattle pasture systems influences soil microbial populations and their GHG production. This was achieved through a field and a laboratory microcosm study. First, grazed pastures sod seeded with non-bloat legumes were surveyed for microbial community structure, enzyme activities, and daily GHG emissions. A second study used stable isotope tracers, isotopomer ratios, and gene copy and transcript abundances to determine the effects of increasing cattle urine N content on N-cycling microbes and N_2O emissions under controlled conditions.

5.1 Summary of Findings

Non-bloat legumes were not found to influence daily pasture soil N_2O emissions on days where soil sampling for microbial properties was conducted. However, time influenced daily N_2O emissions, and a wider range of fluxes was observed in cicer milkvetch pastures. Links were suggested between cicer milkvetch, relative AMF abundance, and daily N_2O emissions by structural equation modeling (SEM) in 2017. The presence of non-bloat legumes in pastures had a small but significant effect on soil microbial community structure and was related to increasing soil NO_3^- content. Seasonal pasture progression and soil moisture played the largest roles in microbial community structure and GHG fluxes. While differences were minimal, microbial communities did structure according to non-bloat legume treatment. Legume pasture soil NO_3^- tended to be higher in 2017, which was reflected in SEM suggesting legumes increased pasture soil NO_3^- content. Microbial extracellular enzyme activity was not different between treatments but β-glucosidase (βG) and N-acetyl-β-D-glucosaminidase (NAG) varied with time in 2017 and 2018, respectively. Lower NAG activity was suggested in cicer milkvetch pastures by SEM. This may be the result of increased plant N inputs reducing demand for soil N, or a reduced abundance of AMF reducing overall AMF necromass, resulting in less NAG being produced to recover N from chitin.

Addition of urine increased N_2O emissions under controlled conditions. Doubling urine urea content from 3.5 g L^{-1} (low urea) to 7.0 g L^{-1} (high urea) did not increase the cumulative N_2O flux but doubled urea-derived CO_2 and N_2O emissions. Toxicity effects on microbial communities were observed in high urea soils, which delayed N_2O fluxes and reduced emission factors. Soil CO_2 fluxes increased with urea content resulting in similar emission factors between treatments. CO_2 emissions directly derived from the ^{13}C labeled urea doubled with a doubling of urea content. The delayed appearance of labeled urea N_2O fluxes relative to the initial peak suggests that other urine and/or soil N compounds were nitrified and denitrified to N_2O prior to urea. Isotopomer ratios revealed different N_2O emission sources between control and urine-treated soils; in both high and low urea soils, denitrification was the primary source of N_2O. It is notable that one out of four replicate microcosms produced excessive N_2O that was three to four times greater than treatment means with no corresponding shift in CO_2 flux or isotopomer ratios, implying that nitrifiers and denitrifiers both increased N_2O emissions proportionally.

Nitrifier and denitrifier responses to urine addition varied between functional groups. Responses varied between no effect (AOA), shifts in transcription rates only (*nirK* and *nosZ-I*), and shifts in both transcription rates and population size (AOB, *nirS*, and *nosZ-II*). Despite having a larger population size than AOB, AOA did not uniformly shift transcription activity or population size. In contrast, AOB initially increased transcription rates and later increased population size, demonstrating their primary role in urine patch nitrification. Denitrifiers harboring *nirK* responded more quickly than *nirS*, increasing transcription rates but not gene abundance in response to urine deposition with no relation to urea concentration. Although *nirS* response was slower than *nirK*, transcription rates were higher, gene abundance shifted over time, and transcript increases were proportional to urea content. The tendency of *nirS* populations to be capable of complete denitrification to N_2 (Graf et al., 2014; Hallin et al., 2018) as well as the timing of *nirK* dominance relative to N_2O peaks suggest that *nirK* groups contributed the majority of initial denitrifier N_2O emissions before *nirS* populations increased competition, partially decreasing denitrifier N_2O emission rates during the second peak. Clade I *nosZ* organisms were less abundant and less responsive to urine addition than clade II *nosZ* organisms, producing fewer transcripts and showing almost no change in gene abundance while clade II organisms were more abundant and active than clade I. Clade II transcription also exhibited a stronger relationship to changing urea content. Half of clade II organisms lack the ability to produce N_2O (Graf et al., 2014; Hallin et al., 2018), increasing N_2O sink capacity in the urine amended soils, particularly high urea soils. This large increase in mainly clade II *nosZ* activity decreased treatment *nir:nos* transcript ratios below control levels and further diminished N_2O fluxes from the influx of urine N.

This research found that while incorporation of non-bloat legumes into pasture forage does shift microbial communities, communities did not shift in a way that increases microbial N_2O emissions. The low N and dry conditions of pasture soils were not conducive to large N_2O fluxes. Additionally, while increasing urine N had varying degrees of influence on microbial N cycling communities, it reduced emission factors and did not increase N_2O emissions. This was likely the result of higher urine N increasing toxic effects on microbial N_2O producers and simultaneously increasing soil microbial N_2O reduction capacity. From a microbial perspective, the dry nature of pastures and the toxic effects of increasing urine N makes it unlikely that non-bloat legume incorporation will result in significantly larger N_2O emissions. Forage legumes also provide a benefit as an alternative to GHG-producing synthetic fertilizers while maintaining a potential to

reduce enteric methane emissions. Canadian cattle producers should not be concerned with non-bloat legumes increasing GHG emissions or an increase in carbon tax as they provide both an environmental benefit and an incentive for the environmentally conscious consumer to purchase their products.

5.2 Future Research

The field survey demonstrated that despite dominant seasonal effects, microbial communities do shift when legumes are introduced to a grass pasture. Veldt cicer milkvetch pastures were suggested by SEM to have lower AMF abundance, a potentially causative mechanism for increased N_2O fluxes, however the mechanistic nature of this link remains unresolved. Future studies may investigate this further by testing whether cicer milkvetch plants do in fact have lower associations with AMF and may seek to find a causative explanation. This field survey was designed to represent real-world pasture grazing conditions. As a result, plant composition was variable, soil conditions were heterogeneous, and annual differences in precipitation affected gas fluxes and strongly impacted microbial abundance, community structure and activity. This study found no difference in microbial N_2O emissions under dry pasture conditions since both study years were dryer than average for this region. Future studies may seek to replicate this study with a more homogenous plant and soil composition in a region with greater precipitation to determine the effects of a wetter climate and higher plant N productivity on microbial populations and GHG emissions.

The laboratory incubation tested urea urine concentrations that reflected field study values where cattle were close to a water source. Values were set at 3.5 g L^{-1} to represent field study observations and doubled to 7.0 g L^{-1} to represent increased protein intake and/or animal dehydration. However, cattle urea concentrations can reach up to 20 g L^{-1} (Selbie et al., 2015). Studies analyzing the higher end of possible concentrations, such as from 10 to 20 g L^{-1} urea, could provide further insights into urine N toxicity on microbes and emission factors of higher urine concentrations. Additionally, this study found one in four urine microcosms to be a hotspot which emitted multitudes greater N_2O than the treatment means. The frequency at which this occurred and the unique flux pattern warrant further investigation. A study with more treatment replicates may help to resolve the biological nature of these apparent outliers which could then be analyzed

separately for causation and statistical significance. A study which measures gas fluxes prior to destructive sampling would have more explanatory power.

This laboratory study demonstrated the effects of real cattle urine chemistry on microbial N-cycling populations. Isotope labelling techniques distinguished urea derived GHG fluxes from total GHG fluxes. Since urea comprised 69% of total urine N and 14-16% of total urine C, fluxes derived from soil N and C were not discernible from non-urea derived N and C in the urine. Future studies may seek to quantify a possible soil priming trend caused by urine application. This could be achieved through artificial urine where N and C content are controlled and all components labeled, or by collecting urine from cattle fed $^{15}N^{13}C$ labeled plant materials, including non-bloat legumes.

This study found populations of AOB and *nirS* maintained population shifts at least 240 h after urine deposition. A study with an additional urine application to urine treated soils would determine the effects of urine on a microbial population which has already been affected by urine deposition. This would simulate a second urine deposition on a urine patch in a pasture setting. A second urination event could produce different relative nitrifier:denitrifier N_2O fluxes and community responses compared to a single event. Studies which manipulate soil moisture prior to urination could examine how moisture regime (Banerjee et al., 2016) affects microbial responses to urine deposition. Microbial N-cycling communities have exhibited different responses in wet and dry soils following urine addition (Orwin et al., 2010). Additionally, pasture soil temperatures vary throughout the day. Colder soils rich in urea have been observed to emit more N_2O than warmer soils due to increased decoupling between ammonia oxidation and nitrite oxidation (Venterea, Coulter, & Clough, 2020). In summary, manipulation of the number and frequency of urination events, soil moisture regime, and soil temperature applied to a single soil could provide a wider range of results still representative of the variable conditions which pastures experience.

6. LITERATURE CITED

Alemu, A. W., Janzen, H., Little, S., Hao, X., Thompson, D. J., Baron, V., … Kröbel, R. (2017). Assessment of grazing management on farm greenhouse gas intensity of beef production systems in the Canadian Prairies using life cycle assessment. *Agricultural Systems*, *158*, 1–13. doi: 10.1016/j.agsy.2017.08.003

Ambus, P., Petersen, S. O., & Soussana, J. F. (2007). Short-term carbon and nitrogen cycling in urine patches assessed by combined carbon-13 and nitrogen-15 labelling. *Agriculture, Ecosystems and Environment*, *121*(1–2), 84–92. doi: 10.1016/j.agee.2006.12.007

Avrahami, S., Conrad, R., & Braker, G. (2002). Effect of Soil Ammonium Concentration on N_2O Release and on the Community Structure of Ammonia Oxidizers and Denitrifiers. *Applied and Environmental Microbiology*, *68*(11), 5685–5692. doi: 10.1128/AEM.68.11.5685

Baggs, E. M. (2011). Soil microbial sources of nitrous oxide: Recent advances in knowledge, emerging challenges and future direction. *Current Opinion in Environmental Sustainability*, *3*, 321–327. doi: 10.1016/j.cosust.2011.08.011

Bakken, L. R., & Frostegård, Å. (2017). Sources and sinks for N_2O, can microbiologist help to mitigate N_2O emissions? *Environmental Microbiology*, *19*(12), 4801–4805. doi: 10.1111/1462-2920.13978

Banerjee, S., Helgason, B., Wang, L., Winsley, T., Ferrari, B. C., & Siciliano, S. D. (2016). Legacy effects of soil moisture on microbial community structure and N_2O emissions. *Soil Biology and Biochemistry*, *95*, 40–50. doi: 10.1016/j.soilbio.2015.12.004

Barneze, A. S., Mazzetto, A. M., Zani, C. F., Misselbrook, T., & Cerri, C. C. (2014). Nitrous oxide emissions from soil due to urine deposition by grazing cattle in Brazil. *Atmospheric Environment*, *92*, 394–397. doi: 10.1016/j.atmosenv.2014.04.046

Bates, D., Maechler, M., Bolker, B., & Walker, S. (2015). Fitting Linear Mixed-Effects Models Using lme4. *Journal of Statistical Software*, *67*(1), 1–48.

Bell, C. W., Fricks, B. E., Rocca, J. D., Steinweg, J. M., McMahon, S. K., & Wallenstein, M. D. (2013). High-throughput Fluorometric Measurement of Potential Soil Extracellular Enzyme Activities. *Journal of Visualized Experiments*, (81), 1–16. doi: 10.3791/50961

Bertram, J. E., Orwin, K. H., Clough, T. J., Condron, L. M., Sherlock, R. R., & O'Callaghan, M. (2012). Effect of soil moisture and bovine urine on microbial stress. *Pedobiologia*, *55*(4), 211–218. doi: 10.1016/j.pedobi.2012.03.004

Black, A. S. (1992). Soil acidification in urine- and urea-affected soil. *Australian Journal of Soil Research*, *30*(6), 989–999. doi: 10.1071/SR9920989

Bligh, E. G., & Dyer, W. J. (1959). A rapid method of total lipid extraction and purification. *Canadian Journal of Biochemistry and Physiology*, *37*(8), 911–917.

Boon, A., Robinson, J. S., Chadwick, D. R., & Cardenas, L. M. (2014). Effect of cattle urine addition on the surface emissions and subsurface concentrations of greenhouse gases in a UK peat grassland. *Agriculture, Ecosystems and Environment*, *186*, 23–32. doi: 10.1016/j.agee.2014.01.008

Bowatte, S., Hoogendoorn, C. J., Newton, P. C. D., Liu, Y., Brock, S. C., & Theobald, P. W. (2018). Grassland plant species and cultivar effects on nitrous oxide emissions after urine application. *Geoderma*, *323*, 74–82. doi: 10.1016/j.geoderma.2018.03.001

Brinkhaus, A. G., Bee, G., Silacci, P., Kreuzer, M., & Dohme-Meier, F. (2016). Effect of exchanging Onobrychis viciifolia and Lotus corniculatus for Medicago sativa on ruminal fermentation and nitrogen turnover in dairy cows. *J. Dairy Sci*, *99*, 4384–4397. doi: 10.3168/jds.2015-9911

Cabral, A. R., Capanema, M. A., Gebert, J., Moreira, J. F., & Jugnia, L. B. (2010). Quantifying Microbial Methane Oxidation Efficiencies in Two Experimental Landfill Biocovers Using Stable Isotopes. *Water, Air, & Soil Pollution*, *209*(1–4), 157–172. doi: 10.1007/s11270-009-0188-4

Cain, J. A., Solis, N., & Cordwell, S. J. (2014). *Beyond gene expression: The impact of protein post-translational modifications in bacteria* (Vol. 97). Elsevier. doi: 10.1016/j.jprot.2013.08.012

Carey, C. J., Dove, N. C., Beman, J. M., Hart, S. C., & Aronson, E. L. (2016). Meta-analysis reveals ammonia-oxidizing bacteria respond more strongly to nitrogen addition than ammonia-oxidizing archaea. *Soil Biology and Biochemistry*, *99*, 158–166. doi: 10.1016/j.soilbio.2016.05.014

Cavicchioli, R., Ripple, W. J., Timmis, K. N., Azam, F., Bakken, L. R., Baylis, M., … Webster, N. S. (2019). Scientists' warning to humanity: Microorganisms and climate change. *Nature Reviews Microbiology*. doi: 10.1038/s41579-019-0222-5

Chantigny, M. H., & Angers, D. A. (2008). Extraction and Characterization of Dissolved Organic Matter. In M. R. Carter & E. G. Gregorich (Eds.), *Soil Sampling and Methods of Analysis* (2nd ed., pp. 649–667). Boca Raton: CRC Press.

Chen, M., Chen, B., & Marschner, P. (2008). Plant growth and soil microbial community structure of legumes and grasses grown in monoculture or mixture. *Journal of Environmental Sciences*, *20*(10), 1231–1237. doi: 10.1016/S1001-0742(08)62214-7

Chodak, M., Gołębiewski, M., Morawska-Płoskonka, J., Kuduk, K., & Niklińska, M. (2015). Soil chemical properties affect the reaction of forest soil bacteria to drought and rewetting stress. *Annals of Microbiology*, *65*(3), 1627–1637. doi: 10.1007/s13213-014-1002-0

Clark, I. M., Buchkina, N., Jhurreea, D., Goulding, K. W. T., & Hirsch, P. R. (2012). Impacts of nitrogen application rates on the activity and diversity of denitrifying bacteria in the Broadbalk Wheat Experiment. *Philosophical Transactions of the Royal Society B: Biological Sciences*, *367*(1593), 1235–1244. doi: 10.1098/rstb.2011.0314

Clough, T. J., Sherlock, R. R., Mautner, M. N., Milligan, D. B., Wilson, P. F., Freeman, C. G., & McEwan, M. J. (2003). Emission of nitrogen oxides and ammonia from varying rates of applied synthetic urine and correlations with soil chemistry. *Australian Journal of Soil Research*, *41*(3), 421. doi: 10.1071/SR02105

Crecchio, C., & Stotzky, G. (1998). Binding of DNA on humic acids: Effect on transformation of Bacillus subtilis and resistance to DNase. *Soil Biology and Biochemistry*, *30*(8–9), 1061–1067. doi: 10.1016/S0038-0717(97)00248-4

Dewhurst, R. J., Delaby, L., Moloney, A., Boland, T., & Lewis, E. (2009). Nutritive value of forage legumes used for grazing and silage. *Irish Journal of Agricultural and Food Research*, *48*(2), 167–187.

Di, H. J., Cameron, K. C., Podolyan, A., & Robinson, A. (2014). Effect of soil moisture status and a nitrification inhibitor, dicyandiamide, on ammonia oxidizer and denitrifier growth and nitrous oxide emissions in a grassland soil. *Soil Biology and Biochemistry*, *73*, 59–68. doi: 10.1016/j.soilbio.2014.02.011

Di, H. J., Cameron, K. C., Shen, J. P., Winefield, C. S., O'Callaghan, M., Bowatte, S., & He, J. Z. (2009). Nitrification driven by bacteria and not archaea in nitrogen-rich grassland soils. *Nature Geoscience*, *2*(9), 621–624. doi: 10.1038/ngeo613

Di, H. J., Cameron, K. C., Shen, J.-P., Winefield, C. S., O'Callaghan, M., Bowatte, S., & He, J.-Z. (2010). Ammonia-oxidizing bacteria and archaea grow under contrasting soil nitrogen conditions. *FEMS Microbiology Ecology*, *72*(3), 386–394. doi: 10.1111/j.1574-6941.2010.00861.x

Di, H. J., Cameron, K. C., Sherlock, R. R., Shen, J.-P., He, J.-Z., & Winefield, C. S. (2010). Nitrous oxide emissions from grazed grassland as affected by a nitrification inhibitor, dicyandiamide, and relationships with ammonia-oxidizing bacteria and archaea. *Journal of Soils and Sediments*, *10*(5), 943–954. doi: 10.1007/s11368-009-0174-x

Dijkstra, J., Oenema, O., van Groenigen, J. W., Spek, J. W., van Vuuren, A. M., & Bannink, A. (2013). Diet effects on urine composition of cattle and N_2O emissions. *Animal*, *7*(s2), 292–302. doi: 10.1017/S1751731113000578

Domeignoz-Horta, L. A., Philippot, L., Peyrard, C., Bru, D., Breuil, M.-C., Bizouard, F., … Spor, A. (2017). Peaks of in situ N_2O emissions are influenced by N_2O-producing and reducing microbial communities across arable soils. *Global Change Biology*, *00*, 1–11. doi: 10.1111/gcb.13853

Drenovsky, R. E., Elliott, G. N., Graham, K. J., & Scow, K. M. (2004). Comparison of phospholipid fatty acid (PLFA) and total soil fatty acid methyl esters (TSFAME) for characterizing soil microbial communities. *Soil Biology and Biochemistry*, *36*(11), 1793–1800. doi: 10.1016/j.soilbio.2004.05.002

Duff, S. M. G., Sarath, G., & Plaxton, W. C. (1994). The role of acid phosphatases in plant phosphorus metabolism. *Physiologia Plantarum*, *90*(4), 791–800. doi: 10.1111/j.1399-3054.1994.tb02539.x

Edwards, J. A., Santos-Medellín, C. M., Liechty, Z. S., Nguyen, B., Lurie, E., Eason, S., … Sundaresan, V. (2018). Compositional shifts in root-associated bacterial and archaeal microbiota track the plant life cycle in field-grown rice. *PLOS Biology*, *16*(2), e2003862. doi: 10.1371/journal.pbio.2003862

Eivazi, F., & Tabatabai, M. A. (1977). Phosphatases in soils. *Soil Biology and Biochemistry*, *9*(3), 167–172. doi: 10.1016/0038-0717(77)90070-0

Eivazi, F., & Tabatabai, M. A. (1988). Glucosidases and galactosidases in soils. *Soil Biology and Biochemistry*, *20*(5), 601–606. doi: 10.1016/0038-0717(88)90141-1

Ekenler, M., & Tabatabai, M. A. (2002). β-glucosaminidase activity of soils: Effect of cropping systems and its relationship to nitrogen mineralization. *Biology and Fertility of Soils*, *36*(5), 367–376. doi: 10.1007/s00374-002-0541-x

Environment and Climate Change Canada. (2017). *National Inventory Report 1990-2015 (Part 1): Greenhouse Gas Sources and Sinks in Canada. Canada's Submission to the United Nations Framework Convention on Climate Change*. Gatineau, Quebec.

Enwall, K., Throbäck, I. N., Stenberg, M., Söderström, M., & Hallin, S. (2010). Soil Resources Influence Spatial Patterns of Denitrifying Communities at Scales Compatible with Land Management. *Applied and Environmental Microbiology*, *76*(7), 2243–2250. doi: 10.1128/AEM.02197-09

Fox, J., & Weisberg, S. (2019). An {R} Companion to Applied Regression (Version 3). Thousand Oaks, CA: Sage.

Frostegård, Å., Tunlid, A., & Bååth, E. (2011). Use and misuse of PLFA measurements in soils. *Soil Biology and Biochemistry*, *43*(8), 1621–1625. doi: 10.1016/j.soilbio.2010.11.021

Fuchslueger, L., Bahn, M., Fritz, K., Hasibeder, R., & Richter, A. (2014). Experimental drought reduces the transfer of recently fixed plant carbon to soil microbes and alters the bacterial community composition in a mountain meadow. *New Phytologist*, *201*(3), 916–927. doi: 10.1111/nph.12569

Garg, M. R., Sherasia, P. L., Bhanderi, B. M., Phondba, B. T., Shelke, S. K., & Makkar, H. P. S. (2013). Effects of feeding nutritionally balanced rations on animal productivity, feed conversion efficiency, feed nitrogen use efficiency, rumen microbial protein supply, parasitic load, immunity and enteric methane emissions of milking animals under field condi. *Animal Feed Science and Technology*, *179*(1–4), 24–35. doi: 10.1016/j.anifeedsci.2012.11.005

Gleeson, D. B., Müller, C., Banerjee, S., Ma, W., Siciliano, S. D., & Murphy, D. V. (2010). Response of ammonia oxidizing archaea and bacteria to changing water filled pore space. *Soil Biology and Biochemistry*, *42*(10), 1888–1891. doi: 10.1016/j.soilbio.2010.06.020

Grace, J. B. (2006). *Structural Equation Modeling and Natural Systems*. Cambridge, UK: Cambridge University Press.

Graf, D. R. H., Jones, C. M., & Hallin, S. (2014). Intergenomic comparisons highlight modularity of the denitrification pathway and underpin the importance of community structure for N_2O emissions. *PLoS ONE, 9*(12). doi: 10.1371/journal.pone.0114118

Gregorich, E., Janzen, H. H., Helgason, B., & Ellert, B. (2015). Nitrogenous Gas Emissions from Soils and Greenhouse Gas Effects. *Advances in Agronomy, 132*, 39–74. doi: 10.1016/bs.agron.2015.02.004

Grogan, D. W., & Cronan, J. E. (1997). Cyclopropane ring formation in membrane lipids of bacteria. *Microbiology and Molecular Biology Reviews, 61*(4), 429–441.

Hallin, S., Philippot, L., Löffler, F. E., Sanford, R. A., & Jones, C. M. (2018). Genomics and Ecology of Novel N_2O-Reducing Microorganisms. *Trends in Microbiology, 26*, 43–55. doi: 10.1016/j.tim.2017.07.003

Hamilton, E. W., & Frank, D. A. (2001). Can Plants Stimulate Soil Microbes and Their Own Nutrient Supply? Evidence from a Grazing Tolerant Grass. *Ecology, 82*(9), 2397–2402. doi: 10.1890/0012-9658(2001)082[2397:CPSSMA]2.0.CO;2

Hammerl, V., Kastl, E.-M., Schloter, M., Kublik, S., Schmidt, H., Welzl, G., … Gschwendtner, S. (2019). Influence of rewetting on microbial communities involved in nitrification and denitrification in a grassland soil after a prolonged drought period. *Scientific Reports, 9*(1), 1–10. doi: 10.1038/s41598-018-38147-5

Hamonts, K., Balaine, N., Moltchanova, E., Beare, M., Thomas, S., Wakelin, S. A., … Clough, T. J. (2013). Influence of soil bulk density and matric potential on microbial dynamics, inorganic N transformations, N_2O and N_2 fluxes following urea deposition. *Soil Biology and Biochemistry, 65*, 1–11. doi: 10.1016/j.soilbio.2013.05.006

Hargreaves, S. K., & Hofmockel, K. S. (2015). A modified incubation method reduces analytical variation of soil hydrolase assays. *European Journal of Soil Biology, 67*, 1–4. doi: 10.1016/J.EJSOBI.2014.12.002

He, J. Z., Hu, H. W., & Zhang, L. M. (2012). Current insights into the autotrophic thaumarchaeal ammonia oxidation in acidic soils. *Soil Biology and Biochemistry, 55*, 146–154. doi: 10.1016/j.soilbio.2012.06.006

Helgason, B. L., Walley, F. L., & Germida, J. J. (2009). Fungal and bacterial abundance in long-term no-till and intensive-till soils of the Northern Great Plains. *Soil Science Society of America Journal, 73*(1), 120–127. doi: 10.2136/sssaj2007.0392

Helgason, B. L., Walley, F. L., & Germida, J. J. (2010). Long-term no-till management affects microbial biomass but not community composition in Canadian prairie agroecosytems. *Soil Biology and Biochemistry, 42*, 2192–2202. doi: 10.1016/j.soilbio.2010.08.015

Henry, S., Bru, D., Stres, B., Hallet, S., & Philippot, L. (2006). Quantitative Detection of the nosZ Gene, Encoding Nitrous Oxide Reductase, and Comparison of the Abundances of 16S rRNA, narG, nirK, and nosZ Genes in Soils. *Applied and Environmental Microbiology, 72*(8), 5181–5189. doi: 10.1128/AEM.00231-06

Henry, Sonia, Baudoin, E., López-Gutiérrez, J. C., Martin-Laurent, F., Brauman, A., & Philippot, L. (2004). Quantification of denitrifying bacteria in soils by nirK gene targeted real-time PCR. *Journal of Microbiological Methods*, *59*(3), 327–335. doi: 10.1016/j.mimet.2004.07.002

Higgins, S. A., Welsh, A., Orellana, L. H., Konstantinidis, K. T., Chee-Sanford, J. C., Sanford, R. A., … Löffler, F. E. (2016). Detection and diversity of fungal nitric oxide reductase genes (p450nor) in agricultural soils. *Applied and Environmental Microbiology*, *82*(10), 2919–2928. doi: 10.1128/AEM.00243-16

Hink, L., Lycus, P., Gubry-Rangin, C., Frostegård, Å., Nicol, G. W., Prosser, J. I., & Bakken, L. R. (2017). Kinetics of NH_3-oxidation, NO-turnover, N_2O-production and electron flow during oxygen depletion in model bacterial and archaeal ammonia oxidisers. *Environmental Microbiology*, *19*(12), 4882–4896. doi: 10.1111/1462-2920.13914

Hink, L., Nicol, G. W., & Prosser, J. I. (2017). Archaea produce lower yields of N_2O than bacteria during aerobic ammonia oxidation in soil. *Environmental Microbiology*, *19*(12), 4829–4837. doi: 10.1111/1462-2920.13282

Jones, C. M., Graf, D. R., Bru, D., Philippot, L., & Hallin, S. (2013). The unaccounted yet abundant nitrous oxide-reducing microbial community: A potential nitrous oxide sink. *The ISME Journal*, *7*(2), 417–426. doi: 10.1038/ismej.2012.125

Jones, C. M., & Hallin, S. (2010). Ecological and evolutionary factors underlying global and local assembly of denitrifier communities. *The ISME Journal*, *4*(5), 633–641. doi: 10.1038/ismej.2009.152

Junier, P., Molina, V., Dorador, C., Hadas, O., Kim, O. S., Junier, T., … Imhoff, J. F. (2010). Phylogenetic and functional marker genes to study ammonia-oxidizing microorganisms (AOM) in the environment. *Applied Microbiology and Biotechnology*, *85*(3), 425–440. doi: 10.1007/s00253-009-2228-9

Karimi, R., Pogue, S. J., Kröbel, R., Beauchemin, K. A., Schwinghamer, T., & Henry Janzen, H. (2020). An updated nitrogen budget for Canadian agroecosystems. *Agriculture, Ecosystems & Environment*, *304*, 107046. doi: 10.1016/j.agee.2020.107046

Lamb, E., Shirtliffe, S., & May, W. (2011). Structural equation modeling in the plant sciences: An example using yield components in oat. *Canadian Journal of Plant Science*, *91*(4), 603–619. doi: 10.4141/cjps2010-035

Lauber, C. L., Strickland, M. S., Bradford, M. A., & Fierer, N. (2008). The influence of soil properties on the structure of bacterial and fungal communities across land-use types. *Soil Biology and Biochemistry*, *40*(9), 2407–2415. doi: 10.1016/j.soilbio.2008.05.021

Laughlin, R. J., & Stevens, R. J. (2002). Evidence for fungal dominance of denitrification and codenitrification in a grassland soil. *Soil Science Society of America Journal*, (2), 1540–1548. doi: 10.2136/sssaj2002.1540

Lenth, R. (2020). emmeans: Estimated Marginal Means, aka Least-Square Means (Version 1.4.6).

Levy-Booth, D. J., Campbell, R. G., Gulden, R. H., Hart, M. M., Powell, J. R., Klironomos, J. N., … Dunfield, K. E. (2007). Cycling of extracellular DNA in the soil environment. *Soil Biology and Biochemistry, 39*(12), 2977–2991. doi: 10.1016/j.soilbio.2007.06.020

Lewicka-Szczebak, D., Augustin, J., Giesemann, A., & Well, R. (2017). Quantifying N_2O reduction to N_2 based on N_2O isotopocules – validation with independent methods (helium incubation and ^{15}N gas flux method). *Biogeosciences*, *14*(3), 711–732. doi: https://doi.org/10.5194/bg-14-711-2017

Lin, D., McCulley, R. L., Nelson, J. A., Jacobsen, K. L., & Zhang, D. (2020). Time in pasture rotation alters soil microbial community composition and function and increases carbon sequestration potential in a temperate agroecosystem. *Science of The Total Environment*, *698*(134233), 1–9. doi: 10.1016/j.scitotenv.2019.134233

Loeppky, H., Hiltz, M., Bittman, S., & Frick, B. (1996). Seasonal changes in yield and nutritional quality of cicer milkvetch and alfalfa in northeastern Saskatchewan. *Canadian Journal of Plant Science*, 441–446.

Lycus, P., Lovise Bøthun, K., Bergaust, L., Peele Shapleigh, J., Reier Bakken, L., & Frostegård, Å. (2017). Phenotypic and genotypic richness of denitrifiers revealed by a novel isolation strategy. *The ISME Journal*, *11*(10), 2219–2232. doi: 10.1038/ismej.2017.82

Madigan, M. T., Martinko, J. M., Bender, K. S., Buckley, D. H., & Stahl, D. A. (2015). Functional Diversity of Bacteria. In K. Churchman, N. McFadden, A. Williams, & M. Early (Eds.), *Brock Biology of Microorganisms* (14th ed., pp. 433–478). Glenview: Pearson Education.

Marsden, K. A., Jones, D. L., & Chadwick, D. R. (2016). The urine patch diffusional area: An important N_2O source? *Soil Biology and Biochemistry*, *92*, 161–170. doi: 10.1016/j.soilbio.2015.10.011

Marshall, C. B., McLaren, J. R., & Turkington, R. (2011). Soil microbial communities resistant to changes in plant functional group composition. *Soil Biology and Biochemistry*, *43*(1), 78–85. doi: 10.1016/j.soilbio.2010.09.016

Martens-Habbena, W., Berube, P. M., Urakawa, H., de la Torre, J. R., & Stahl, D. A. (2009). Ammonia oxidation kinetics determine niche separation of nitrifying Archaea and Bacteria. *Nature*, *461*, 976–979. doi: 10.1038/nature08465

Maynard, D., Kalra, Y., & Crumbaugh, J. (2008). Nitrate and Exchangeable Ammonium Nitrogen. In M. R. Carter & E. G. Gregorich (Eds.), *Soil Sampling and Methods of Analysis* (2nd ed., pp. 97–106). Boca Raton: CRC Press.

McLeod, E. M., Banerjee, S., Bork, E. W., Hall, L. M., & Hare, D. D. (2015). Structural equation modeling reveals complex relationships in mixed forage swards. *Crop Protection*, *78*, 106–113. doi: 10.1016/j.cropro.2015.08.019

Meinhardt, K. A., Stopnisek, N., Pannu, M. W., Strand, S. E., Fransen, S. C., Casciotti, K. L., & Stahl, D. A. (2018). Ammonia-oxidizing bacteria are the primary N_2O producers in an ammonia-oxidizing archaea dominated alkaline agricultural soil. *Environmental Microbiology*, *20*(6), 2195–2206. doi: 10.1111/1462-2920.14246

Michotey, V., Méjean, V., & Bonin, P. (2000). Comparison of Methods for Quantification of Cytochrome cd1-Denitrifying Bacteria in Environmental Marine Samples. *Applied and Environmental Microbiology*, *66*(4), 1564–1571.

Monaghan, R. M., & Barraclough, D. (1992). Some chemical and physical factors affecting the rate and dynamics of nitrification in urine-affected soil. *Plant and Soil*, *143*, 11–18.

Monaghan, R. M., & Barraclough, D. (1993). Nitrous oxide and dinitrogen emissions from urine-affected soil under controlled conditions. *Plant and Soil*, *151*(1), 127–138. doi: 10.1007/BF00010793

Moran, M. A., Satinsky, B., Gifford, S. M., Luo, H., Rivers, A., Chan, L.-K., … Hopkinson, B. M. (2013). Sizing up metatranscriptomics. *The ISME Journal*, *794*(10), 237–243. doi: 10.1038/ismej.2012.94

Morley, N., Baggs, E. M., Dörsch, P., & Bakken, L. (2008). Production of NO, N_2O and N_2 by extracted soil bacteria, regulation by NO_2 and O_2 concentrations. *FEMS Microbiology Ecology*, *65*(1), 102–112. doi: 10.1111/j.1574-6941.2008.00495.x

Németh, D. D., Wagner-Riddle, C., & Dunfield, K. E. (2014). Abundance and gene expression in nitrifier and denitrifier communities associated with a field scale spring thaw N2O flux event. *Soil Biology and Biochemistry*, *73*, 1–9. doi: 10.1016/j.soilbio.2014.02.007

Nicol, G. W., Leininger, S., Schleper, C., & Prosser, J. I. (2008). The influence of soil pH on the diversity, abundance and transcriptional activity of ammonia oxidizing archaea and bacteria. *Environmental Microbiology*, *10*(11), 2966–2978. doi: 10.1111/j.1462-2920.2008.01701.x

Niklaus, P. A., Le Roux, X., Poly, F., Buchmann, N., Scherer-Lorenzen, M., Weigelt, A., & Barnard, R. L. (2016). Plant species diversity affects soil–atmosphere fluxes of methane and nitrous oxide. *Oecologia*, *181*(3), 919–930. doi: 10.1007/s00442-016-3611-8

Niklaus, P. A., Wardle, D. A., & Tate, K. R. (2006). Effects of plant species diversity and composition on nitrogen cycling and the trace gas balance of soils. *Plant and Soil*, *282*(1–2), 83–98. doi: 10.1007/s11104-005-5230-8

Novinscak, A., Goyer, C., Zebarth, B. J., Burton, D. L., Chantigny, M. H., & Filion, M. (2016). Novel P450nor gene detection assay used to characterize the prevalence and diversity of soil fungal denitrifiers. *Applied and Environmental Microbiology*, *82*(15), 4560–4569. doi: 10.1128/AEM.00231-16

Oksanen, J., Blanchet, F. G., Friendly, M., Kindt, R., Legendre, P., McGlinn, D., … Wagner, H. (2018). *vegan: Community Ecology Package*. Retrieved from https://cran.r-project.org/package=vegan

Orwin, K. H., Bertram, J. E., Clough, T. J., Condron, L. M., Sherlock, R. R., O'Callaghan, M., … Baird, D. B. (2010). Impact of bovine urine deposition on soil microbial activity, biomass, and community structure. *Applied Soil Ecology*, *44*(1), 89–100. doi: 10.1016/j.apsoil.2009.10.004

Pedersen, A. R. (2017). *HMR: Flux Estimation with Static Chamber Data*. Retrieved from https://cran.r-project.org/package=HMR

Petersen, S. O., Roslev, P., & Bol, R. (2004). Dynamics of a Pasture Soil Microbial Community after Deposition of Cattle Urine Amended with 13C Urea. *Applied and Environmental Microbiology*, *70*(11), 6363–6369. doi: 10.1128/AEM.70.11.6363

Petersen, S. O., Stamatiadis, S., & Christofides, C. (2004). Short-term nitrous oxide emissions from pasture soil as influenced by urea level and soil nitrate. *Plant and Soil*, *267*(1–2), 117–127. doi: 10.1007/s11104-005-4688-8

Powell, J. M., & Broderick, G. A. (2011). Transdisciplinary Soil Science Research: Impacts of Dairy Nutrition on Manure Chemistry and the Environment. *Soil Science Society of America Journal*, *75*(6), 2071–2078. doi: 10.2136/sssaj2011.0226

R Core Team. (2019). R: A language and environment for statistical computing (Version 3.6.0). Vienna, Austria: R Foundation for Statistical Computing.

R Core Team. (2020). R: A language and environment for statistical computing. (Version 3.6.3). Vienna, Austria: R Foundation for Statistical Computing.

Regan, K., Stempfhuber, B., Schloter, M., Rasche, F., Prati, D., Philippot, L., … Marhan, S. (2017). Spatial and temporal dynamics of nitrogen fixing, nitrifying and denitrifying microbes in an unfertilized grassland soil. *Soil Biology and Biochemistry*, *109*, 214–226. doi: 10.1016/j.soilbio.2016.11.011

Rex, D., Clough, T. J., Richards, K. G., de Klein, C., Morales, S. E., Samad, M. S., … Lanigan, G. J. (2018). Fungal and bacterial contributions to codenitrification emissions of N_2O and N2 following urea deposition to soil. *Nutrient Cycling in Agroecosystems*, *110*(1), 135–149. doi: 10.1007/s10705-017-9901-7

Rosseel, Y. (2012). lavaan: An R Package for Structural Equation Modeling. *Journal of Statistical Software*, *48*(2), 1–36.

Rotthauwe, J. H., Witzel, K. P., & Liesack, W. (1997). The ammonia monooxygenase structural gene amoA as a functional marker: Molecular fine-scale analysis of natural ammonia-oxidizing populations. *Applied and Environmental Microbiology*, *63*(12), 4704–4712.

Rousk, J., Brookes, P. C., & Bååth, E. (2010). Investigating the mechanisms for the opposing pH relationships of fungal and bacterial growth in soil. *Soil Biology and Biochemistry*, *42*(6), 926–934. doi: 10.1016/j.soilbio.2010.02.009

Schirrmeister, B. E., de Vos, J. M., Antonelli, A., & Bagheri, H. C. (2013). Evolution of multicellularity coincided with increased diversification of cyanobacteria and the Great Oxidation Event. *Proceedings of the National Academy of Sciences*, *110*(5), 1791–1796. doi: 10.1073/pnas.1209927110

Schmidt, C. S., Richardson, D. J., & Baggs, E. M. (2011). Constraining the conditions conducive to dissimilatory nitrate reduction to ammonium in temperate arable soils. *Soil Biology and Biochemistry*, *43*(7), 1607–1611. doi: 10.1016/J.SOILBIO.2011.02.015

Selbie, D. R., Buckthought, L. E., & Shepherd, M. A. (2015). The Challenge of the Urine Patch for Managing Nitrogen in Grazed Pasture Systems. *Advances in Agronomy*, *129*, 229–292. doi: 10.1016/bs.agron.2014.09.004

Seo, J., & Lee, K.-J. (2004). Post-translational modifications and their biological functions: Proteomic analysis and systematic approaches. *Journal of Biochemistry and Molecular Biology*, *37*(1), 35–44. doi: 10.5483/BMBRep.2004.37.1.035

Shoun, H., Fushinobu, S., Jiang, L., Kim, S.-W., & Wakagi, T. (2012). Fungal denitrification and nitric oxide reductase cytochrome P450nor. *Philosophical Transactions of The Royal Society B*, *367*, 1186–1194. doi: 10.1098/rstb.2011.0335

Sinsabaugh, R. L., & Follstad Shah, J. J. (2012). Ecoenzymatic Stoichiometry and Ecological Theory. *Annual Review of Ecology, Evolution, and Systematics*, *43*, 313–343. doi: 10.1146/annurev-ecolsys-071112-124414

Sipilä, T. P., Yrjälä, K., Alakukku, L., & Palojärvi, A. (2012). Cross-site soil microbial communities under tillage regimes: Fungistasis and microbial biomarkers. *Applied and Environmental Microbiology*, *78*(23), 8191–8201. doi: 10.1128/AEM.02005-12

Sloat, L. L., Gerber, J. S., Samberg, L. H., Smith, W. K., Herrero, M., Ferreira, L. G., … West, P. C. (2018). Increasing importance of precipitation variability on global livestock grazing lands. *Nature Climate Change*, *8*(3), 214–218. doi: 10.1038/s41558-018-0081-5

Sterngren, A. E., Hallin, S., & Bengtson, P. (2015). Archaeal Ammonia Oxidizers Dominate in Numbers, but Bacteria Drive Gross Nitrification in N-amended Grassland Soil. *Frontiers in Microbiology*, *6*. doi: 10.3389/fmicb.2015.01350

Stevenson, B. A., Hunter, D. W. F., & Rhodes, P. L. (2014). Temporal and seasonal change in microbial community structure of an undisturbed, disturbed, and carbon-amended pasture soil. *Soil Biology and Biochemistry*, *75*, 175–185. doi: 10.1016/j.soilbio.2014.04.010

Storer, K., Coggan, A., Ineson, P., & Hodge, A. (2018). Arbuscular mycorrhizal fungi reduce nitrous oxide emissions from N_2O hotspots. *New Phytologist*, *220*(4), 1285–1295. doi: 10.1111/nph.14931

Sun, Y., Chen, H. Y. H., Jin, L., Wang, C., Zhang, R., Ruan, H., & Yang, J. (2020). Drought stress induced increase of fungi:bacteria ratio in a poplar plantation. *CATENA*, *193*, 104607. doi: 10.1016/j.catena.2020.104607

Sutka, R. L., Ostrom, N. E., Ostrom, P. H., Breznak, J. A., Gandhi, H., Pitt, A. J., & Li, F. (2006). Distinguishing Nitrous Oxide Production from Nitrification and Denitrification on the Basis of Isotopomer Abundances. *Applied and Environmental Microbiology*, *72*(1), 638–644. doi: 10.1128/AEM.72.1.638-644.2006

Teutscherova, N., Vazquez, E., Arango, J., Arevalo, A., Benito, M., & Pulleman, M. (2019). Native arbuscular mycorrhizal fungi increase the abundance of ammonia-oxidizing bacteria, but suppress nitrous oxide emissions shortly after urea application. *Geoderma*, *338*, 493–501. doi: 10.1016/J.GEODERMA.2018.09.023

Thies, J. E. (2015). Molecular Approaches to Studying the Soil Biota. In E. A. Paul (Ed.), *Soil Microbiology, Ecology, and Biochemistry* (4th ed., pp. 151–186). Oxford: Academic Press.

Throbäck, I. N., Enwall, K., Jarvis, Å., & Hallin, S. (2004). Reassessing PCR primers targeting nirS, nirK and nosZ genes for community surveys of denitrifying bacteria with DGGE. *FEMS Microbiology Ecology*, *49*(3), 401–417. doi: 10.1016/j.femsec.2004.04.011

Tourna, M., Freitag, T. E., Nicol, G. W., & Prosser, J. I. (2008). Growth, activity and temperature responses of ammonia-oxidizing archaea and bacteria in soil microcosms. *Environmental Microbiology*, *10*(5), 1357–1364. doi: 10.1111/j.1462-2920.2007.01563.x

Treusch, A. H., Leininger, S., Kletzin, A., Schuster, S. C., Klenk, H.-P., & Schleper, C. (2005). Novel genes for nitrite reductase and Amo-related proteins indicate a role of uncultivated mesophilic crenarchaeota in nitrogen cycling: Role of mesophilic crenarchaeota in nitrogen cycling. *Environmental Microbiology*, *7*(12), 1985–1995. doi: 10.1111/j.1462-2920.2005.00906.x

Uwizeye, A., Boer, I. J. M. de, Opio, C. I., Schulte, R. P. O., Falcucci, A., Tempio, G., … Gerber, P. J. (2020). Nitrogen emissions along global livestock supply chains. *Nature Food*, 1–10. doi: 10.1038/s43016-020-0113-y

van Groenigen, J. W., Kuikman, P. J., de Groot, W. J. M., & Velthof, G. L. (2005). Nitrous oxide emission from urine-treated soil as influenced by urine composition and soil physical conditions. *Soil Biology and Biochemistry*, *37*(3), 463–473. doi: 10.1016/J.SOILBIO.2004.08.009

van Groenigen, J. W., Velthof, G. L., van der Bolt, F. J. E., Vos, A., & Kuikman, P. J. (2005). Seasonal variation in N_2O emissions from urine patches: Effects of urine concentration, soil compaction and dung. *Plant and Soil*, *273*, 15–27. doi: 10.1007/s11104-004-6261-2

Venterea, R. T., Coulter, J. A., & Clough, T. J. (2020). Nitrite accumulation and nitrogen gas production increase with decreasing temperature in urea-amended soils: Experiments and modeling. *Soil Biology and Biochemistry*, *142*, 107727. doi: 10.1016/j.soilbio.2020.107727

Wei, W., Isobe, K., Shiratori, Y., Nishizawa, T., Ohte, N., Ise, Y., … Senoo, K. (2015). Development of PCR primers targeting fungal nirK to study fungal denitrification in the environment. *Soil Biology and Biochemistry*, *81*, 282–286. doi: 10.1016/j.soilbio.2014.11.026

White, D. C., Davis, W. M., Nickels, J. S., King, J. D., & Bobbie, R. J. (1979). Determination of the sedimentary microbial biomass by extractible lipid phosphate. *Oecologia*, *40*(1), 51–62. doi: 10.1007/BF00388810

Willers, C., Jansen van Rensburg, P. J., & Claassens, S. (2015). Phospholipid fatty acid profiling of microbial communities-a review of interpretations and recent applications. *Journal of Applied Microbiology*, *119*(5), 1207–1218. doi: 10.1111/jam.12902

Williams, R., & Haynes, R. J. (1994). Comparison of initial wetting pattern, nutrient concentrations in soil solution and the fate of 15N-labelled urine in sheep and cattle urine patch areas of pasture soil. *Plant and Soil*, *162*, 49–59.

Wittorf, L., Jones, C. M., Bonilla-Rosso, G., & Hallin, S. (2018). Expression of nirK and nirS genes in two strains of Pseudomonas stutzeri harbouring both types of NO-forming nitrite reductases. *Research in Microbiology*, *169*(6), 343–347. doi: 10.1016/j.resmic.2018.04.010

Wu, T., Chellemi, D. O., Martin, K. J., Graham, J. H., & Rosskopf, E. N. (2007). Discriminating the effects of agricultural land management practices on soil fungal communities. *Soil Biology and Biochemistry*, *39*(5), 1139–1155. doi: 10.1016/j.soilbio.2006.11.024

Xi, N., Chu, C., & Bloor, J. M. G. (2018). Plant drought resistance is mediated by soil microbial community structure and soil-plant feedbacks in a savanna tree species. *Environmental and Experimental Botany*, *155*, 695–701. doi: 10.1016/j.envexpbot.2018.08.013

Yamulki, S., Wolf, I., Bol, R., Grant, B., Brumme, R., Veldkamp, E., & Jarvis, S. C. (2000). Effects of dung and urine amendments on the isotopic content of N_2O released from grasslands. *Rapid Communications in Mass Spectrometry*, *14*(15), 1356–1360. doi: 10.1002/1097-0231(20000815)14:15<1356::AID-RCM30>3.0.CO;2-C

Yoon, S., Nissen, S., Park, D., Sanford, R. A., & Löffler, E. (2016). Nitrous oxide reduction kinetics distinguish bacteria harboring clade I nosZ from those harboring clade II nosZ. *Applied and Environmental Microbiology*, *82*(13), 3793–3800. doi: 10.1128/AEM.00409-16.Editor

Zhou, Y., Zhu, H., Fu, S., & Yao, Q. (2017). Variation in Soil Microbial Community Structure Associated with Different Legume Species Is Greater than that Associated with Different Grass Species. *Frontiers in Microbiology*, *8*. doi: 10.3389/fmicb.2017.01007

APPENDIX A. FIELD SURVEY ENVIRONMENTAL AND VEGETATION DATA

Table A1: Sampling date average daily weather and moisture conditions.

Year	Date	Air Temp.	Soil Temp.	Soil Moisture	24 h Precip.	7 d Precip.
		°C	°C	g g^{-1}	mm	mm
2017	June 23	10.0	-*N/A*-	0.16	3.0	15.9
	July 19	15.2	-*N/A*-	0.13	0.5	1.1
	Aug. 09	16.3	-*N/A*-	0.24	16.8	28.4
	Aug. 30	17.8	-*N/A*-	0.11	0.1	0.1
	Sept. 20	9.8	-*N/A*-	0.27	14.1	24.8
2018	June 13	16.1	12.4	0.16	0.3	0.8
	July 03	16.1	14.3	0.13	0.0	9.4
	July 25	14.1	14.7	0.19	0.0	18.8
	Aug. 16	16.3	15.1	0.13	0.0	0.0
	Sept. 04	8.8	11.2	0.11	0.0	0.3

Table A2: Pasture forage yields prior to and following the grazing period. Paddocks sampled June 21 and July 19, 2017; June 21 and August 13, 2018.

Year	Treatment	Rep	Pre-Grazing Forage Yield	Post-Grazing Forage Yield
			kg dry matter ha^{-1}	
2017	Control	1	2844	1207
		2	3190	1485
		3	3345	1815
	CMV	1	3597	3008
		2	3406	2868
		3	4086	2947
	Sainfoin	1	3485	3013
		2	3182	2201
		3	3252	2100
2018	Control	1	3421	735
		2	2842	1787
		3	3694	3817
	CMV	1	3522	2754
		2	3282	2642
		3	5112	2308
	Sainfoin	1	3743	2034
		2	2894	1548
		3	3896	2844

Table A3: Vegetation composition data for paddocks 2017 and 2018.

Year	Season	Treatment	Rep	Grass	Weeds	Legume	Non-Bloat Leg.
				% Cover			
2017	Spring	Control	1	96	1	4	
		Control	2	97	2	2	
		Control	3	100	1		
		CMV	1	69	8	7	16
		CMV	2	48	12	17	23
		CMV	3	58	4	13	25
		Sainfoin	1	69	12	17	3
		Sainfoin	2	58	6	33	4
		Sainfoin	3	61	10	24	6
2017	Fall	Control	1	100			
		Control	2	98	2		
		Control	3	99	1		
		CMV	1	77	3	12	8
		CMV	2	60	8	13	19
		CMV	3	47	10	20	23
		Sainfoin	1	73	10	9	9
		Sainfoin	2	68	7	22	3
		Sainfoin	3	71	10	14	6
2018	Spring	Control	1	96	4		
		Control	2	98	2		
		Control	3	99	1		
		CMV	1	72.75	3.5	8.75	15
		CMV	2	54.5	4.25	17.75	23.5
		CMV	3	55.75	7.5	20.5	16.25
		Sainfoin	1	81.5	4.25	11	3.25
		Sainfoin	2	64.25	6.75	23.25	5.75
		Sainfoin	3	77.25	6.5	15	3
2018	Fall	Control	1	99	1		
		Control	2	99	1		
		Control	3	99	1		
		CMV	1	94.25	1.5	0.25	4
		CMV	2	83.75	4.25	5.75	6.25
		CMV	3	76	4.75	6.75	12.5
		Sainfoin	1	93.25	2.5	3.5	0.75
		Sainfoin	2	91.75	2	5.75	0.5
		Sainfoin	3	91.88	4.62	3.25	0.25

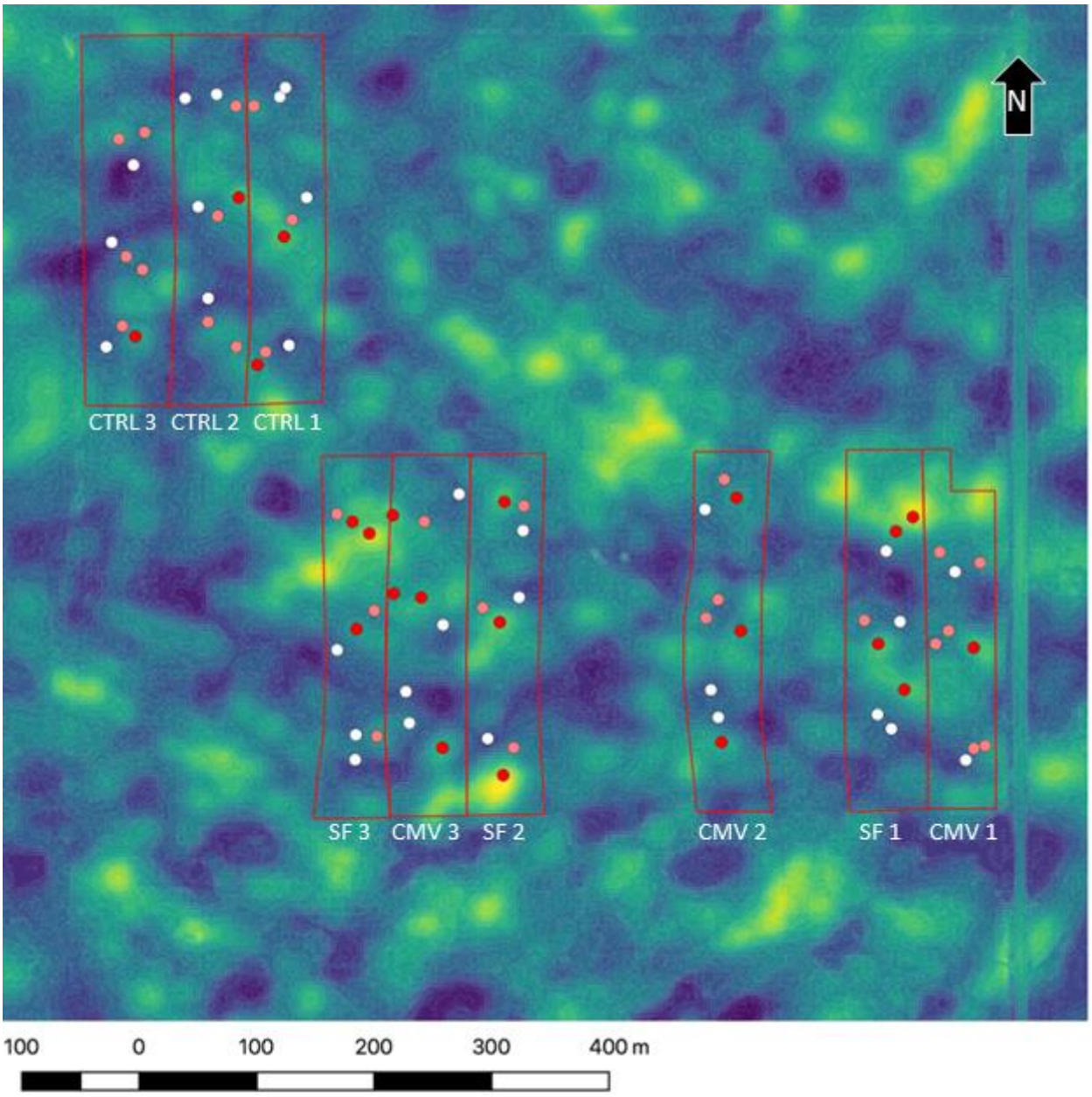

Figure A1: Termuende research ranch plot layout, chamber positions, and landscape topography. Red outlines represent cicer milkvetch (CMV), sainfoin (SF), and control (CTRL) paddock boundaries. Dots represent GHG chamber positions at elevated (red), sloped (pink), and depression (white) positions along slopes within each paddock. Topography is represented along a color gradient representing high (yellow) and low (blue) elevations. Represented elevations are relative to the surrounding area within 100 m.

APPENDIX B. SEASONAL AND ANNUAL TREATMENT DIFFERENCES OF FIELD SURVEY PLFA, ENZYME ACTIVITY, AND SOIL PROPERTY DATA

Table B1: Treatment PLFA abundance means and standard deviations.

Year	Treatment	Gram+	Gram-	Actinobact.	AMF	Fungi	Total
		nmol g^{-1} soil					
2017	Control	25.8 ± 4.1	35.1 ± 4.6	10.8 ± 1.7	6.3 ± 1.2	1.5 ± 0.3	112 ± 16
	CMV	24.4 ± 3.2	33.8 ± 5.1	10.6 ± 1.4	5.5 ± 1.4	1.5 ± 0.4	107 ± 14
	Sainfoin	25.4 ± 4.6	34.3 ± 6.2	10.4 ± 2.0	6.0 ± 1.6	1.6 ± 0.4	110 ± 19
2018	Control	28.7 ± 3.9	37.7 ± 6.5	12.1 ± 1.8	6.3 ± 1.2	2.0 ± 0.5	124 ± 19
	CMV	28.6 ± 4.2	37.9 ± 6.0	12.6 ± 1.9	5.7 ± 1.0	2.3 ± 0.6	124 ± 18
	Sainfoin	28.4 ± 5.2	36.7 ± 6.6	12.1 ± 1.9	5.7 ± 1.0	2.2 ± 0.6	122 ± 21

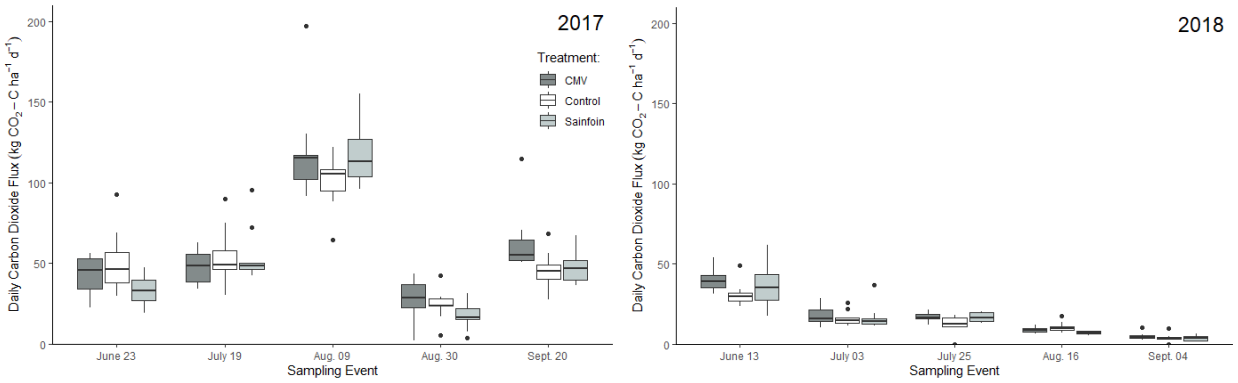

Figure B1: Daily soil carbon dioxide emissions.

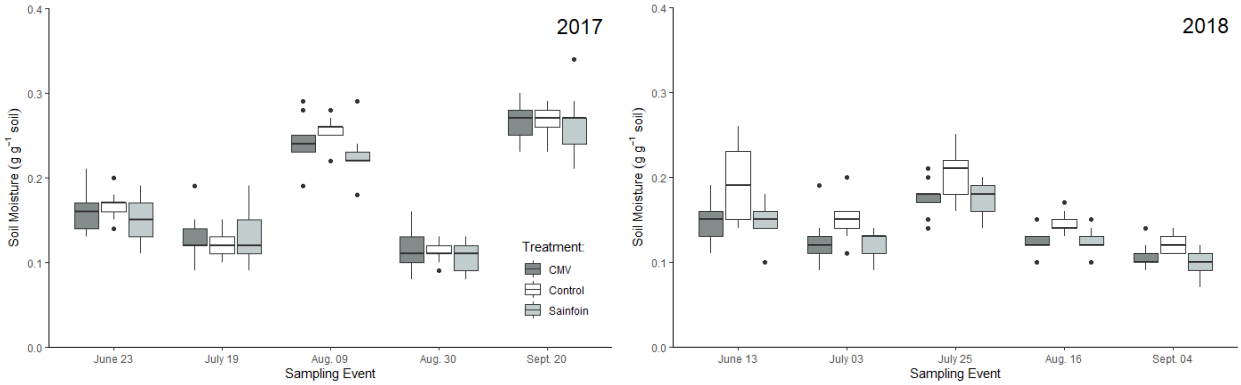

Figure B2: Soil moisture.

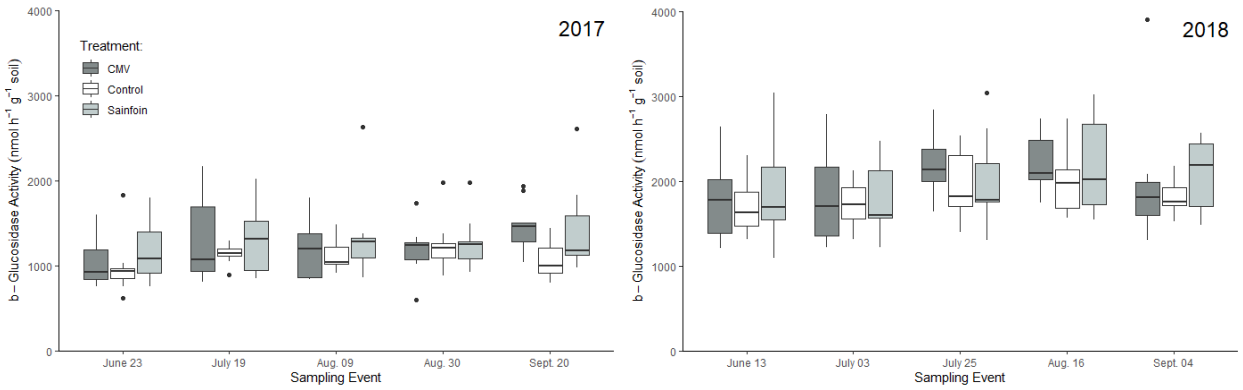

Figure B3: β-Glucosidase activity.

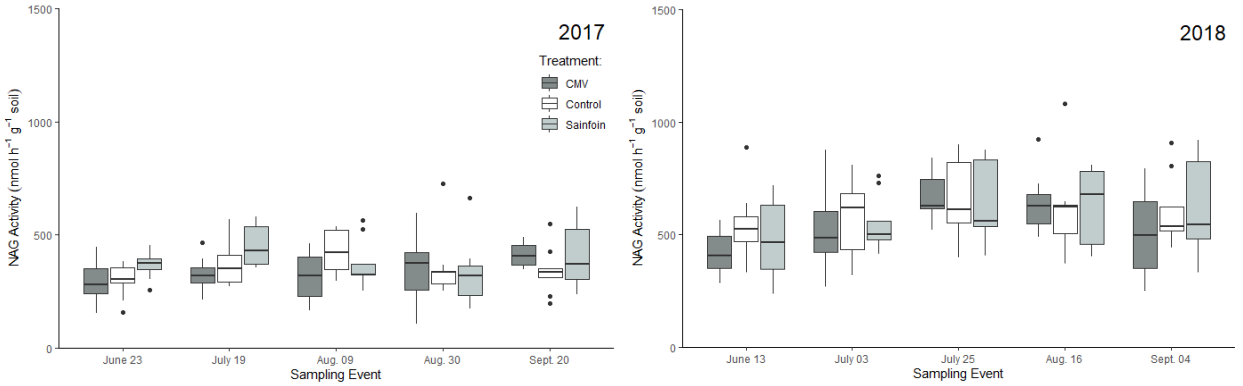

Figure B4: NAG activity.

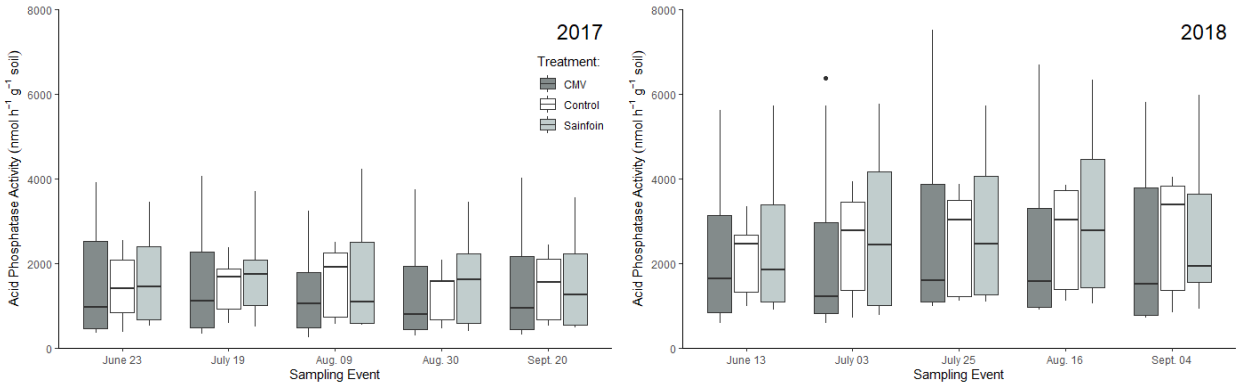

Figure B5: Acid phosphatase activity.

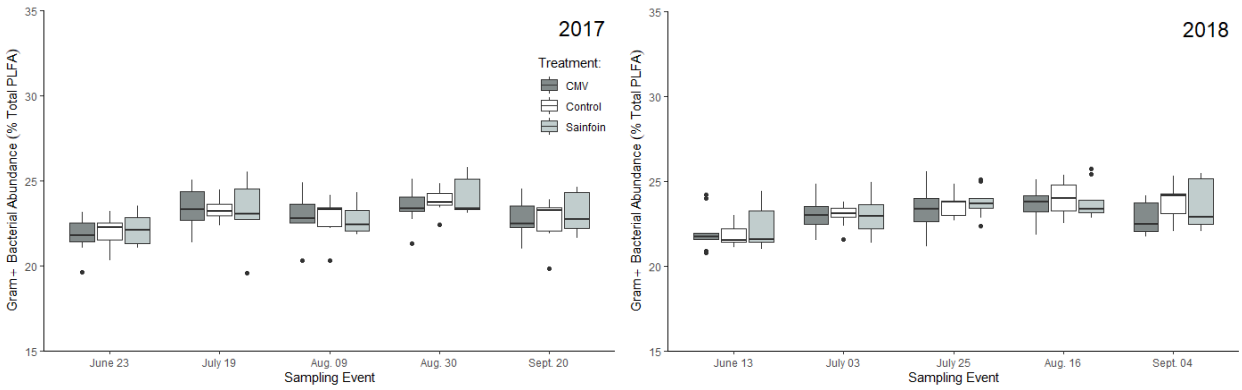

Figure B6: Gram+ PLFA abundance.

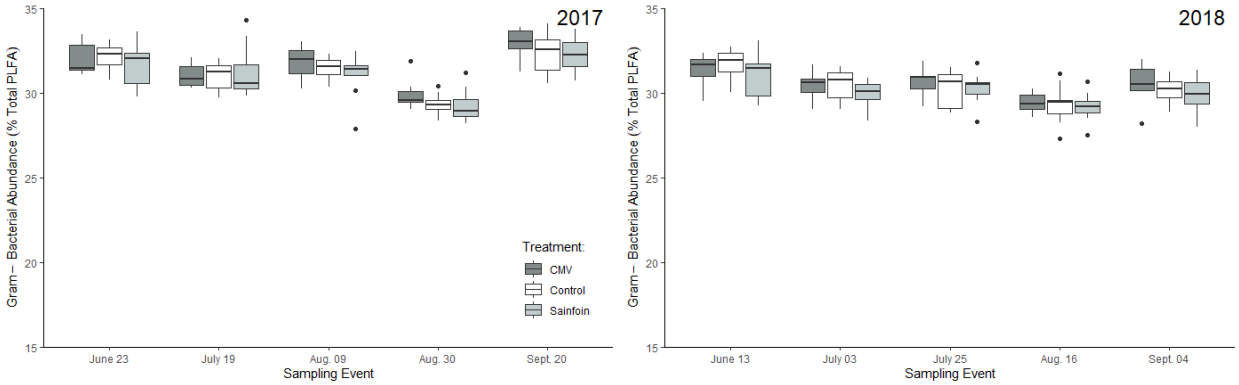

Figure B7: Gram- PLFA abundance.

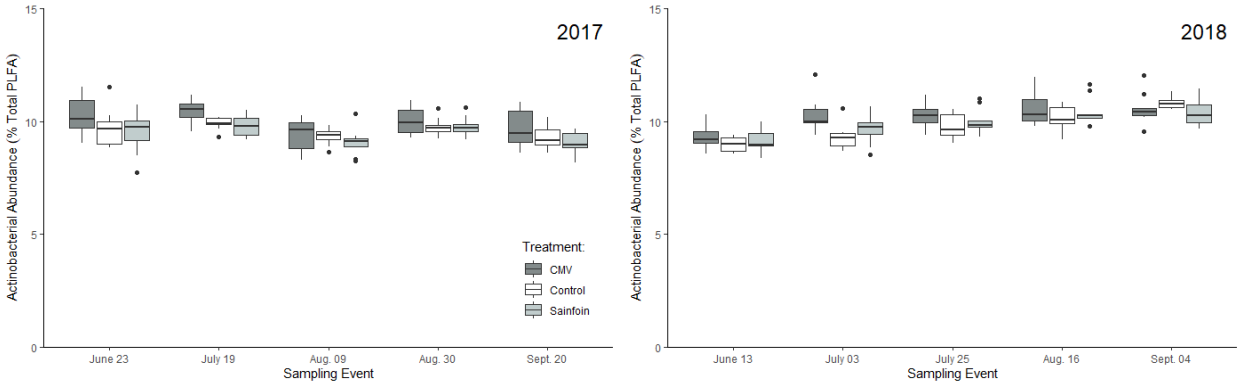

Figure B8: Actinobacteria PLFA abundance.

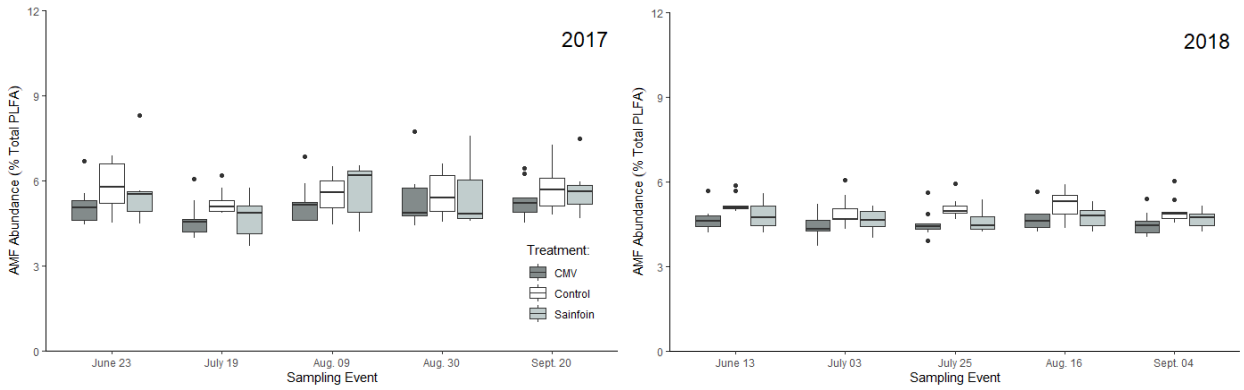

Figure B9: AMF PLFA abundance.

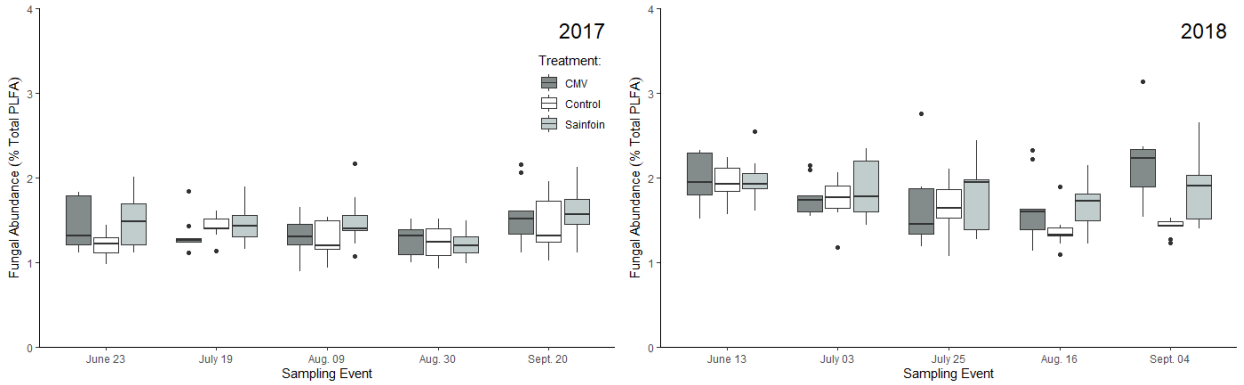

Figure B10: Fungal PLFA abundance.

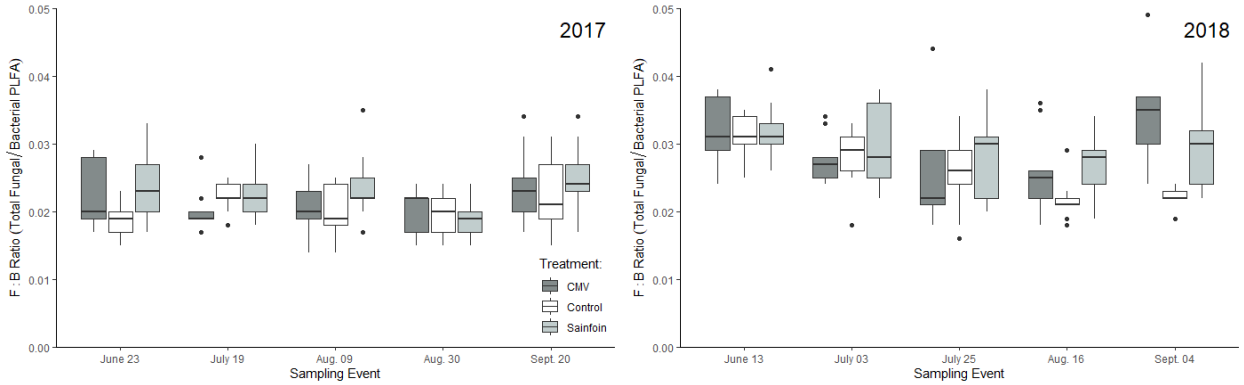

Figure B11: Ratio of fungal:bacterial PLFA counts.

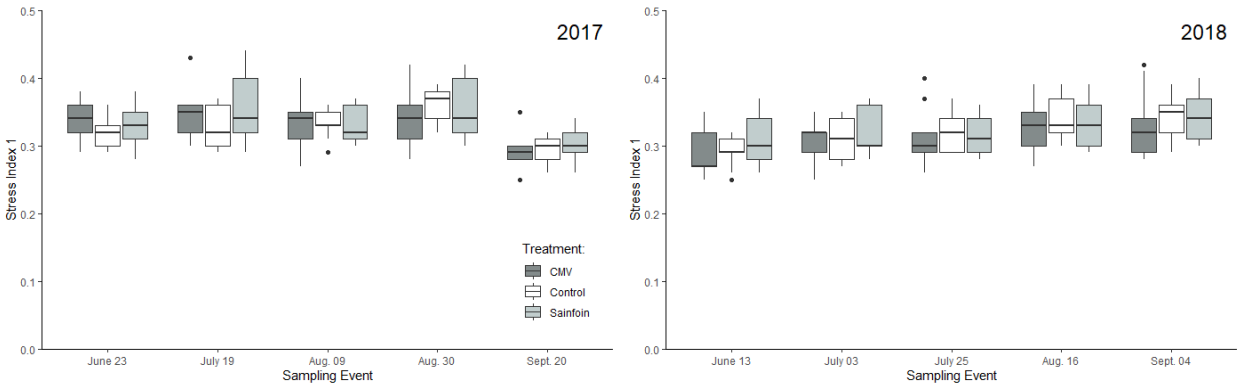

Figure B12: PLFA stress index 1.

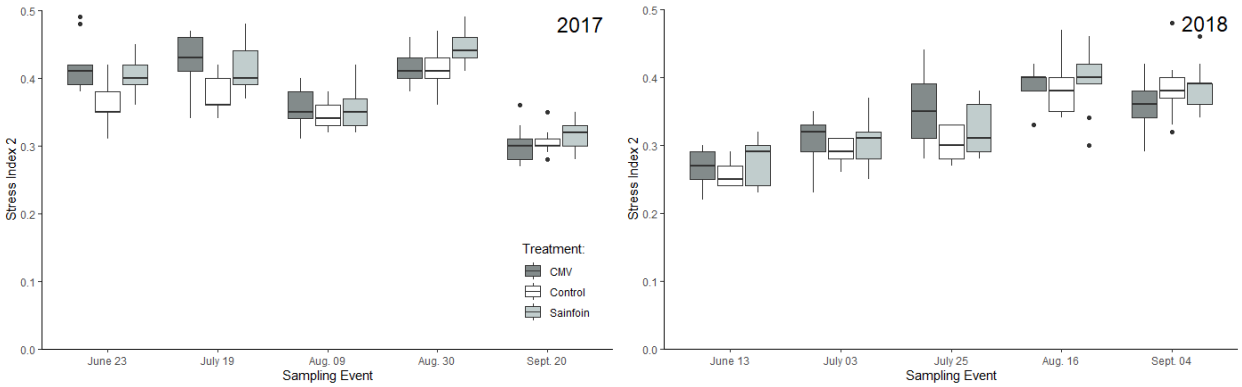

Figure B13: PLFA stress index 2.

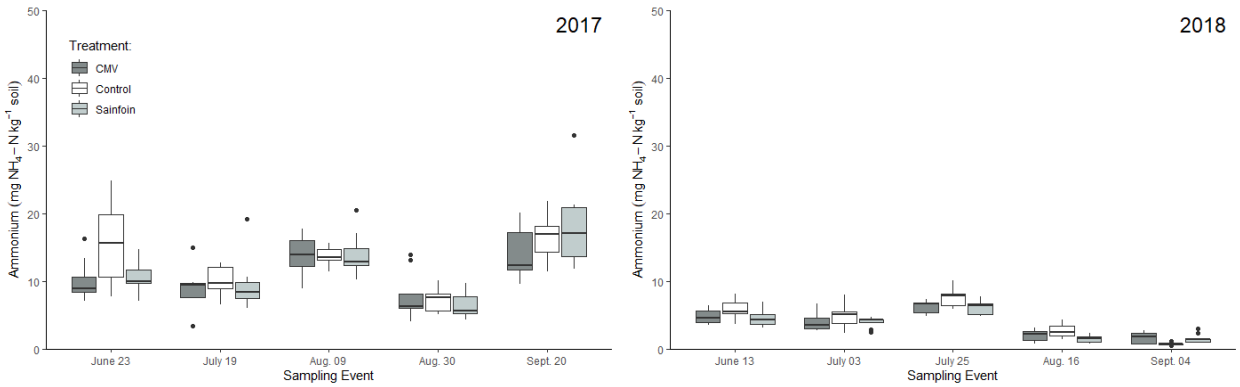

Figure B14: Soil ammonium.

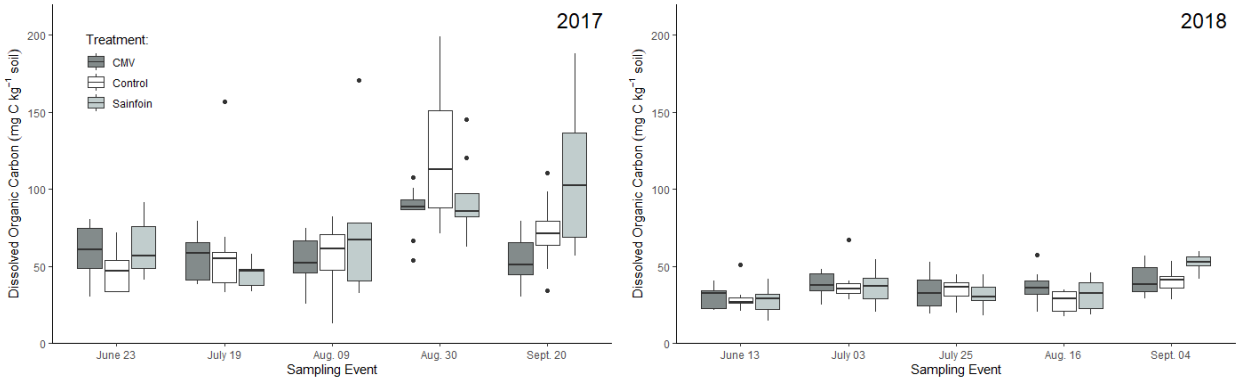

Figure B15: Soil dissolved organic carbon.

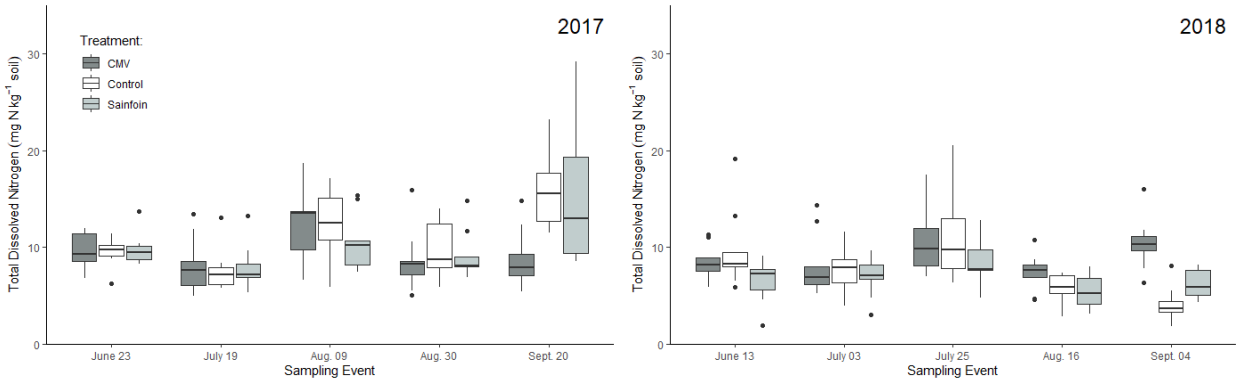

Figure B16: Soil total dissolved nitrogen.

APPENDIX C. FIELD STUDY ANOVA AND PERMANOVA TABLES

Table C1: 2017 field study Type III ANOVA F test model results.

Flux Model	Term	df	Res. df	F value	Pr (> F)	
Daily N_2O Flux	(Intercept)	1	43.3	4.07	0.0500	*
	Treatment	2	43.3	0.53	0.5947	
	Time	4	114	9.24	< 0.0001	***
	Treatment:Time	8	114	1.06	0.3951	
β-Glucosidase	(Intercept)	1	19.9	4206	< 0.0001	***
	Treatment	2	19.9	0.57	0.5754	
	Time	4	114	2.14	0.0805	.
	Treatment:Time	8	114	0.74	0.6567	
N-acetyl glucosaminidase	(Intercept)	1	81.4	71.2	< 0.0001	***
	Treatment	2	81.4	1.15	0.3215	
	Time	4	114	1.61	0.1775	
	Treatment:Time	8	114	1.59	0.1360	
Acid Phosphatase	(Intercept)	1	14.8	10.7	0.0052	**
	Treatment	2	14.8	0.09	0.9116	
	Time	4	114	0.13	0.9714	
	Treatment:Time	8	114	0.10	0.9991	
G+ PLFA	(Intercept)	1	16.3	2137	< 0.0001	***
	Treatment	2	16.3	0.16	0.8545	
	Time	4	114	4.10	0.0039	**
	Treatment:Time	8	114	0.25	0.9793	
G- PLFA	(Intercept)	1	61.0	8845	< 0.0001	***
	Treatment	2	61.0	0.87	0.4255	
	Time	4	114	12.0	< 0.0001	***
	Treatment:Time	8	114	0.67	0.7144	
Actinobacteria PLFA	(Intercept)	1	34.4	1969	< 0.0001	***
	Treatment	2	34.4	3.01	0.0624	.
	Time	4	114	4.78	0.0013	**
	Treatment:Time	8	114	0.39	0.9251	
AMF PLFA	(Intercept)	1	13.1	200.5	< 0.0001	***
	Treatment	2	13.1	0.95	0.4102	
	Time	4	114	1.39	0.2431	
	Treatment:Time	8	114	0.43	0.9033	

Table C1 *(continued)*: 2017 field study Type III ANOVA F test model results.

Flux Model	Term	df	Res. df	F value	Pr (> F)	
Fungal PLFA	(Intercept)	1	54.2	266.3	< 0.0001	***
	Treatment	2	54.2	2.72	0.0748	.
	Time	4	114	2.15	0.0782	.
	Treatment:Time	8	114	0.99	0.4445	
F:B Ratio	(Intercept)	1	44.9	229.1	< 0.0001	***
	Treatment	2	44.9	2.46	0.0971	.
	Time	4	114	1.63	0.1706	
	Treatment:Time	8	114	1.05	0.4005	
PLFA Stress1	(Intercept)	1	16.2	510.5	< 0.0001	***
	Treatment	2	16.2	0.56	0.5840	
	Time	4	114	4.38	0.0025	**
	Treatment:Time	8	114	0.75	0.6458	
PLFA Stress 2	(Intercept)	1	22.7	1177	< 0.0001	***
	Treatment	2	22.7	6.47	0.0060	**
	Time	4	114	30.0	< 0.0001	***
	Treatment:Time	8	114	2.45	0.0175	*
Total PLFA	(Intercept)	1	40.4	435.7	< 0.0001	***
	Treatment	2	40.4	0.28	0.7590	
	Time	4	114	4.12	0.0038	**
	Treatment:Time	8	114	2.29	0.0261	*
Soil NO_3^-	(Intercept)	1	16.4	79.5	< 0.0001	***
	Treatment	2	16.4	0.17	0.8451	
	Time	4	114	18.2	< 0.0001	***
	Treatment:Time	8	114	2.58	0.0125	*
Soil NH_4^+	(Intercept)	1	47.7	26.7	< 0.0001	***
	Treatment	2	47.7	2.14	0.1286	
	Time	4	114	2.55	0.0432	*
	Treatment:Time	8	114	2.24	0.0297	*
Total Dissolved N	(Intercept)	1	28.1	421.3	< 0.0001	***
	Treatment	2	28.1	0.01	0.9855	
	Time	4	114	3.24	0.0146	*
	Treatment:Time	8	114	2.82	0.0069	**
Dissolved Organic C	(Intercept)	1	34.0	36.3	< 0.0001	***
	Treatment	2	34.0	0.66	0.5245	
	Time	4	114	2.61	0.0387	*
	Treatment:Time	8	114	3.36	0.0017	**

Table C2: 2018 field study Type III ANOVA F test model results.

Flux Model	Term	df	Res. df	F value	Pr (> F)	
Daily N_2O Flux	(Intercept)	1	20.2	10.9	0.0035	**
	Treatment	2	20.2	0.12	0.8889	
	Time	4	114	2.72	0.0331	*
	Treatment:Time	8	114	1.69	0.1071	
β-Glucosidase	(Intercept)	1	20.7	90.8	< 0.0001	***
	Treatment	2	20.7	0.22	0.8081	
	Time	4	114	1.98	0.1028	
	Treatment:Time	8	114	0.15	0.9968	
N-acetyl glucosaminidase	(Intercept)	1	27.2	44.4	< 0.0001	***
	Treatment	2	27.2	0.91	0.4136	
	Time	4	114	3.78	0.0063	**
	Treatment:Time	8	114	0.46	0.8786	
Acid Phosphatase	(Intercept)	1	16.1	9.89	0.0062	**
	Treatment	2	16.1	0.05	0.9515	
	Time	4	114	0.18	0.9479	
	Treatment:Time	8	114	0.06	0.9999	
G+ PLFA	(Intercept)	1	11.5	2010	< 0.0001	***
	Treatment	2	11.5	0.11	0.8975	
	Time	4	114	4.42	0.0023	**
	Treatment:Time	8	114	0.70	0.6907	
G- PLFA	(Intercept)	1	15.5	5601	< 0.0001	***
	Treatment	2	15.5	0.49	0.6212	
	Time	4	114	5.69	0.0003	***
	Treatment:Time	8	114	0.40	0.9165	
Actinobacteria PLFA	(Intercept)	1	17.4	1458	< 0.0001	***
	Treatment	2	17.4	0.48	0.6273	
	Time	4	114	8.36	< 0.0001	***
	Treatment:Time	8	114	1.74	0.0973	.
AMF PLFA	(Intercept)	1	12.8	610.5	< 0.0001	***
	Treatment	2	12.8	2.25	0.1451	
	Time	4	114	0.84	0.5042	
	Treatment:Time	8	114	0.11	0.9989	
Fungal PLFA	(Intercept)	1	36.0	258.5	< 0.0001	***
	Treatment	2	36.0	0.03	0.9659	
	Time	4	114	4.22	0.0032	**
	Treatment:Time	8	114	2.10	0.0412	*

Table C2 *(continued)*: 2018 field study Type III ANOVA F test model results.

Flux Model	Term	df	Res. df	F value	Pr (> F)	
F:B Ratio	(Intercept)	1	34.0	245.7	< 0.0001	***
	Treatment	2	34.0	0.06	0.9377	
	Time	4	114	4.15	0.0036	**
	Treatment:Time	8	114	2.15	0.0370	*
PLFA Stress1	(Intercept)	1	12.9	331.9	< 0.0001	***
	Treatment	2	12.9	0.39	0.6877	
	Time	4	114	2.78	0.0301	*
	Treatment:Time	8	114	0.39	0.9227	
PLFA Stress 2	(Intercept)	1	17.8	304.5	< 0.0001	***
	Treatment	2	17.8	0.30	0.7453	
	Time	4	114	18.4	< 0.0001	***
	Treatment:Time	8	114	1.53	0.1533	
Total PLFA	(Intercept)	1	30.8	358.3	< 0.0001	***
	Treatment	2	30.8	0.10	0.9068	
	Time	4	114	2.17	0.0769	.
	Treatment:Time	8	114	0.23	0.9853	
Soil NO_3^-	(Intercept)	1	70.3	17.5	< 0.0001	***
	Treatment	2	70.3	0.15	0.8615	
	Time	4	114	6.87	< 0.0001	***
	Treatment:Time	8	114	1.57	0.1405	
Soil NH_4^+	(Intercept)	1	43.7	154.9	< 0.0001	***
	Treatment	2	43.7	3.53	0.03792	*
	Time	4	114	31.3	< 0.0001	***
	Treatment:Time	8	114	2.12	0.03974	*
Total Dissolved N	(Intercept)	1	60.9	325.9	< 0.0001	***
	Treatment	2	60.9	3.65	0.0318	*
	Time	4	114	1.98	0.1016	
	Treatment:Time	8	114	4.44	0.0001	***
Dissolved Organic C	(Intercept)	1	30.3	79.5	< 0.0001	***
	Treatment	2	30.3	0.09	0.9161	
	Time	4	114	2.36	0.0577	.
	Treatment:Time	8	114	2.09	0.0420	*

Table C3: 2017 field survey PerMANOVA results. Terms added sequentially.

Term	df	SS	r^2	F	Pr (> F)
Moisture	1	0.021	0.111	54.5	0.001
CO_2	1	0.002	0.010	4.7	0.003
TDN	1	0.002	0.009	4.4	0.001
Treatment	2	0.010	0.053	13.1	0.001
DOC	1	0.007	0.040	19.5	0.001
Nitrate	1	0.014	0.075	37.0	0.001
Ammonium	1	0.001	0.007	3.5	0.006
pH	1	0.002	0.010	5.1	0.002
Time	4	0.035	0.186	22.8	0.001
Gram-	1	0.012	0.062	30.6	0.001
Gram+	1	0.008	0.042	20.7	0.001
Actinobact.	1	0.013	0.069	33.8	0.001
Fungi	1	0.004	0.020	10.0	0.001
AMF	1	0.006	0.030	14.9	0.001
Stress1	1	0.005	0.029	14.2	0.001
Stress2	1	0.002	0.013	6.5	0.001
Residual	114	0.044	0.232		
Total	134	0.187	1		

Table C4: 2018 field survey PerMANOVA results. Terms added sequentially.

Term	df	SS	r^2	F	Pr (> F)
Moisture	1	0.021	0.074	55.7	0.001
CO_2	1	0.062	0.216	163.4	0.001
TDN	1	0.002	0.005	4.0	0.007
Treatment	2	0.015	0.052	19.8	0.001
DOC	1	0.006	0.020	15.4	0.001
Nitrate	1	0.006	0.023	17.1	0.001
Ammonium	1	0.012	0.041	31.2	0.001
pH	1	0.021	0.074	56.1	0.001
Time	4	0.046	0.159	30.1	0.001
Gram-	1	0.008	0.028	21.1	0.001
Gram+	1	0.011	0.039	29.7	0.001
Actinobact.	1	0.012	0.040	30.4	0.001
Fungi	1	0.007	0.025	19.1	0.001
AMF	1	0.008	0.028	21.0	0.001
Stress1	1	0.004	0.013	10.0	0.001
Stress2	1	0.003	0.010	7.6	0.001
Residual	114	0.043	0.151		
Total	134	0.287	1		

APPENDIX D. N_2O OUTLIER FLUXES AND SOIL MICROCOSM DATA

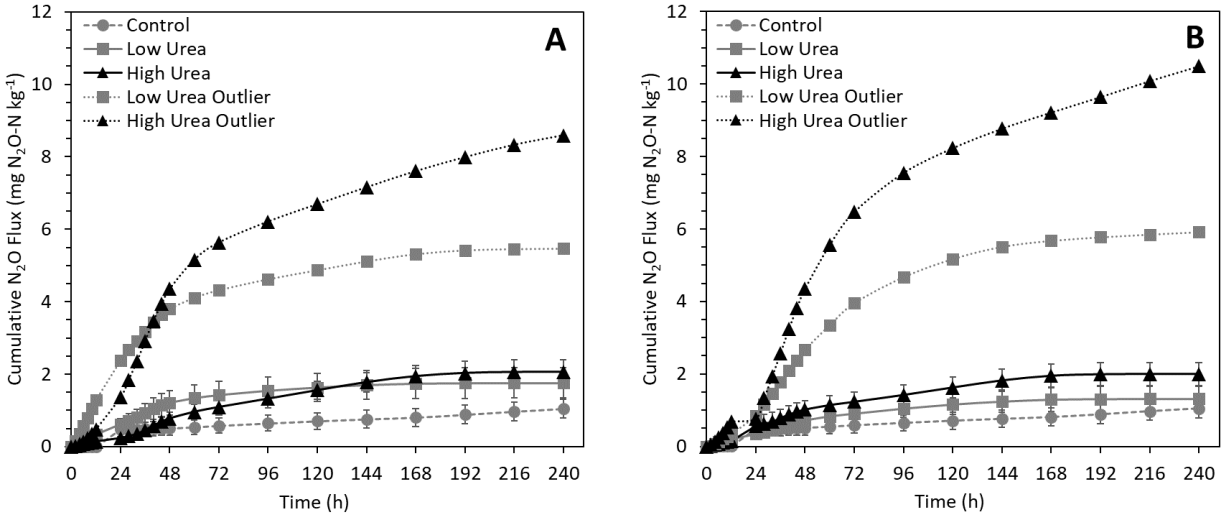

Figure D1: Outlier N_2O cumulative fluxes relative to treatment means for unlabeled urea (A) and $^{13}C^{15}N$ labeled urea (B) microcosms. Error bars represent SE.

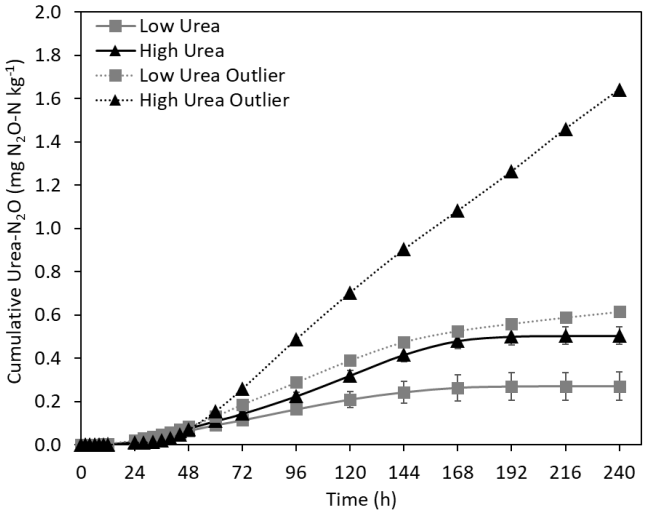

Figure D2: Outlier cumulative urea-N_2O fluxes relative to treatment means. Error bars represent SE. Emission factors for outlier low and high urea-N are 0.65% and 0.85%, respectively.

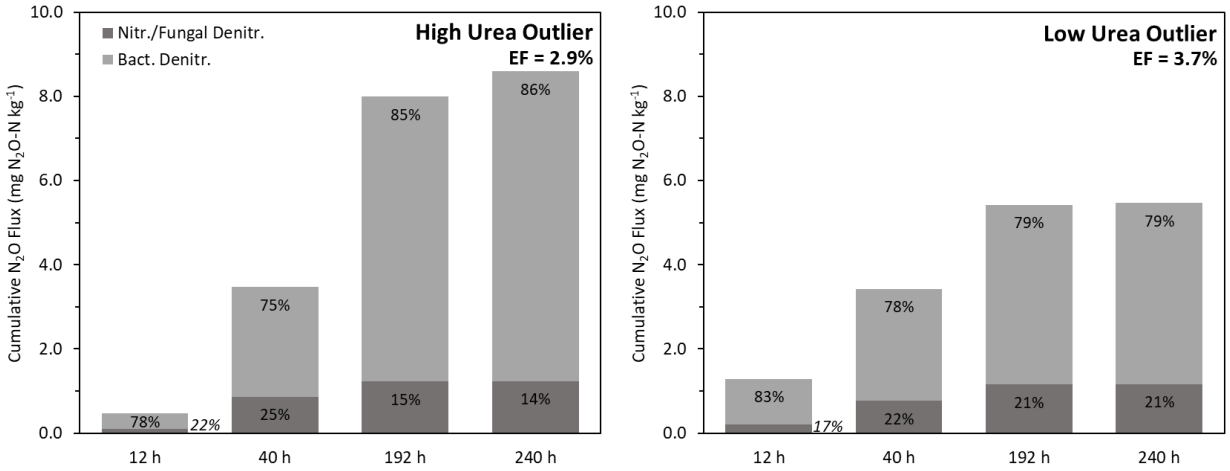

Figure D3: Relative contributions of nitrifiers and denitrifiers to total N_2O in N_2O outlier soils after 12, 40, 192, and 240 h. Cumulative emission factors (EF) are listed as mg N_2O-N produced per mg urine-N added.

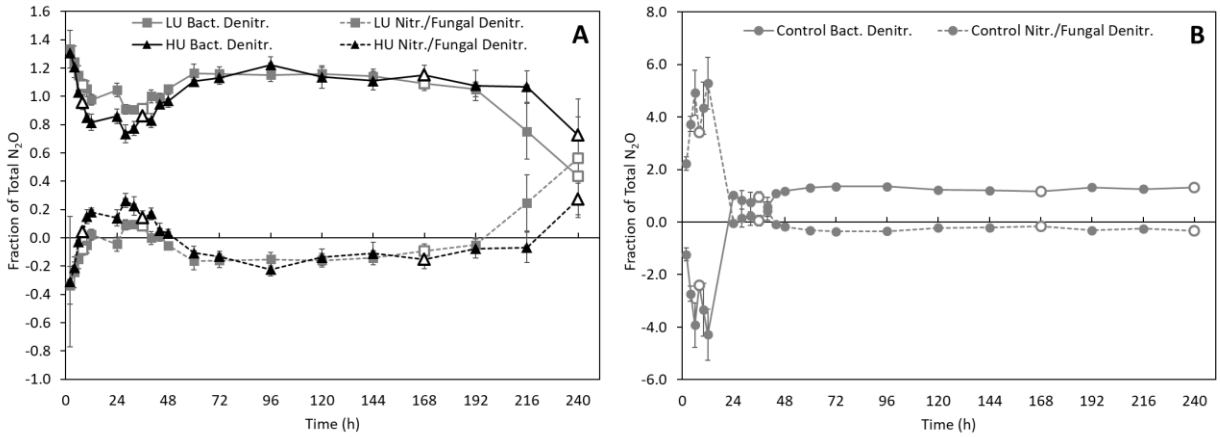

Figure D4: Unadjusted N_2O source partition fraction values from low urea (LU) and high urea (HU) urine treatments (A) and controls (B). Error bars represent SE.

Table D1: Average microcosm soil pH, ammonium, and nitrate content ± SE.

Treatment	Time	pH	Soil NH_4^+-N	Soil NO_3^--N
	h		mg kg^{-1}	mg kg^{-1}
Pre-Condition	0	7.22 ± 0.03	5.60 ± 0.20	190 ± 2
3.5 g L^{-1}	8	7.44 ± 0.01	128 ± 2	208 ± 1
	36	7.47 ± 0.01	131 ± 3	155 ± 12
	168	7.17 ± 0.04	91.1 ± 23.5	214 ± 34
	240	7.13 ± 0.00	8.12 ± 1.41	319 ± 3
7.0 g L^{-1}	8	7.52 ± 0.02	213 ± 9	209 ± 6
	36	7.36 ± 0.01	195 ± 1	104 ± 6
	168	7.29 ± 0.05	193 ± 24	173 ± 56
	240	7.08 ± 0.01	8.12 ± 0.48	311 ± 29
Control	240	7.18 ± 0.01	6.87 ± 0.37	218 ± 4
3.5 g L^{-1} ($^{15}N^{13}C$)	240	7.11 ± 0.02	6.60 ± 0.71	315 ± 5
7.0 g L^{-1} ($^{15}N^{13}C$)	240	7.06 ± 0.02	9.29 ± 2.55	339 ± 1

APPENDIX E. qPCR PRIMERS, THERMOCYCLER CONDITIONS, AND REPRESENTATIVE ORGANISMS

Table E1: qPCR target genes, master mixes, and primers used.

Gene	Primer	Sequence (5' → 3')	Product (bp)
Arch. *amoA*	Crenamo23F (Tourna, Freitag, Nicol, & Prosser, 2008)	ATGGTCTGGCTWAGACG	629
	Crenamo616r48x (Nicol et al., 2008) [a]	GCCATCCABCKRTANGTCCA	
Bact. *amoA*	amoA1F	GGGGTTTCTACTGGTGGT	491
	amoA2R (Rotthauwe, Witzel, & Liesack, 1997)	CCCCTCKGSAAAGCCTTCTTC	
nirK	nirKH1F	ATYGGCGGVAYGGCGA	165
	nirKH1R (Sonia Henry et al., 2004)	GCCTCGATCAGRTTRTGGTT	
nirS	Cd3aF (Michotey, Méjean, & Bonin, 2000)	GTSAACGTSAAGGARACSGG	410
	R3cd (Throbäck, Enwall, Jarvis, & Hallin, 2004)	GASTTCGGRTGSGTCTTGA	
nosZ clade I	nosZ2F	CGCRACGGCAASAAGGTSMSSGT	267
	nosZ2R (Henry, Bru, Stres, Hallet, & Philippot, 2006)	CAKRTGCAKSGCRTGGCAGAA	
nosZ clade II	nosZ-II-F	CTIGGICCIYTKCAYAC	698
	nosZ-II-R (Jones, Graf, Bru, Philippot, & Hallin, 2013)	GCIGARCARAAITCBGTRC	

[a] *Crenamo616r degenerate primer*

Table E2: Thermocycler conditions for qPCR. Cycles consisted of denaturation (D), annealing (A), extension (E), and measurement (M) to denature possible primer-dimers at measurement.

Gene	SYBR MM	Primer Conc.	Thermal Cycle [a]	Efficiency	r^2
		uM		%	
Arch. *amoA*	Platinum	0.5	D: 60s 95°C A: 60s 55°C E: 60s 72°C M: 60s 80°C [45x]	90.4	0.995
Bact. *amoA*	PowerUp	0.9	D: 45s 95°C A: 45s 55°C E: 45s 72°C M: 60s 80°C [40x]	90.8	0.999
nirK [b]	PowerUp	F: 0.6; R: 0.8	D: 15s 95°C A: 30s 58°C E: 30s 72°C M: 15s 80°C [40x]	101.3	0.995
nirS [b]	PowerUp	1.0	D: 15s 95°C A: 30s 60°C E: 30s 72°C M: 15s 80°C [40x]	95.0	0.998
nosZ clade I [b]	PowerUp	1.0	D: 15s 95°C A: 30s 60°C E: 30s 72°C M: 15s 80°C [40x]	96.6	0.998
nosZ clade II [b]	Platinum	2.0	D: 15s 95°C A: 30s 58°C E: 30s 72°C M: 15s 80°C [45x]	109.2	0.992

[a] All methods started with 2 min 50 °C UDG activation and 2 min 95 °C DNA polymerase activation and initial denaturation.

[b] Initial 6 cycles of touchdown qPCR using stated method denaturation, annealing, and extension cycles with an initial annealing temperature +5°C and decreasing -1°C with each cycle until reaching stated temperature.

Table E3: representative organisms and genes cloned for absolute qPCR.

Gene	**Representative Organism**
Arch. *amoA*	Synthesized from Fosmid 54D9 sequence (Treusch et al., 2005)
Bact. *amoA*	*Nitrosomonas europa*
nirK	Synthesized from *Sinorhizobium meliloti nirK* sequence
nirS	*Pseudomonas stutzeri*
nosZ clade I	*Pseudomonas stutzeri*
nosZ clade II	Equimolar mix of 10 cloned *nosZ-II* amplicons derived from environmental samples and confirmed by DNA sequencing.

APPENDIX F. ANOVA TABLES FOR GAS FLUX AND GENE ABUNDANCE MODELS

Table F1: Gas flux model ANOVA results (Type III F-test).

Flux Model	Term	df	Res. df	F value	Pr (> F)	
Hourly N_2O	(Intercept)	1	52.1	2.14	0.1468	
	Treatment	2	52.1	16.3	< 0.0001	***
	Time	21	147	23.9	< 0.0001	***
	Treatment:Time	42	147	28.5	< 0.0001	***
Hourly CO_2	(Intercept)	1	88.8	8.77	0.0039	**
	Treatment	2	88.8	201.3	< 0.0001	***
	Time	21	189	251.8	< 0.0001	***
	Treatment:Time	42	189	29.6	< 0.0001	***
Cumulative N_2O	(Intercept)	1	11.5	0.8	0.3993	
	Treatment	2	11.5	0.2	0.8252	
	Time	21	147	46.2	< 0.0001	***
	Treatment:Time	42	147	4.3	< 0.0001	***
Cumulative CO_2	(Intercept)	1	11.7	403.7	< 0.0001	***
	Treatment	2	11.7	36.7	< 0.0001	***
	Time	21	189	2644	< 0.0001	***
	Treatment:Time	42	189	73.4	< 0.0001	***
Hourly Urea-N_2O	(Intercept)	1	49.5	138.6	< 0.0001	***
	Treatment	1	49.5	0.287	0.5948	***
	Time	21	84	21.0	< 0.0001	***
	Treatment:Time	21	84	3.36	< 0.0001	***
Hourly Urea-CO_2	(Intercept)	1	130.7	205	< 0.0001	***
	Treatment	1	130.7	8.31	0.00462	***
	Time	21	125	413.6	< 0.0001	***
	Treatment:Time	21	125	10.1	< 0.0001	***
Cumulative Urea-N_2O	(Intercept)	1	39.3	342.4	< 0.0001	***
	Treatment	1	39.3	1.18	.2840	
	Time	21	84	202.5	< 0.0001	***
	Treatment:Time	21	84	4.37	< 0.0001	***
Cumulative Urea-CO_2	(Intercept)	1	8.4	69.0	< 0.0001	***
	Treatment	1	8.4	5.76	0.0420	*
	Time	21	125	379.4	< 0.0001	***
	Treatment:Time	21	125	237.6	< 0.0001	***

Table F1 *(continued)*: Gas flux model ANOVA results (Type III F-test).

Flux Model	Term	df	Res. df	F value	Pr (> F)	
Bacterial Denitrifier	(Intercept)	1	142	537	< 0.0001	***
N_2O	Treatment	2	142	72.3	< 0.0001	***
	Time	21	189	8.50	< 0.0001	***
	Treatment:Time	42	189	9.19	< 0.0001	***
Nitrifier/Fungal	(Intercept)	1	142	0.28	0.5948	
Denitrifier N_2O	Treatment	2	142	72.3	< 0.0001	***
	Time	21	189	8.50	< 0.0001	***
	Treatment:Time	42	189	9.19	< 0.0001	***

Table F2: Gene Abundance (DNA) ANOVA results (Type III F-test).

Gene	Term	df	F value	Pr (> F)	
Arch. *amoA*	Treatment	2	1.10	0.3452	
	Time	3	0.50	0.6838	
	Treatment:Time	6	3.63	0.0066	**
	Residuals	35			
Bact. *amoA*	Treatment	2	5.49	0.0083	**
	Time	3	23.4	< 0.0001	***
	Treatment:Time	6	18.3	< 0.0001	***
	Residuals	36			
nirK	Treatment	2	0.70	0.5042	
	Time	3	1.79	0.1656	
	Treatment:Time	6	3.36	0.0098	**
	Residuals	36			
nirS	Treatment	2	7.19	0.0024	**
	Time	3	10.1	< 0.0001	***
	Treatment:Time	6	9.25	< 0.0001	***
	Residuals	36			
nosZ Clade I	Treatment	2	3.48	0.0417	*
	Time	3	2.16	0.1097	
	Treatment:Time	6	3.54	0.0074	**
	Residuals	36			
nosZ Clade II	Treatment	2	5.14	0.0111	*
	Time	3	6.82	0.0010	***
	Treatment:Time	6	13.1	< 0.0001	***
	Residuals	35			
Total *nir*	Treatment	2	0.48	0.6232	
	Time	3	0.95	0.4261	
	Treatment:Time	6	2.88	0.0215	*
	Residuals	36			
Total *nos*	Treatment	2	5.06	0.0117	*
	Time	3	6.54	0.0013	**
	Treatment:Time	6	13.1	< 0.0001	***
	Residuals	35			
Total *nir*:*nos*	Treatment	2	2.33	0.1119	
	Time	3	1.92	0.1449	
	Treatment:Time	6	8.10	< 0.0001	***
	Residuals	35			

Table F3: Gene Transcript Abundance (mRNA) ANOVA results (Type III F-test).

Gene Model	Term	df	F value	Pr (> F)	
Arch. *amoA*	Treatment	2	1.28	0.2916	
	Time	3	1.60	0.2080	
	Treatment:Time	6	2.07	0.0845	.
	Residuals	33			
Bact. *amoA*	Treatment	2	2.82	0.0743	.
	Time	3	2.27	0.0991	.
	Treatment:Time	6	3.59	0.0076	**
	Residuals	33			
nirK	Treatment	2	47.6	< 0.0001	***
	Time	3	14.0	< 0.0001	***
	Treatment:Time	6	15.3	< 0.0001	***
	Residuals	33			
nirS	Treatment	2	4.96	0.0131	*
	Time	3	18.8	< 0.0001	***
	Treatment:Time	6	10.5	< 0.0001	***
	Residuals	33			
nosZ Clade I	Treatment	2	7.83	0.0016	**
	Time	3	10.8	< 0.0001	***
	Treatment:Time	6	14.2	< 0.0001	***
	Residuals	33			
nosZ Clade II	Treatment	2	92.8	< 0.0001	***
	Time	3	92.2	< 0.0001	***
	Treatment:Time	6	34.4	< 0.0001	***
	Residuals	32			
Total *nir*	Treatment	2	13.3	< 0.0001	***
	Time	3	13.2	< 0.0001	***
	Treatment:Time	6	11.3	< 0.0001	***
	Residuals	33			
Total *nos*	Treatment	2	57.8	< 0.0001	***
	Time	3	47.8	< 0.0001	***
	Treatment:Time	6	33.6	< 0.0001	***
	Residuals	32			
Total *nir*:*nos*	Treatment	2	15.8	< 0.0001	***
	Time	3	14.2	< 0.0001	***
	Treatment:Time	6	6.77	0.0001	***
	Residuals	32			